Nuclear Safety
NEA/CSNI/R(2022)10
March 2025
www.oecd-nea.org

Best Practice Guidelines for the Use of CFD in Nuclear Reactor Safety Applications – 2024 Update

OECD
BETTER POLICIES FOR BETTER LIVES

NEA
NUCLEAR ENERGY AGENCY

Nuclear Energy Agency

NEA/CSNI/R(2022)10

Unclassified English text only

19 March 2025

NUCLEAR ENERGY AGENCY
COMMITTEE ON THE SAFETY OF NUCLEAR INSTALLATIONS

Best Practice Guidelines for the Use of CFD in Nuclear Reactor Safety Applications – 2024 Update

JT03562423

ORGANISATION FOR ECONOMIC CO-OPERATION AND DEVELOPMENT

The OECD is a unique forum where the governments of 38 democracies work together to address the economic, social and environmental challenges of globalisation. The OECD is also at the forefront of efforts to understand and to help governments respond to new developments and concerns, such as corporate governance, the information economy and the challenges of an ageing population. The Organisation provides a setting where governments can compare policy experiences, seek answers to common problems, identify good practice and work to co-ordinate domestic and international policies.

The OECD member countries are: Australia, Austria, Belgium, Canada, Chile, Colombia, Costa Rica, Czechia, Denmark, Estonia, Finland, France, Germany, Greece, Hungary, Iceland, Ireland, Israel, Italy, Japan, Korea, Latvia, Lithuania, Luxembourg, Mexico, the Netherlands, New Zealand, Norway, Poland, Portugal, the Slovak Republic, Slovenia, Spain, Sweden, Switzerland, Türkiye, the United Kingdom and the United States. The European Commission takes part in the work of the OECD.

OECD Publishing disseminates widely the results of the Organisation's statistics gathering and research on economic, social and environmental issues, as well as the conventions, guidelines and standards agreed by its members.

NUCLEAR ENERGY AGENCY

The OECD Nuclear Energy Agency (NEA) was established on 1 February 1958. Current NEA membership consists of 34 countries: Argentina, Australia, Austria, Belgium, Bulgaria, Canada, Czechia, Denmark, Finland, France, Germany, Greece, Hungary, Iceland, Ireland, Italy, Japan, Korea, Luxembourg, Mexico, the Netherlands, Norway, Poland, Portugal, Romania, Russia (suspended), the Slovak Republic, Slovenia, Spain, Sweden, Switzerland, Türkiye, the United Kingdom and the United States. The European Commission and the International Atomic Energy Agency also take part in the work of the Agency.

The mission of the NEA is:

- to assist its member countries in maintaining and further developing, through international co-operation, the scientific, technological and legal bases required for a safe, environmentally friendly and economical use of nuclear energy for peaceful purposes;
- to provide authoritative assessments and to forge common understandings on key issues, as input to government decisions on nuclear energy policy and to broader OECD policy analyses in areas such as energy and sustainable development.

Specific areas of competence of the NEA include the safety and regulation of nuclear activities, radioactive waste management and decommissioning, radiological protection, nuclear science, economic and technical analyses of the nuclear fuel cycle, nuclear law and liability, and public information. The NEA Data Bank provides nuclear data and computer program services for participating countries.

COMMITTEE ON THE SAFETY OF NUCLEAR INSTALLATIONS (CSNI)

The Committee on the Safety of Nuclear Installations (CSNI) addresses Nuclear Energy Agency (NEA) programmes and activities that support maintaining and advancing the scientific and technical knowledge base of the safety of nuclear installations.

The Committee constitutes a forum for the exchange of technical information and for collaboration between organisations, which can contribute, from their respective backgrounds in research, development and engineering, to its activities. It has regard to the exchange of information between member countries and safety R&D programmes of various sizes in order to keep all member countries involved in and abreast of developments in technical safety matters.

The Committee reviews the state of knowledge on important topics of nuclear safety science and techniques and of safety assessments, and ensures that operating experience is appropriately accounted for in its activities. It initiates and conducts programmes identified by these reviews and assessments in order to confirm safety, overcome discrepancies, develop improvements and reach consensus on technical issues of common interest. It promotes the co-ordination of work in different member countries that serve to maintain and enhance competence in nuclear safety matters, including the establishment of joint undertakings (e.g. joint research and data projects), and assists in the feedback of the results to participating organisations. The Committee ensures that valuable end-products of the technical reviews and analyses are provided to members in a timely manner, and made publicly available when appropriate, to support broader nuclear safety.

The Committee focuses primarily on the safety aspects of existing power reactors, other nuclear installations and new power reactors; it also considers the safety implications of scientific and technical developments of future reactor technologies and designs. Further, the scope for the Committee includes human and organisational research activities and technical developments that affect nuclear safety.

Acknowledgements

The members of the Nuclear Energy Agency (NEA), the Committee on the Safety of Nuclear Installations (CSNI) and the Working Group on Analysis and Management of Accidents (WGAMA) acknowledge the significant contributions of those individuals who had a key role in the preparation of the summary report, and those who had a leadership role in the conduct and success of the NEA activity *Best Practice Guidelines for the Use of CFD in Nuclear Reactor Safety Applications – 2024 Update*, such as the writing group. Additional thanks are extended to all the task group members who reviewed and contributed to the paper and to Christèle Tephany M'Pania (NEA) for her editorial support.

This document was approved by the CSNI at its 71st session on 30-31 May 2022 (NEA/SEN/SIN(2022)4, not publicly available).

Note: References are at the end of each section, the numbering restarts to 1 at the next section.

Writing group co-ordination

Philippe FREYDIER	EDF, France
Mathieu GUINGO	EDF, France
Stephan KELM	Forschungszentrum Jülich, Germany
Pierre RUYER	IRSN, France

Contributors to the revision

Martina ADORNI	NEA
Ulrich BIEDER	CEA, France
Ingo CREMER	Framatome, Germany
Graham MACPHERSON	Frazer-Nash Consultancy Ltd, United Kingdom
Raksmy NOP	CEA, France
Angel PAPUKCHIEV	GRS, Germany
Krishna PODILA	Canadian Nuclear Laboratories
Dave POINTER	Oak Ridge National Laboratory, United States
Tommi RÄMÄ	Fortum Power and Heat Oy, Finland
Jérôme ROY	IRSN, France
Brian SMITH	Retired from PSI, Switzerland
Juan URIBE	University of Manchester, EDF Energy, United Kingdom
Richard UNDERHILL	Frazer-Nash Consultancy Ltd, United Kingdom
Pascal VEBER	Vattenfall, Sweden
Clément VIRON	IRSN, France
Daniele VIVALDI	IRSN, France
Mingjun. WANG	XJTU, China

Table of contents

List of figures

List of tables

List of abbreviations and acronyms

ADI	Alternative direction implicit
AFM	Algebraic flux model
AHFM	Algebraic heat flux models
AICC	Adiabatic isochoric complete combustion
BCD	Bounded central differencing
BDT	Boron dilution transients
BPG	Best Practice Guideline
CAD	Computer aided design
CD	Central differencing
CEA	Commissariat à l'énergie atomique et aux énergies alternatives (French Alternative Energies and Atomic Energy Commission)
CFD	Computational fluid dynamics
CFL	Courant-Friedrichs-Lewy
CHF	Critical heat flux
CHT	Conjugate heat transfer
CSAU	Code scaling, applicability, and uncertainty
CSM	Computational structural mechanics
CSNI	Committee on the Safety of Nuclear Installations
DDT	Deflagration to detonation transition
DES	Detached eddy simulation
DNS	Direct numerical simulation
ECC	Emergency core cooling
ECCS	Emergency core cooling system
EDF	Électricité de France
ELES	Embedded large eddy simulation
ERCOFTAC	European Research Community on Flow, Turbulence and Combustion
EVM	Eddy viscosity models
FAC	Flow-accelerated corrosion
FDS	Fire Dynamic Simulator
FEA	Finite element analysis
FoM	Figure of merit
FSCK	Full spectrum correlated k
FSI	Fluid-structure interaction

GCI	Grid convergence index
GIF	Generation IV International Forum
GRS	Gesellschaft für Anlagen- und Reaktorsicherheit (German nuclear safety research organisation)
GUI	Graphical user interface
HTC	Heat transfer coefficient
HTGR	High-temperature gas reactors
ICFMP	International collaborative fire model project
IET	Integral effect tests
IR	Importance ranking
IRSN	Institut de Radioprotection et de Sûreté Nucléaire (French Institute for Radiological Protection and Nuclear Safety)
KL	Knowledge level
LBL	Line-by-line
LES	Large eddy simulation
LFR	Lead-cooled fast reactors
LMFBR	Liquid Metal Fast Breeder Reactor
LMFR	Liquid metal-cooled fast reactors
LOCA	Loss-of-coolant accident
LOL	Lower oxygen limit
LS	Level set
MAC	Marker-and-cell
MC	Monte Carlo
MoC	Method of characteristics
MSB	Multi-assembly sealed basket
MSR	Molten salt reactors
NEA	Nuclear Energy Agency
NIST	National Institute of Standards and Technology (United States)
NRG	Nuclear Research and Consultancy Group (Netherlands)
NRS	Nuclear reactor safety
NS	Navier-Stokes
PCA	Permanent Court of Arbitration
PCT	Peak Clad Temperature
PSA	Probabilistic safety assessments
PSI	Paul Scherrer Institute
PTS	Pressurised thermal shock

PWR	Pressurised water reactor
QA	Quality assurance
RANS	Reynolds-averaged Navier-Stokes
RPV	Reactor pressure vessel
RSM	Reynolds stress models
RTE	Radiative transfer equation
SAR	Safety Analysis Report
SAS	Scale adaptive simulation
SFR	Sodium-cooled fast reactors
SGDH	Simple gradient diffusion hypothesis
SMC	Second moment closure
SNAP	Symbolic Nuclear Analysis Programme
SNBCK	Statistical narrow band correlated k
SOR	Successive-over-relaxation
SST	Shear stress transport
TH	Thermal-hydraulic
UPTF	Upper plenum test facility
UQ	Uncertainty quantification
V&V	Verification and validation
VCC	Ventilated concrete cask
VOF	Volume of fluid
WGAMA	Working Group on Analysis and Management of Accidents (NEA)
WSGG	Weighted-sum-of-gray-gases
ZLES	Zonal large eddy simulation

Executive summary

The aim of this second revision of the *Best Practice Guidelines (BPG)* is to provide guidance to the user of computational fluid dynamics (CFD) codes, both novice and experienced, in the field of nuclear reactor safety (NRS). It gives a complete set of guidelines for a wide range of single-phase applications of CFD to NRS problems. The original document, *Best Practice Guidelines for the Use of CFD in Nuclear Reactor Safety Applications* [1] has known two successive revisions, one in 2015 [2], and the present report. Changes are summarised in Annex II.

Computational fluid dynamics (CFD) codes are scientific computing tools that consider explicitly 3-D geometric features while solving momentum, heat and mass balances through a fluid domain. The use of CFD in the field of nuclear reactor safety (NRS) thermal hydraulics has been identified as the most relevant approach for several issues, for which access to data at a local scale can bring a real benefit. The development of CFD codes is fast evolving and their implication in safety assessment studies has been increasing sharply over the past two decades. The specificities of such tools raise the question of adapted methodologies for those studies.

The "Quick guide introduction" at the beginning of this *Best Practice Guideline* (BPG) should be most helpful to novice CFD users as it provides some essential guidelines, avoiding the need to search for them in the entire and (necessarily quite long) BPG document.

This core of the BPG document contains a large set of detailed considerations about the application of CFD for NRS-related studies. This collection of experts' analyses about generic issues covers the whole process of performing a CFD study:

- **Problem definition**, which is the basis for all further steps; the phenomena identification and ranking table (PIRT) approach is a useful tool here.
- **Tool selection**: the most appropriate tool may, or not, be a CFD code; component or system codes can be more appropriate in some cases.
- **Physical models**: for single-phase flows, the choice of a turbulence model is often the most important choice to be made; heat transfer modelling and, when appropriate, fluid-structure interaction modelling may also be important.
- **Numerical settings**: meshing (i.e. discretisation of the spatial domain) is an essential and often time-consuming step in a CFD study.
- **Results interpretation**.
- **Qualification of the tool for the application**:
  - verification (solving the equations correctly).
  - validation (solving the right equations).
  - and uncertainty quantification.
- **Study documentation**.

This is complemented by some more specific considerations focused on a set of applications, either because of the specific physical phenomena that need to be modelled, or because these applications raise the question of coupling CFD with other physics. Gathering all this information in a single reference document is one of the most important results of this activity.

This document can thus serve as a basis for several issues regarding the use of CFD for NRS applications.

First, it can be used to build a rigorous methodology for a CFD-based study by specialists. The document also can be used as a guide for the assessment of the CFD-based NRS study.

As reflected in the document, producing a CFD analysis of an NRS issue implies much more than just generating input data and taking note of calculation results. The main recommendation is clearly to include documentation at each step in the corresponding NRS study. Trusting the result obtained from a CFD simulation implies that several considerations must be addressed. Moreover, although the equations solved come close to describing the elementary physics of fluid flows (closer at least than in more global approaches), a set of models are still required (for turbulence for single-phase flows) that need justifications and analysis of applicability. According to the relatively high computational cost of CFD numerical simulations in industrial configurations, some compromises may have to be considered regarding the accuracy of the solution by optimising the mesh size, for example; this must be compensated by a corresponding analysis of induced errors. For the specific point of uncertainty quantification, the guide provides some generic discussions regarding the issue and references but the current state of the art of CFD studies reveals that methodologies (mainly issued from system scale studies) still require some adaptation to be used without inducing excessive computational efforts in “real” industrial problems.

A future perspective for this activity is a regular updating of the document according to the most recent progress in the field of CFD as well as a potential transformation of the guide into more dedicated guides for specific applications.

References

1. NEA (2007), “Best Practice Guidelines for the use of CFD in Nuclear Reactor Safety Applications”, OECD Publishing, Paris, www.oecd-nea.org/jcms/pl_18444.
2. NEA (2015), “Best Practice Guidelines for the Use of CFD in Nuclear Reactor Safety Applications – Revision”, OECD Publishing, Paris, www.oecd-nea.org/jcms/pl_19548.

A Quick guide introduction

The purpose of this section is to provide a brief introduction to the concepts presented in this best practice document to serve as a checklist for novice users or a refresher for the more experienced analyst. This quick start guide is not a comprehensive manual and is not a substitute for the careful review of the best practices discussed in depth in this document.

Any analysis should be completed as a structured series of documented, repeatable steps. This is especially true for analyses related to safety, with substantial and far-reaching consequences potentially resulting from errors. This guide is therefore structured as a series of steps to be completed as part of an analysis campaign. This guide is intended to be informative to the user and is not a substitute for legal, regulatory or institutional guidance or requirements in your home country, region or institute.

Step 0. Before you begin

In any engineering analysis, the analyst must establish a strategy for the completion of the analysis before work begins. Is your nuclear reactor safety (NRS) analysis a computational fluid dynamics (CFD) problem? How will you document your analysis? How will you document the development of your model? How will you document changes made to the model based on review of the results, benchmarking against other codes, or validation against available data?

In the past several decades, reactor systems and containments have generally been modelled as networks of 0-D and 1D elements. With the fast development of powerful computers and numerical computation methods, the use of CFD methods to solve thermal-hydraulic issues is attracting great attention in the nuclear engineering community. The users should clarify whether the problem encountered is a system-level, meso-scale or micro-scale issue. The users, especially beginners, are suggested to keep in mind that not all the problems can be solved using CFD approaches in NRS analysis.

In modern computing, the use of version control systems to document the changes made to computer code and the reasons for those changes has become standard practice. The use of version control approaches to document the development of CFD models is highly recommended. In engineering analyses, the users may develop a numbering scheme for their files and document their changes in a spreadsheet or text file that they update with each change. Alternatively, the developer of CFD models can implement inline documentation strategies directly if working with the source code or with text-based input files. The spirit of these strategies can be extended to the development of models in interactive user environments by keeping careful notes explaining each option selected as the model is developed. The approach does not matter as much as establishing a structured approach that allows the analyst to be certain that the model is implemented as they believe it to be implemented.

Step 1. Fully define the problem

Before any decisions can be made about the model itself, the problem must be sufficiently well understood and documented to support selection of appropriate methods.

A *Define the computational domain*

An accurate and reasonable description of the geometry of the components or system is essential for a successful CFD analysis. Most often, domain geometries will be defined from computer aided design (CAD) models. For more information see Section 6.2. It is also recommended to reconsider some choices for the possibly simplified or ignored

geometrical details with respect to the work on the identification of the influencing phenomena (see below). Furthermore, the timeframe of the scenario needs to be defined to understand the needs for initial and boundary conditions as well as to obtain an estimate of the overall effort in transient simulations.

B *Define materials and their properties*

Materials which appear in the model must be known and the thermophysical properties associated with each material must be available. Individual properties are commonly defined in CFD models as algebraic equations, lookup tables, or, if appropriate, constant values.

C *Identify quantities of interest*

At a minimum, the analyst should identify the quantities of interest that will be extracted from the simulation, e.g. peak temperature in a material, bulk velocity, pressure drop. If possible, the analyst should identify the locations of data extraction and/or the cross-sectional views that may be desired to facilitate consideration of these positions in the construction of the computational mesh.

D *Identify phenomena*

Before physical models can be selected, the important (with respect to their influence on the quantities of interest) phenomena that are expected to appear in a simulation must be identified. For simple problems, it may be tempting to think that the relative likelihood that a phenomenon is important may be intuitive based on experience. However, it is important to take a rigorous approach that begins with estimation of characteristic non-dimensional parameters such as Reynolds or Rayleigh numbers. For more complex systems or more challenging conditions, the structured approach of the PIRT may be helpful in identifying phenomena to consider. See Section 3.2 for additional information.

E *Define boundary conditions*

The boundary conditions at the defined domain's limits.

<u>Steady state simulations</u>

In steady state simulations, boundary conditions are typically defined as constant values or fixed spatial distributions. Boundary conditions should be based on average data extracted from experiments or other analyses.

<u>Unsteady simulations</u>

Unsteady flows may either arise on their own due to instabilities or flow separation, and/or result from the boundary conditions, reflecting the unsteady fluctuations in flow or thermal conditions at the CFD model boundaries. This can be accomplished in two ways:

1. Direct specification of constant or time-dependent conditions from experimental data or other analyses. In this case, data must be available to support the development of boundary conditions.
2. Unsteady boundary conditions that are dependent upon solved parameters. In this case, the domain must be carefully selected to facilitate the extraction of synthetic boundary condition data. These synthetic data can be for example obtained with precursor simulations or recycling methods.

Step 2. Select an appropriate simulation tool

Once the problem has been completely defined, the correct tool can be selected to deliver an assessment of the desired quantities of interest from a model that adequately represents the expected phenomena. Options may include system codes, component or so-called subchannel codes, or CFD codes of many varieties. An analysis may combine one or more models. For more information on simulation tool options, see Section 4.

As part of the selection of the appropriate simulation tools, it is important to consider the verification and validation (V&V) as well as quality assurance programme associated with the code or software suite to ensure that is proven to be capable of modelling all the identified phenomena within the expected range of application. In case of lacks in the V&V basis, a corresponding assessment must be done by the user prior to the analysis. For more information on code verification expectations, see Section 8.

Step 3. Select physical models

Any selected simulation tool is likely to have a wide variety of physical models that can be selected by the user for application to a particular problem. The analyst will have to select the most appropriate model based on the expected phenomena and conditions in the modelled domain as well as the V&V basis. Four such decisions are discussed below, but others may be necessary depending on the specific details of the defined problem.

A. Turbulence

Steady RANS	*Unsteady RANS*	*Hybrid LES/LES*
All turbulent fluctuations are modelled based on a turbulence closure model using a steady state simulation method. In case instabilities are an important aspect of the simulation, an unsteady solution method can be used to reach a quasi-steady state, which can be averaged in time.	An unsteady simulation method is used, and the computational model has a sufficiently refined mesh resolution in the required areas to directly simulate very large-scale unsteady flow structures such as vortex shedding or wake oscillations, while shear-driven turbulence is mostly modelled by the RANS turbulence model.	LES models always require an accurate unsteady simulation method and sufficiently refined mesh in all the computational domains to resolve most of the turbulence that occurs in the system. A sub grid-scale model is used only to approximate the turbulence contributions from vortex structures smaller than the mesh resolution. With respect to computational efficiency, hybrid methods can be employed that switch from RANS to LES according to the ratio of mesh and turbulence length scales (detached eddy simulation, scale adaptive simulation) or a geometric definition (embedded or zonal LES).

Turbulence may be resolved all the way to the wall if a sufficiently refined mesh is used, with the first cell having a non-dimensional boundary layer thickness less than 1 (i.e. y+ < 1). More often, they may be coupled with a wall function describing near-wall behaviour.	Unsteady RANS models are more likely to resolve turbulence all the way to the wall, but wall functions may still be applied.	LES can resolve turbulence all the way to the wall (wall-resolved LES) but can also be still compatible with wall functions (wall-modelled LES), while DES relies in a URANS solution near the wall.

The selection of turbulence modelling strategy is certainly the most encountered decision facing a CFD analyst and perhaps the most controversial. In this best practice guide, consideration is given to steady Reynolds-averaged Navier-Stokes (RANS) methods, Unsteady RANS, hybrid RANS/LES approaches or full large eddy simulation (LES) methods. direct numerical simulation (DNS) methods are not discussed at length since they are typically limited to small domain analysis and rather simple geometries.

For additional information on turbulence model selection see Section 5.1.

B. Heat transfer

In the development of a CFD model, the analyst must decide which heat transfer phenomena, if any, must be included in the model.

Turbulent heat transfer

In (U)RANS approaches, turbulent heat transport is often modelled using the simple gradient diffusion hypothesis (SGDH) i.e. assuming that an additional turbulent thermal conductivity can be obtained from the eddy viscosity by defining a turbulent Prandtl number. The user must consider the validity of this approach (challenged e.g. for liquid metal flows) and define this model coefficient (usually in the range of 0.7 to 0.9)

Conjugate heat transfer

The second question is often whether conjugate heat transfer between the fluid and solid regions must be simulated. The inclusion of conjugate heat transfer may impose additional requirements on the computational mesh, which are often very specific to the code(s) being used. Analysts should carefully review code documentation for conjugate heat transfer requirements.

Thermal radiation

Nuclear reactor systems and components often experience high temperatures and the contributions of thermal radiation to the total heat transfer may be significant. Even in purely fluid systems, thermal radiation may play a significant role in redistributing energy within the domain and the fluid may be a participating medium. The analyst should confirm the potential significance of thermal radiation through approximate hand calculations.

For additional information on heat transfer modelling see Section 5.2.

C. *Multiphase flows*

This best practice guide primarily addresses incompressible single-phase models, but the guidance provided herein is directly applicable to some multiphase systems and extensible to others. Three common configurations in nuclear systems are discussed here.

Free surface flows	*Spargers or sprays*	*Boiling flows*
Free surface flows have a large interface between a primarily gas phase and a primarily liquid phase. Free surface flows can often be treated as incompressible, and a variety of numerical simulation strategies can be applied, including Lagrangian methods such as front tracking, or Eulerian methods such as volume of fluid (VOF), level set or Arbitrary Lagrangian-Eulerian (ALE) methods. For more information, see Section 5.3.	Spargers inject gas into a primarily liquid volume. Sprays inject liquid into a primarily gas volume. Sparger and spray systems may be treated as if they are free surface problems or in manor more like boiling flows. Selection of modelling strategy should consider the desired quantities of interest and the availability of validation data to support the application. For more information, see [NEA (2010), *Extension of CFD Codes Application to Two-Phase Flow Safety Problems: Phase 2*, www.nea-oecd.org/jcms/pl_18898]	Boiling flows are common in nuclear reactor cores or heat exchangers, depending on the specific design and analysis conditions. Models most commonly use a Eulerian approach with the two-phase flow treated either as a mixture or a two-fluid model with one phase dispersed in the other. For more information, see [NEA (2010), *Extension of CFD Codes Application to Two-Phase Flow Safety Problems: Phase2*, www.nea-oecd.org/jcms/pl_18898]

D. Fluid-structure interaction

Interactions between the fluid flowing through structures and the deformation of structural components themselves are quite common, and the analyst must decide if or how to represent these interactions in their models.

Interactions due to pressure forces	*Interactions due to turbulence*
Flows through nuclear reactor components impose pressure on the surfaces of the solid components. These pressures, especially in impinging flows, may cause deflections of those components. Further, nuclear reactor geometries often have many parallel flow paths, creating different pressures on opposite sides of a structure. Such conditions may result in displacements in that component. The selection of modelling strategy for interactions if this type should consider potential time scales of the interactions. Coupled reduced order models or mesh adaptation strategies may be sufficient to adequately represent the changes in the domain.	Turbulent flows through or across nuclear reactor components may introduce vibration of those components through either impingement or shear. Flow-induced vibration is of particular concern for thin-walled components with high aspect ratios such as fuel rods or heat exchanger tubes. The fluctuating nature of the interaction and the interaction of both the solid and the liquid fields might require a tightly coupled strategy to be employed.

For additional information on best practices in problems exhibiting fluid-structure interactions, see Section 5.4.

Step 4. Develop numerical model

When the problem is well defined and the physical modelling strategy selected, the computational model can be developed. However, important decisions remain for the analyst, including how to represent the geometry with a computational mesh, how to discretise the equations to be solved, and how to define the convergence of the simulation.

A. Mesh development

Development of the computational mesh is often the most time-consuming effort in the development of a CFD model. For the mesh creation, the analyst must be mindful of three major concerns:

1. Is the mesh sufficiently fine to resolve the flow features of interest with the methodology to be applied?
2. Is the mesh consistent with the requirements of the phenomenological models applied, especially the turbulence model?
3. Is the mesh of adequate quality to produce a reliable numerical result?

The first two questions related to resolution adequacy are typically addressed by completing a series of simulations using meshes with different mesh size characteristics and comparing the results. In some cases, to limit the time and computational burden, such tests may be completed on small subdomains that consider only a part of the overall domain geometry. Best practice guidance typically suggests that analysts confirm grid convergence, implying that further refinement of the mesh is not expected to change the results, at least the targeted quantities. This criterion can be difficult to establish for complex geometries or flows with unsteadiness, and even much more challenging if unstructured meshes are used. The solution verification strategies described in Section 8.5 may be applied as a framework for confirmation of mesh adequacy.

The third question related to mesh quality is typically addressed by a series of mesh quality checks (proposed in most CFD codes) that evaluate the individual mesh elements. Computational element characteristics that are evaluated may include (the important characteristics naturally depend on the employed numerical approach):

- angles that are too large or small;
- faces that are too small in area;
- high aspect ratios;
- large discontinuities in the size of adjacent elements;
- specific details associated with the vertex numbering scheme used by the code.

For additional information about mesh development strategies, please see Section 6.2.

B. Discretisation scheme selection

Most modern CFD codes automate the selection of the discretisation scheme based on the physical models activated, but nearly all codes also allow the analyst to override those selections. The selection of the discretisation scheme is always an effort to balance the numerical diffusion error associated with lower order schemes with undesirable oscillatory behaviours associated with higher order schemes. In general, the use of purely first order discretisation schemes should be avoided in unsteady simulations but may be necessary for

convergence in true steady state solutions. Additional information about discretisation schemes can be found in Section 6.3. The solution verification approach described in Section 8.5 can be applied to confirm the acceptability of discretisation scheme selections.

C. Assessment of the model

Once the numerical model has been created, it needs to be independently assessed by a qualified person, who checks e.g.:

- if there is a validation/qualification basis for the use of this simulation tool to model the defined problem;
- if the numerical model accurately represents the defined problem (as specified in Step 1). Are all deviations/assumptions justified?
- if it uses the proper physical models (and their selections justified);
- that this assessment is ideally conducted before the model is used to generate results to avoid that identified shortcoming require changes and re-running the simulation(s).

D. Convergence monitoring

The monitoring of convergence as the simulation progresses is critical to determine whether the simulation result has reached the desired accuracy. In cases where the analytical solution is known, the simulation prediction can be compared directly, and an error calculated. However, this is never the case in industrial CFD applications. More often, consistency and stability are used as a surrogate for accuracy when deciding to stop the iterative solution process.

Nearly all modern CFD codes are developed based on residual form equations where the residual values provide some direct measure of the stability of the solution for that equation. Monitoring of these residuals is a necessary, but often not sufficient, component of convergence monitoring. Since the quantities of interest are known from the careful definition of the problem in Step 1, the progression of these quantities should also be directly monitored for asymptotic convergence to a stable value. Convergence tolerances for both the residuals and asymptotic convergence monitors are specific to the problem of interest and the adequacy of selected targets should be checked by allowing the simulation to further mature and comparing the results. Additional information on convergence controls can be found in Section 6.4. Step

E. Interpretation of results

Interpretation of simulation results calls upon the skills of the analyst to determine whether observed phenomena or conditions align with expected real world behaviours. The review of results often begins with qualitative comparison of predicted flow structures and quantities of interest with analyst expectations. Analysts should carefully confirm that predicted flow and thermal fields are within the limitations of the physical models and the material property models that were used. The location of flow structures for which special mesh resolution regions were developed should be confirmed to ensure that they fall within the anticipated region. Predicted values of non-dimensional scaling parameters such as Reynolds or Rayleigh number should be compared with expected values.

Step 6. Building confidence in the results

Obtaining a successful CFD result is often considered as a victory because of the difficulty of resolving flow fields through large domains with complex geometry that are common to

nuclear reactor safety analyses. However, it is important that a successful model be further exercised to establish confidence in the predictions. Four approaches to building confidence in predictions may be part of this step.

A. Solution verification

Solution verification studies should be completed for every analysis as a de minimis evaluation of the quality of the simulation results. In solution verification, the spatial and temporal discretisation errors are evaluated to approximate the error in the predicted result due to these sources of error. Richardson extrapolation methods are typically applied to calculate an extrapolated solution that is used as the basis for error estimation. Solutions using three or more spatial mesh sizes or time steps are typically required to facilitate the evaluation. Many journals now require or at least recommend the reporting of solution verification results as part of a publication focused on CFD analysis. Additional information on solution verification methods can be found in Section 8.5.

B. Uncertainty quantification

While the analyst has worked to carefully define the problem in Step 1, there are inevitably many uncertainties in the problem specification. Uncertainties in the geometric configuration result from manufacturing tolerances. Material databases have inherent uncertainties that are multiplied by the errors in the algebraic relationships that are fit to the data points. Boundary and initial conditions have at best measurement uncertainties associated with the instrumentation used to evaluate them. They are not always fully specified at the CFD scale and choices for building a full numerical set of conditions may also induce uncertainties. Moreover, the models of physical phenomena or some algebraic constants within those models also provide sources of uncertainties that mostly must be considered with respect to their validation (see below). While the CFD simulation hopefully produces one stable and consistent value for a quantity of interest, all the uncertainties combine to establish a probability distribution that describes likely values for that quantity of interest. A variety of deterministic or stochastic methods can be applied to evaluate the propagation of the uncertainties in the problem definition through the model and establish an uncertainty band around the predicted value. Such campaigns can be computationally expensive but may be essential to understanding the nature of the system. Additional information on uncertainty quantification can be found in Section 10.

C. Code-to-code benchmarking

Many institutions have access to multiple methodologies that are applicable to a problem of interest, or multiple institutions may partner to compare the results from different codes developed and validated by each participant. Such exercises can be useful to find errors in model implementation or identify oversights in code verification. Code-to-code benchmarking can also help to build consensus opinion about the applicability of certain models or methods. Indeed, at its heart, this best practice guide is some form of benchmarking of user experiences. While useful, code-to-code benchmarking is not a surrogate for direct validation of a simulation result against experimental data and CFD analysts should be careful not to assign false confidence in predictions based solely on code-to-code benchmarking.

D. Validation

Validation of simulation predictions against high-quality experimental data or high-fidelity simulations (DNS, wall-resolved LES) is the foundation of confidence in an analysis. In many cases where a CFD analysis is performed, a direct analogue of the problem of interest is not available in an experimental test facility, so direct validation of the problem of interest is often not possible. Instead, the CFD analyst must construct a compelling validation argument from a series of validation tests using experiments or high-fidelity simulations which include characterisation of phenomena relevant to the problem. Validation methodologies are discussed in more detail in Section 9.

1. General introduction

1.1. Report contents

The primary purpose of this report is to provide practical guidance for the application of single-phase computational fluid dynamics (CFD) to the analysis of nuclear reactor safety (NRS). The use of CFD programmes solving Reynolds-averaged Navier-Stokes (RANS) equations on both regular and unstructured meshes will be considered, as well as use of large eddy simulation (LES), and detached eddy simulation (DES). Little will be said about direct numerical simulation (DNS) as it is only practical for a very limited range of applications. There was an attempt in this report to cover the full range of issues associated with a high-quality analysis. This begins with proper definition of the problem to be solved, permitting selection of an appropriate simulation tool. For the probable range of tools, generic guidance is provided on a selection of physical models and on numerical issues including creation of an appropriate spatial grid. To complete the process of analysis, guidance for verification of the input model is also provided, as well as validation of results and documentation of the process.

Although the primary target audience could be less experienced CFD users, the document should be valuable to a wider audience. High-quality CFD analysis is a complex process with many steps, and many opportunities to forget important details. More experienced CFD users should find value in the checklist of steps and considerations provided at the end of the document. Project managers should find the discussion useful in establishing the level of effort for a new analysis. Regulators should find this to be a valuable source of questions to ask those using CFD to support licensing requests.

There are already several other useful documents providing guidelines for the use of CFD. The most notable in reactor safety analysis was produced by the ECORA project [1]. The European Research Community on Flow, Turbulence and Combustion (ERCOFTAC) produced a more general set of guidelines for creation of CFD input models [2, 3]. Similar guidelines were produced specifically for marine applications by MARNET [4]. The AIAA has produced a short guidelines document on verification and validation [5]. More details on verification and validation can be found in a book by Patrick Roache [6], and publications by William Oberkampf and his colleagues at Sandia National Laboratories [7, 8].

This work was intended to be as internally complete as possible and specific guidance that might also be available in the above publications is provided here in the context of NRS and the authors' experience with CFD. However, "internally complete" does not imply that the document is exhaustive. No attempt is made to cover the full history of turbulence theory and modelling, nor the full range of turbulence models available today for CFD applications. For more details on these subjects, a text on CFD is recommended, such as the recent work by David Wilcox [9] or Stephen B. Pope [10].

For any specific application (e.g. mixing in a lower plenum) detailed information can be gathered and recorded on spatial nodalisation, code specific model selection, and experimental basis for validation. The intent is that this report be updated as needed and followed by a series of best practice guideline reports for specific NRS applications.

General overview of the report

After a review of other best practice guidelines, and discussion with many CFD practitioners and developers, guidance has been assembled covering a fully verified and validated NRS analysis. The report begins with a summary of NRS-related CFD analysis in countries represented by the authors, to give a feeling for the existing range of

experience. Some key terminology in the field is defined. These definitions are not meant simply for novices, but also provide experienced users with an understanding of how some terms (e.g. verification and validation) are used within this report.

Chapter 3 deals with definition of the problem and its solution approach. This includes isolation of the portion of the NRS problems most in need of CFD and use of a standard thermal-hydraulic (TH) safety code to provide boundary conditions for the CFD based upon less detailed simulation of the balance of plant. The chapter discusses the phenomena identification and ranking table (PIRT) process, which identifies phenomena critical to the problem, provides a basis for selection of an appropriate simulation tool, and establishes the foundation for the validation process needed for a high level of confidence in the results. The chapter contains an example of application of the PIRT methodology. The chapter also discusses theory and modelling needs associated with several special phenomena important to NRS but not commonly modelled in the CFD community.

Chapter 4 is about the more precise determination of adequate simulation tools, making it possible to justify the need for a CFD approach for a given problem if any, but also addressing the use of CFD as part of the numerical strategy. In this latter case, questions regarding coupling must be addressed.

Chapter 5 discusses the selection of physical models available as user options. As is appropriate for single-phase CFD, most of the emphasis is on selection of turbulence models. Recommendations are provided for a high-level selection between (unsteady) Reynolds-averaged Navier-Stokes ((U)RANS), large eddy simulation (LES), and hybrid approaches such as detached eddy simulation (DES). Specific turbulence models available with each of these approaches are also described. Recommendations are also provided for models associated with buoyancy, heat transfer, free surfaces and fluid-structure interactions.

Chapter 6 focuses on the numerical approximations available to solve the flow equations. Guidelines are provided for nodalisation and for choice of discrete approximations to the differential equations. Guidance is also given on convergence of iterative solutions and numerical techniques for following free surfaces. Results from any simulation must be properly justified.

Chapter 7 discusses the general assessment strategy. Chapter 8 covers approaches to limiting errors associated with discretisation and numerical solution methods (verification). This step is a necessary precursor to quantifying errors associated with physical models (validation) as described in Chapter 9. For a given application case, an uncertainty quantification process must be included in the study and Chapter 10 provides some references. All these steps must, of course, be properly documented both for immediate review and archival purposes. Guidance on documentation is provided in Chapter 11.

Chapter 12 provides some examples of NRS applications. These are not intended as comprehensive illustrations of best practices but illustrate some of these practices for specific NRS applications. The first two examples are boron dilution and pressurised thermal shock. These scenarios have been analysed for many years by a few organisations, and references to some of these other studies can be found in Chapter 1. The third example explores the use of FLUENT for simulation of dry cask storage of spent fuel. This example is highly suited to single-phase CFD analysis.

References

1. Menter, F. (2002), “CFD best practice guidelines for CFD code validation for reactor-safety applications”, European Commission, 5th EURATOM Framework Programme, report, EVOLECORA-D1.

2. Casey, M. and T. Wintergerste (2000), "ERCOFTAC best practice guidelines: Special interest group on 'quality and trust in industrial CFD', Version 1".
3. Casey, M., and T. Wintergerste (2002), "The best practice guidelines for CFD - A European initiative on quality and trust", American Society of Mechanical Engineers, Pressure Vessels and Piping Division (Publication) PVP, v 448, n 1, p 1-10.
4. WS Atkins Consultants (2002), "Best Practices Guidelines for Marine Applications of CFD", *MARNETCFD Report*.
5. AIAA (1998), "AIAA guide for the verification and validation of computational fluid dynamics simulations", *AIAA Report G-077-1988*.
6. Roache, P.J. (1998), "Verification and validation in computational science and engineering", Hermosa Publishers.
7. Oberkampf, W.L. and T.G. Trucano (2002), "Verification and validation in computational fluid dynamics," *Progress in Aerospace Sciences*, Vol. 38, pp. 209-272.
8. Oberkampf, W.L., T.G. Trucano and C. Hirsch (2004), "Verification, Validation and Predictive Capability in Computational Engineering and Physics", *Applied Mechanics Reviews, Vol. 57*, pp. 345-384.
9. Wilcox, D.C. (2006), *Turbulence Modeling for CFD*, Third Edition, DCW Industries.
10. Pope, S.B. (2000), *Turbulent Flows*, First Edition, Cambridge University Press.

1.2. Background of report

In May 2002, an "exploratory meeting of experts to define an action plan on the application of computational fluid dynamics (CFD) codes to nuclear reactor safety problems" was held in Aix-en-Provence, France. The outcome was a recommendation that three writing groups be created to provide recommendations on:

1. Guidelines for use of CFD in nuclear reactor safety applications.
2. Assessment of CFD codes for nuclear reactor safety problems.
3. Extension of CFD codes to two-phase flow safety problems.

The rationale behind this split of efforts was that applications of single-phase CFD were widespread in the nuclear reactor safety (NRS) community and in need of systematic guidelines for use. A need was also identified for an organised and documented collection of appropriate assessment cases. Within the context of NRS, two-phase CFD was considered to still be in its infancy, needing further thought on paths for development and appropriate assessment. The CSNI approved these writing groups at the end of 2002, and work began in March 2003.

The first group's final report was submitted to GAMA in September 2004, summarising existing best practice guidelines (BPG) for CFD, and recommending creation of a BPG document for nuclear reactor safety (NRS) applications. This action was approved by GAMA and CSNI, resulting in the creation of this report.

1.3. History of CFD use in nuclear reactor safety analysis

Systems thermal-hydraulic codes have dominated flow modelling for NRS analysis. However, use of single-phase CFD has already a long history, beginning with specialised codes mainly developed at government laboratories, and expanding rapidly after widespread acceptance of results obtained with commercial and open- source multipurpose CFD packages. Research summaries are provided here for more than historical reasons. References provided in this section are also meant to summarise current worldwide use of CFD in NRS applications, and to give an idea of the existing pool of expertise in the area. However, these summaries simply reflect the experience of the authors of this report. An attempt has not been made in this report to cover activities in all countries concerned with nuclear safety.

2. Terminology

Discussion of terminology must begin with "computational fluid dynamics". At its most general level any computer-based simulation of fluid flow falls in this domain. However, specialists in the field tend to apply two levels of restrictions to use of the phrase. In normal usage CFD implies solution of Navier-Stokes (as opposed to Euler) equations with some special provision for modelling turbulence [1]. With improvements in hardware and software technology, description of a simulation as CFD has also come to normally imply the presence of some sophisticated means of dealing with the problem geometry, usually involving a complex and flexible process for spatial discretisation.

2.1. Spatial mesh

Until recently, CFD tools have tended to work on a regular, logically rectangular mesh. Logically rectangular simply means that you can apply some transformation to the mesh and get a picture that looks like an orderly lattice of rectangular boxes. This mesh class comes in two flavours: orthogonal, where all grid lines meet at right angles; and non-orthogonal, where no restriction is placed on angles between mesh lines. Now, many CFD tools have the capability to work with an unstructured mesh. Common elements here are tetrahedrons, hexahedrons or polyhedrons in 3-D meshes, although mixtures with other geometric cell forms are possible and at times desirable. The primary advantages of an unstructured mesh are the ability to nodalise very complex geometries and better load balancing in parallel calculations. The primary disadvantages of unstructured codes are complexity of software implementations and higher level of errors associated with spatial discretisation.

A third option exists for discretisation of space, overset grid (or Chimera) methods [2]. This technology was largely developed in the United States by the National Aeronautics and Space Administration (NASA) and the Department of Defense (DoD), for analysis of flow past very complex systems, such as the space shuttle. The underlying idea is to break a complex geometry into a collection of much simpler regions. Each region can be resolved with a relatively simple structured mesh, and all meshes have a zone of overlap with their neighbours. One major advantage of the method is the ability to model motion such as rotating turbine blades, changes in position of control surfaces, or manoeuvring of a full body. This capability has also been applied to resolution of vortices shed at trailing edges. The primary disadvantage occurs during development of the portion of the software associated with interpolation of results in the overlap zones between the overset grids.

References

1. Ferziger, J.H. and M. Perić (2002), "Computational Methods for Fluid Dynamics", Third Edition, Springer.
2. Steger, J.L., F.C. Dougherty and J.A. Benek (1983), "A Chimera Grid Scheme", *Advances in Grid Generation*, K.N. Ghia and U. Ghia, eds., ASME FED-Vol. 5, June.

2.2. Turbulence

An early decision in modelling any turbulent flow is the high-level approach to turbulence modelling. Details of this selection are provided in Section 5, but brief definitions of four approaches are provided here as part of basic CFD terminology. Distinctions between the

approaches are based on the standard view of turbulence as a superposition of eddies with a continuous distribution of sizes. Selection of modelling approach is a question of how much of this eddy spectrum is resolved in the direct solution of the Navier-Stokes equations and how much is relegated to special auxiliary models.

2.2.1. Reynolds-averaged Navier-Stokes (RANS)

RANS is most clearly defined in simulations of "steady" flow. The time independent mean flow field is obtained from Navier-Stokes equations, and mean effects of all turbulence are captured in a separate model. In transient simulations, the time averaging imposed on the Navier-Stokes equations is on a large enough scale that everything recognised as turbulence is filtered and must be modelled separately. Nonetheless, unsteady RANS (URANS) enables to resolve large-scale unsteadiness of the flow while modelling the remaining scales.

2.2.2. Direct numerical simulation (DNS)

DNS takes advantage of the fact that turbulence is part of any detailed solution of the Navier-Stokes equation. In this approach a fine enough computational mesh is introduced to resolve all significant scales of turbulence up to the Kolmogorov scale and no special turbulence models are needed. Unfortunately, turbulence theory shows that the ratio of the smallest persistent eddy diameter to the large length scales is roughly proportional to the turbulent Reynolds number to the minus three-quarters power (1/Re3/4). This means that the number of mesh points in 3-D DNS scales like Re9/4 for homogeneous turbulence (neglecting the presence of walls), and only a very limited range of problems, usually on simple geometries, can be solved with DNS on current computers.

2.2.3. Large eddy simulation (LES)

LES is a family of methods that compromise between RANS and DNS. Large-scale eddies are resolved in the flow equation solution, and effects of small-scale eddies are obtained from a special model called sub grid-scale model. This implies a cut-off size in the LES model separating the two scales in the so-called inertial sub-range. The grid refinement is small enough that turbulence models for smaller scales can be significantly simpler than those required for good results with RANS.

2.2.4. Detached eddy simulation (DES)

DES is a further compromise between RANS and LES, to capture key physical phenomena at the lowest possible amount of computer time. A decision is made on spatial regions that are adequately modelled by RANS and those requiring LES. An example is simulation of vortex shedding from the trailing edge of some solid structure, perhaps as part of an acoustic or fatigue analysis. Boundary layers and more far-field flows can be simulated well with RANS. However, a region downstream of the structure would require a finer mesh, and a flag activating LES.

2.3. Verification and validation

When discussing verification and validation (V&V) for a simulation, it is useful to precisely define a few terms. Although there is some variance in definitions within the V&V community, these are generally small. The definitions adopted here were provided by the AIAA [1]. First a specific distinction is drawn between error and uncertainty.

Error - A recognisable deficiency in any phase or activity of modelling and simulation that is not due to lack of knowledge.

Uncertainty - A potential deficiency in any phase or activity of the modelling process that is due to lack of knowledge.

It is also important to distinguish between two types of uncertainties [2]. Aleatory (or stochastic) uncertainty results from a physical process that is fundamentally random. Processes in this class may be totally characterised by known probability density functions, and the only unknown is the state of the random process at any instant. The second class of uncertainty is epistemic and reflects a broader lack of knowledge. One common example is a parameter in a model which is a constant (not stochastic), but for which the value is not precisely known. It is also possible to have unknown information in the specification of a stochastic process (unknown distribution function, unknown mean, unknown variance). In this case the uncertainty is both aleatory and epistemic.

The processes of verification and validation are separated as follows:

Verification - the process of determining that a model implementation accurately represents the developer's conceptual description of the model and the model equations are solved numerically;

Validation - the process of determining the degree to which a model is an accurate representation of the real world from the perspective of the intended uses of the model.

For the user of a CFD code, verification primarily covers quantification of error associated with the selection of mesh, time step, and iteration convergence criteria, and with specification of initial and boundary conditions in an input model. Details of the V&V process are covered in Chapters 8 and 9.

References

1. AIAA (1998), "AIAA guide for the verification and validation of computational fluid dynamics simulations," AIAA Report G-077-1988.
2. Oberkampf, W.L., T.G. Trucano and C. Hirsch (2003), "Verification, validation, and predictive capability in computational engineering and physics", Sandia National Laboratory Report SAND2003-3709, p. 21, February 2003.

3. Problem definition

In this section, two important steps in the problem definition are discussed. The first is a clean isolation of the problem to be analysed and the second is the PIRT (phenomena identification ranking process) process. PIRT was originally defined in the context of classic thermal-hydraulic safety analysis, but the procedures are not specific to that area, and it is gaining acceptance in the wider CFD community. The section is closed with a discussion of considerations of phenomena necessary during the process of problem definition.

3.1. Isolation of the problem

Hitherto, reactor systems and containments have generally been modelled as networks of 0-D and 1D elements. Primary systems have been represented by a series of control volumes, connected by flow junctions; the primary system codes RELAP5, TRACE, CATHARE and ATHLET, for example, are all constructed in this way. The flow conservation equations are applied to the volumes and junctions, and heat transfer and appropriate flow resistance correlations are imposed, depending on the flow regime. It is evident, however, that in some components the flow is far from being 1-D, for example in the upper and lower plenums and downcomer of the reactor pressure vessel (RPV), and to some extent the core region, particularly if driven by non-symmetric loop operation. Natural circulation and mixing in containment volumes are also 3-D phenomena, and several "CFD-type" codes have been specially developed to deal with such flows: for example, GOTHIC, TONUS and GASFLOW. However, the meshes employed are very coarse if compared to CFD standards and rely on correlations rather than resolving boundary layers and underlying physics. Here, the coarse-mesh, system/containment part of the simulation is conveniently delegated as the macro-scale calculation, and the fine mesh, CFD part as the meso- or micro-scale calculation.

A recent example of meso-scale calculation can be found in [1]. Comparative simulations of hydrogen mixing including mitigation in a full containment of type VVER 440/213 for a small break severe accident scenario were carried out with commercial CFD codes and GASFLOW. The CFD meshes were about one order of magnitude higher than that of GASFLOW.

It is inconceivable that CFD approaches will be able soon to completely replace the now well-established system/containment code approach to reactor transients. The number of meshes which would need to be employed would be well beyond the capabilities of present computers, and reliable closure relations for 3- D multiphase situations are still a long way from maturity. Additionally, not readily available CFD code has a neutronics modelling/coupling capability.

A more efficient option would be to perform local CFD computations only where and when a fine mesh resolution is required. The problem with this is that most of the macro-scale phenomena related to safety are transient, and the local meso-scale situation may be strongly influenced by the macro-scale parameters. This means directly interfacing a CFD module to an existing system/containment code to perform a localised 3-D computation within the framework of an overall macro-scale description. This arrangement is attractive since it retains the accumulated experience and reliability of the traditional system/containment code approach but extends their capabilities in modelling meso-scale phenomena. However, the issue of isolating the CFD problem arises, and long transients remain computationally expensive.

Unless there is full coupling between the macro- and meso-scale parts of the simulation, meaning that the CFD computation is carried out throughout the entire system transient, it must be decided whether the coupling between the scales is one-way or two ways.

In the case of one-way coupling (no feedback of the CFD calculation on the macro-scale behaviour), the two calculations can be run independently, with the CFD part of the calculation run in a post-processing mode, with time-dependent boundary conditions supplied by the system/containment calculation. Calculations with a system code usually start from a steady state. When the CFD simulation also starts from the same steady state, the initial conditions for the CFD would be determined from a steady state CFD simulation based upon this initial macro-scale steady state (that is, a steady state is computed with the CFD code using boundary conditions supplied by steady state calculation from the system code). Frequently, however, the CFD simulation starts during the transient, so that this approach cannot be used. Then, a quasi-steady situation should be selected as the initial state for the CFD simulation, and this quasi-steady state is again calculated by the CFD code using corresponding boundary conditions based on the calculation of the system code. Simulations of pressurised thermal shock is a typical example. They usually start at the time when the emergency core cooling system (ECCS) starts to deliver cold water into the primary circuit. At this time, the situation in that part of the primary circuit selected as the computational domain for the CFD simulation does not need to be steady and some conservative assumptions must be adopted (e.g. flow stagnation). Another option would be to start the CFD calculation at an earlier time in the pressurised thermal shock (PTS) transient when some "plateau" in thermal-hydraulic parameters within the selected computational domain is detected in the system calculation. From the point of view of best practice guidelines (BPGs), sensitivity to initial conditions needs to be carried out, the time step for the CFD simulation should be set in accordance with the time variation of the boundary conditions, and an assessment should be made for the validity of assumed flat profiles at the inlets and outlets (using sensitivity studies, if needed). Two-way coupling is more difficult, but some cases could be handled by iteration between the macro-scale and meso-scale computations.

The isolation problem is bypassed if there is full, two-way coupling between the code systems. The disadvantage then is that the meso-scale calculations would have to be performed throughout the transient, even if the 3-D aspects at this scale are not always important, and this brings with it a large CPU overhead and/or restrictions on the number of meshes that could be employed. However, there would be no logistics problem associated with specifying initial conditions: for example, the transient may start from a steady-state flow situation, already established, and known cell-wise, in the 3-D domain. As before, the validity of the 1-D approximations to the velocity, concentration and temperature profiles at the inlets and outlets would need to be examined.

References

1. Huhtanen, R. (Ed) (2005), "Hydrogen management for the VVER-440/213 containment", Phare project service contract No HU2002/000-632-04-01, Final Report, Dec. 2005.

3.2. PIRT

The process of constructing a phenomena identification and ranking table (PIRT) originated as part of the US NRC's code scaling, applicability, and uncertainty (CSAU) evaluation methodology [1]. Phenomena and processes are ranked in the PIRT based on

their influence on the primary safety criteria, and efforts should be focused on the most important points. This process has proven valuable, and its specifications have been broadened over the years [2].

3.2.1. PIRT establishment

The establishment of the PIRT is continuously improved and optimised as the researcher's cognitive level improves [3]. Experts' assessment can be based:

- on calculations and experiments;
- on literature review; and
- on experts' discussion.

The value of PIRT does not lie in the absolute accuracy of results, but in guiding researchers to allocate limited resources to complete the complex research with the acceptable errors.

The establishment of PIRT can be separated in the following steps:

1. *Define the issue* that is driving the need, e.g. a licensing, operational or programmatic issue. The definition may evolve as a hierarchy, starting with federal regulations and descending to a consideration of key physical processes.
2. *Define the specific objectives*. The PIRT objectives are usually specified by the sponsoring agency but should be reviewed for technical accuracy. The PIRT objectives should include a description of the final products to be prepared.
3. *Define the detailed scenario* for which the PIRT is to be prepared. Generally, a specific hardware configuration and specific scenario are specified.
4. *Define the evaluation criterion*. The primary evaluation criterion is the key figure of merit (FoM) used to judge the relative importance of each phenomenon. It must, therefore, be identified before proceeding with the ranking portion of the PIRT effort. It is important that all PIRT panel members come to a common and clear understanding of the primary evaluation criterion and how it will be used in the ranking effort.
5. *Identify, compile, and review* the current knowledge database that captures the relevant experimental and analytical knowledge relative to the physical processes and hardware for which the PIRT is being developed. Each panel member should review and become familiar with the information in the database.
6. *Identify all the possible phenomena*: According to the existing literature and experience, a list of phenomena will be formed by the panel. The phenomena need to be detailed, and there is no need to consider here whether the phenomena affect the evaluation criteria or the current level of cognition in the process.
7. *Develop importance ranking*: After the phenomena have been identified, their importance is ranked based on their effects on each of the identified FoM. Table 3.1 shows the phenomena importance ranking criteria.

Table 3.1. Phenomena importance ranking

Ranking	Description
High(H)	Significant or dominant influence on FoM
Medium(M)	Moderate influence on FoM
Low(L)	Small influence on FoM (including the possibility that the phenomenon is not present or possible)

8. *Evaluate knowledge level:* Determine the knowledge level (KL) of each phenomenon. In this step, the knowledge levels were graded as known (K), partially known (P), and unknown (U). Table 3.2 shows the knowledge level ranking criteria. After the phenomenon importance and knowledge level ranking, those phenomena that need further consideration are then determined. Table 3.3 shows the rules to determine phenomena that need further consideration.

Table 3.2. Knowledge level ranking definitions

Ranking	Description
Known (K)	Phenomenon is well understood and can be accurately modelled
Partially Known (P)	Phenomenon is understood, however, can only be modelled with moderate uncertainty
Unknown (U)	Phenomenon is not well understood. Modelling is currently either not possible or is possible only with large uncertainty

Table 3.3. Determination of phenomena for further consideration

Knowledge Level	Importance ranking (IR)		
	High (H)	Middle (M)	Low (L)
Known (K)	NO	NO	NO
Partially Known (P)	YES	NO	NO
Unknown (U)	YES	YES	NO

9. *Document PIRT results.* The primary objective of this step is to provide sufficient coverage and depth that a knowledgeable reader can understand what was done (process) and the outcomes (results). The essential results to be documented are the phenomena considered and their associated definitions, the importance of each phenomenon and associated rationale for the judgement of importance, the level of knowledge or uncertainty regarding each phenomenon and associated rationale, and the results and rationales for any assessments of extended applicability for the baseline PIRT. Other information may be included as determined by the panel or requested by the sponsor.

3.2.2. An example of PIRT establishment: Flow fields in the lower plenum of M310 PWR

1. *Define the issue*
   The numerous, multi-scale internal structures with complex geometries inside the lower plenum of the reactor pressure vessel have a significant influence on the flow field at the core inlet, which further affects the safety design of nuclear reactors. Therefore, it is necessary to compare the three-dimensional flow fields in the different types of PWR plenums, to increase the understanding of the different internal structures' influence on the flow field, and to provide the guidance for improvement in design of the internal structures. Here, one typical design of the current PWRs, M310, is taken as an example.

2. *Define the specific objectives*
   Generally, the flowrate at the core inlet is designed to be as evenly distributed to provide the same conditions for each fuel assembly. However, the internals inside the lower plenum inevitably affects the flowrate distributions. The objective is to achieve the relationship between the internal structures and flow rate distribution at the core inlet to optimise the diffuser design accordingly in the future.

3. *Define the detailed scenario*
   The study domain includes the downcomer, lower plenum with flow diffuser and the lower part of the reactor core. The study scenario is the normal power generation condition with full and balanced flow rates in the cold legs.

4. *Define the evaluation criterion*
   In this case, one FoM was defined: the difference between the maximum and minimum flowrates through the fuel assemblies at core inlet.

5. *Identify, compile and review the current knowledge base*
   A thorough review and summary of the research status of three-dimensional flow phenomena in the M310 lower plenum, including the related published literature and expert experience, was performed.

6. *Identify all the possible phenomena*
   According to the existing literature and experience, a list of three-dimensional flow phenomena in M310 was set up after the discussion by the expert committee, as shown in Table 3.4 and Figure 3.1.

Table 3.4. List of all flow phenomena inside the M310 lower plenum

Number	**Physical phenomenon**
1	Recirculation flow
2	Flow acceleration along the bottom curvature
3	Obstacle effect from the secondary support structure
4	Flow obstacle effects by the vortex suppression plates
5	Flow straightening and repartitioning

Figure 3.1 The physical phenomena in the M310 lower plenum

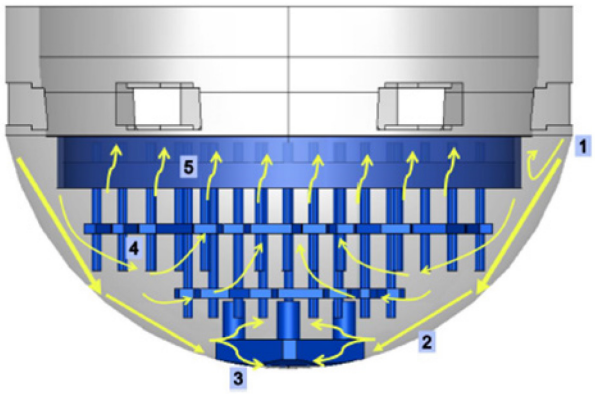

Note: 1- Recirculation flow; 2- Flow acceleration along the bottom curvature; 3- Obstacle effect from the secondary support structure; 4- Flow obstacle effect by the vortex suppression plates; 5- Flow straightening and repartitioning.

7. Develop importance ranking

The importance level of each flow phenomena inside the M310 lower plenum was determined based on its influence on the FoM. The importance levels of flow phenomena inside the M310 lower plenum are summarised in Table 3.5.

Table 3.5. Importance level of each flow phenomena inside the M310 lower plenum

Number	**Physical phenomenon**	**Importance level**
1	Recirculation flow	L
2	Flow acceleration along the bottom curvature	M
3	Obstacle effect from the secondary support structure	M
4	Flow obstacle effects by the vortex suppression plates	M
5	Flow straightening and repartitioning	H

8. Evaluate knowledge level

The knowledge level of each flow phenomena is generally determined based on the corresponding current research status of numerical simulations and related experiments. The knowledge mainly includes the influence of different geometries and local flow phenomena on the global flow characteristics. The knowledge levels of flow phenomena inside the M310 lower plenum are listed in Table 3.6.

Table 3.6. Knowledge level of each flow phenomena inside the M310 lower plenum

Number	**Physical phenomenon**	**Knowledge level**
1	Recirculation flow	P
2	Flow acceleration along the bottom curvature	U
3	Obstacle effect from the secondary support structure	U
4	Flow obstacle effects by the vortex suppression plates	P
5	Flow straightening and repartitioning	U

9. Document PIRT results

The PIRT study results, including the phenomenon definitions, importance rankings, knowledge level rankings, reference parameters regarding the flow phenomena are summarised in Table 3.7.

Table 3.7. The PIRT of flow fields in lower plenum of M310

Number	Physical phenomenon	Importance level	Knowledge level	Reference parameters
1	Recirculation flow	L	P	Expansion ratio
2	Flow acceleration along the bottom curvature	M	U	Curvature of the bottom wall
3	Obstacle effect from the secondary support structure	M	U	Secondary support structure size
4	Flow obstacle effects by the vortex suppression plates	M	P	Vortex suppression plates size Flow hole pattern on the plates
5	Flow straightening and repartitioning	H	U	Flow holes arrangement patterns

Based on Table 3.7 one of the main results is to enforce research on topic five with high importance and low knowledge.

References:

1. Boyack, B. et al. (1989), *Quantifying Reactor Safety Margins: Application of Code Scaling, Applicability, and Uncertainty Evaluation Methodology to a Large-Break, Loss-of-Coolant Accident*, US Nuclear Regulatory Commission Report, NUREG/CR-5249, December 1989.
2. Oberkampf, W.L., T.G. Trucano and C. Hirsch (2004), "Verification, validation and predictive capability in computational engineering and physics", *Applied Mechanics Reviews*, Vol. 57, pp. 345-384.
3. Ball, S.J. et al. (2008), *Next Generation Nuclear Plant Phenomena Identification and Ranking Tables (PIRTs) Vol. 2: Accident and Thermal Fluids Analysis PIRTs*, ORNL/TM-2007/147, Oak Ridge National Laboratory, Oak Ridge, TN.

3.3. Special phenomena, issues

3.3.1. Containment wall condensation

An overview of the containment thermal hydraulics phenomenology can be found in references [1, 2]. It is now recognised that traditional approaches to containment modelling using lumped-parameter models need to be supplemented by 3-D models, and purpose-built "CFD-like" containment codes such as GOTHIC [3], using very coarse meshes (by CFD standards), but with industrial standard turbulence models. Discrepancies remain in validation of these 3-D containment codes, however, and their source cannot always be identified because of lack of detailed information in integral tests. When sufficient computer resources are available, CFD codes, with much finer meshes, have the potential to improve simulation accuracy, but need extended modelling capabilities. A CFD code used for containment simulations must have some provision for condensation of steam on walls or condensers.

Steam condensation in the presence of high non-condensable mass fractions at low gas mass fluxes (i.e. below 2 kg/m^2s) is encountered in the context of passive containment cooling for advanced light water reactors incorporating building condensers. Typical

condenser operating conditions are saturated steam/air mixtures at 110°C with 1 kg/m^3 air partial density on the primary side and boiling water at 100°C on the secondary side.

Two main approaches are available to deal with condensation on the walls of the containment. The first one, described immediately hereafter, relies on a single-phase simulation approach, and requires a specific modelling of the mass transfer of the steam at the wall. The second one, described at the end of the present section, is based on a two-phase approach that is coherent with the modelling of spray systems.

Single-phase approach

It is possible to directly calculate the condensation process from first principles or to introduce empirical models for heat and mass transfer. Both models assume that, in the presence of a non-condensable gas, the thermal inertia and resistance of the condensate layer is negligible and can be ignored. This means that a multi-component, single-phase simulation can be carried out, with the mass transfer of the steam handled by defining it to be at saturation conditions at the wall.

For the direct modelling approach, the computational mesh next to the condensing surface needs to be chosen fine enough for the boundary layer to be resolved in the laminar sublayer ($y^+<4$), where turbulent mass transfer can be neglected [4]. This means that the model has to be used in combination with a low Reynolds number turbulence model, e.g. the k-w SST model. The model may also be used along with a high Reynolds approach; however, it should be clear that the use of wall functions, describing the turbulent momentum, heat and mass transfer can lead to a significant error for strong buoyancy (e.g. mixed convection conditions) or high condensation rates/suction rates. The condensation mass flux to the wall q_m'' is then evaluated from the gradient of the steam mass fraction Y according to Fick's law:

$$q_m'' = -\frac{\rho D}{(1-Y_w)}\frac{\partial Y}{\partial n}$$

in which ρ is the mixture density, D the binary diffusion coefficient, and n is the normal distance from the wall. Saturation conditions are assumed at the wall itself, so that from the local wall surface temperature T_w the partial pressure of steam P_{st} can be found from tables. Since the total pressure is known as one of the local state variables, and stored by the code, the partial pressure of the non-condensable can be derived, and from this the mass fraction of steam at the wall $Y_{w;}$ the mass fraction gradient is assumed linear near the wall and may be determined from differences with local values. The latent heat is extracted from the fluid cell and placed in the wall material (for a conjugate heat transfer problem) to be conducted away internally, while sensible heat transfer to the wall is handled by the code in the normal way. A summary of the modelling assumptions and strategies to implement the model in a CFD code is given in [5]

For the non-local model, fine mesh resolution near the condensing wall is not required, and a suitable mass/heat transfer correlation is used to represent condensation for the mesh cell next to the wall. In principle, any standard heat transfer correlation can be used (e.g. Gido-Koestel [6]), and the mass transfer calculated by dividing by the latent heat at the steam partial pressure. As before, the condensate film is ignored in this treatment. An alternative treatment which employs the turbulent mass transfer coefficient based on the wall function concept rather than a heat transfer correlation is applied in reference [7]. It must be remembered, however, that if a correlation is used, it corresponds to the total heat transfer, including the sensible heat, so this must not be added again by the code. Besides, the

physical modelling involving simultaneously heat and mass transfer using species inter-diffusion, Soret effect and Dufour effect is discussed in reference [8].

Currently, no definite guidelines exist for choosing between use of a correlation or a wall function approach when using a non-local model. The wall function approach has the advantage of being consistent with the rest of the near-wall modelling in the simulation and is simpler to implement. However, a correlation may be more exact in special cases like rough walls or finned tubes, which are not resolved in the mesh. A difficulty with correlations is that they were not derived for local values but for a global or averaged estimation over a total wall and not a tiny piece of it. Therefore, uncertainties arise in calculating required averaged parameters like bulk temperature or height of condensate film along a wall. Care is needed when applying heat transfer correlations to provide a mesh independent calculation and to stay within the limits under which the correlation was derived.

Thus, from the standpoint of best practice guidelines, it is necessary to ensure the following.

The fluid mesh cell next to the condensing surface should be appropriate to the condensing model chosen. Fick's law model should be applied within the laminar sublayer (for concentration) to avoid modelling errors introduced by wall functions, and the correlation model outside the turbulent boundary layer. The concentration gradients tend to be sharper than those for heat and momentum transfer, and consistency checks need to be made that the fluid mesh is appropriate for all transport quantities.

Two-phase approach

A different treatment of the problem relies on the modelling of the condensation by a two-phase flow approach [9]. It has been validated on the experiments COPAIN and TOSQAN ISP47. In particular, the convergence in space as the mesh was refined turned out to be satisfactory. Moreover, whereas in the two former "single-phase" approaches the fluid necessary flows along a fixed wall, a two-phase approach permits modelling of the entrainment of the gas by the condensate that is streaming along the *real* wall. Last, but not least, such a two-phase approach is consistent with a refined modelling of sprays (the sprays and the condensate streaming on the walls can be handled simultaneously within a single approach and a single code).

References

1. Studer, E. et al. (2020), "Challenges in containment thermal hydraulics", *Nuclear Technology*, Vol. 206, pp. 1361-1373.
2. Kelm, S., H. Müller and H.-J. Allelein (2019), "A Review of the CFD modelling progress triggered by ISP-47 on containment thermal hydraulics", *Nuclear Science and Engineering*, Vol. 193(1-2), pp. 63-80.
3. George, Th. L., et al. (1997), *GOTHIC containment analysis package - User Manual. Numerical Applications*, Inc., NAI 8907-02 Rev. 7, prepared for EPRI (RP4444-1).
4. Smith, B.L., M. Milelli and S. Shepel (2003), "Aspects of nuclear reactor simulation requiring the use of advanced CFD models", IAEA-TECDOC-1379, *Proceedings of a joint technical meeting IAEA and OECD/NEA on Use of Computational Fluid Dynamics Codes for Safety Analysis of Nuclear Reactor Systems, Pisa (Italy),* 11-14 November 2002.

5. IAEA (2003), TECDOC-1379, *Proceedings of a Joint Technical Meeting IAEA and OECD/NEA on Use of Computational Fluid Dynamics Codes for Safety Analysis of Nuclear Reactor Systems, Pisa (Italy),* 11-14 November 2002.
6. Vijaya Kumar, G. et al. (2021), "Implementation of a CFD model for wall condensation in the presence of non-condensable gas mixtures", *Applied Thermal Engineering, Vol. 187*, 25 March 2021, doi.org/10.1016/j.applthermaleng.2021.116546.
7. Gido, R.G. and A. Koestel (1983), "Containment condensing heat transfer", *2nd International Topical Meeting on Nuclear Reactor Thermal-Hydraulics (NURETH-2),* Santa Barbara, CA, United States, 11-14 January 1983.
8. Dehbi. A. (2013), "On the adequacy of wall functions to predict condensation rates from steam-noncondensable gas mixtures", *Nuclear Engineering and Design,* Vol. 265, December 2013, pp. 25-34.
9. Jian, N., E. Studer and B. Podvin (2020), "Physical modelling of simultaneous heat and mass transfer: species interdiffusion, Soret effect and Dufour effect", *International Journal of Heat and Mass Transfer*, Vol. 156.
10. Mimouni, S., A. Foissac, and J. Laviéville (2011), "CFD modelling of wall steam condensation by a two-phase flow approach", *Nuclear Engineering and Design*, Vol. 241, pp. 4445-4455.

3.3.2. Pipe wall affected by flow-accelerated corrosion

Flow-accelerated corrosion must be distinguished from erosion-corrosion because the fundamental mechanisms for the two corrosion modes are different:

- **Flow-accelerated corrosion** (FAC) is a corrosion mechanism in which a normally protective oxide layer on a metal surface dissolves in fast flowing water. The underlying metal corrodes to recreate the oxide, and thus the metal loss continues.
- **Erosion-corrosion** is a degradation of material surface due to mechanical action. The mechanism can be described as follows: (1) mechanical erosion of the material, or protective (or passive) oxide layer on its surface; (2) enhanced corrosion of the material if the corrosion rate of the material depends on the thickness of the oxide layer.

The secondary circuit of a PWR is usually made of carbon steel. FAC on a pipe wall can bring about wall thinning of secondary piping to an extent that the pipe wall thickness reaches the minimum thickness required by the design criterion. This phenomenon has resulted in severe piping ruptures at the Surry nuclear plant in 1989 and the Mihama plant in 2004. FAC is a form of localised attack that occurs in areas where the turbulence intensity at the metal surface is high enough to cause disruption of the normally protective oxide surface film.

Programmes for inspecting pipe wall thinning exist at all plants. Inspection locations are generally established in accordance with the inspection programme guidelines of each country. The inspection frequency for pipe wall thickness measurements is based on a combination of predicted and measured FAC rates. Kastner's correlation [1] has been mostly used as the prediction formula of the thinning behaviour of carbon steel piping by FAC. It should, however, be noticed that this formula only estimates the maximum amount of thinning and gives no information on its distribution.

Detailed ultra-sonic wave measurements of the distribution of pipe wall thinning were performed after the Mihama accident to find the causes of the pipe rupture in one of the secondary flow circuits (the rupture was in the condensate system, upstream of the feed-water pumps) and to elucidate the phenomenon. The 3-D turbulent flow in the secondary cooling system of the Mihama Plant has been analysed by modern CFD codes to simulate the measured distribution of thinning [3].

An investigation of the relation between the calculated values of turbulence intensity and the thinning obtained by the Kastner's correlation revealed that the calculated kinetic energy of turbulence near the pipe wall surface would have good correlation with the wall thinning.

The measured thinning distribution on the pipe wall downstream of the orifice agreed well with the calculated distribution of turbulent kinetic energy near the wall surface by the CFD codes. This 3D-CFD calculation was extended to the full secondary piping system to study the reasons for the enhancement in the wall thinning in one plant secondary loop (A-loop) relative to that in another loop (B-loop) and found the following differences of flow pattern in A and B piping:

- Strong counter-clockwise rotating flow was generated in the first elbow of A-loop piping.
- Weak clockwise rotating flow was generated in the first elbow of B-loop piping.

These differences caused the different circumferential distribution of calculated turbulence energy near the wall surface behind the orifices of the A and B loops. The distribution of calculated turbulent energy was found to have some similarities to the measured wall thinning distribution. Both showed uneven distribution in the A-loop, and uniform distribution in the B-loop.

Experience analysing the Mihama accident has produced several specific guidelines for application of CFD to this class of problem. The coolant in the secondary piping system at normal operation is considered to flow in a steady turbulent condition. The standard k-ε turbulent model can provide satisfactory results for calculating this flow. However, the scaled test performed after the Mihama accident revealed oscillating and twisting flow in the A-loop. This required transient analysis using LES to model the turbulent flow.

A standard wall function is applicable to the steady turbulent flow of normal operation. However, for the observed oscillatory flows a non-slip boundary condition with fine mesh near the wall using the low Reynolds number turbulence models or wall-resolved LES models may be better than wall function. This would provide high accuracy evaluation of turbulent kinetic energy near the pipe needed for evaluation of wall thinning by FAC. The same is also true for RSM.

Special consideration must also be given to spatial discretisation. The shape of roundness of the corner in pipe junctions should be exactly reflected in the calculation grid because details of the junction shape have a strong effect on the flow dynamics.

References

1. Kastner, W. et al. (1990), "Calculation code for erosion corrosion induced wall thinning in piping systems", *Nuclear Engineering and Design*, Vol. 119, pp. 431- 438.
2. Morii, T., H. Terasakaand and E. Hirano (2000), "Benchmark Analysis of Rapid Boron Dilution Transient by the PLASHY Code", (in the frame of the OECD Int. Standard Problem ISP-43 for code assessment on rapid boron dilution transients),

Proceedings of the NTHAS2 Conference (second Japan-Korea symposium on nuclear thermal hydraulics and safety), Fukuoka (Japan), 15-18 October 2000, pp. 625-632.

3. Kansaï Electric Power Company (KEPCO), Mitsubihi Heavy Industry (MHI) (2005), Appendix 4 of the *Final report on the Secondary Piping Rupture Accident at Mihama Power Station, Unit 3 of the Kansai Electric Power Co., Inc.,* (in Japanese), report of the Ministry of Economy, Trade and Industry, Japan.

3.3.3. Thermal cycling

Thermal striping (presence of high-frequency thermal fluctuation on the inner surface of a component) can be the cause of the propagation of deep cracks in the component wall. Failures of parts of structures of nuclear power plants caused by thermal fatigue have been experienced at Civaux (France), Genkai Unit 1 (Japan), Tihange Unit 1 (Belgium), Farley Unit 2 (United States), the Dounreay Prototype Fast Reactor (United Kingdom), Tsuruga Unit 2 (Japan), and Loviisa (Finland). Thermal striping is a complex phenomenon involving several fields of science: thermal hydraulics (which can produce the thermal fluctuations), stress analysis (which can transform the thermal loads into mechanical stresses), and science of materials (which can describe the effects of mechanical stresses on behaviour of cracks). Therefore, multi-physics coupling of codes is required.

In thermal-hydraulic analysis of thermal fatigue it is necessary to know how different frequencies and amplitudes of time-dependent mechanical stress affect crack propagation to evaluate the suitability of a selected computational model to analyse the problem of thermal fatigue. Based on experience described in Chapuliot et al. [1], the frequency range from 0.1 Hz to 10 Hz should be studied. The upper bound of frequencies (10 Hz) is also found in Ref. [3]. Higher frequencies are not so dangerous from the point of view of crack propagation (but it is not so clear from the point of view of initiation).

Thermal fluctuations of various frequencies and amplitudes can be caused by vortex shedding, turbulence, or by large-scale instabilities or unsteadiness like pulses, pump fluctuations and gravity waves. Some low-frequency fluctuations depend on geometry and even of the plant-specific conditions which may cause problems with selection of the computational domain and formulation of boundary conditions. Critical geometries are represented mainly by T-junctions, valves and parallel jets (e.g. in upper plenums). Simulation approaches can be based on RANS, U-RANS or on LES/VLES/DES models. For RANS cases the unsteady nature is implicitly modelled, and so additional approximations are needed to recreate the instantaneous thermal fluctuations and their corresponding frequencies and amplitudes. Some unsteadiness can be observed when U-RANS is used; however, this smooth sinusoidal form for temperature fluctuations does not include the effects due to higher frequency small-scale turbulence. There are simulations using a “pseudo-DNS calculation”, that is, using the assumption of unsteady laminar flow with fine grids and small-time steps (but not sufficiently fine enough to be considered as a true DNS). As a general statement, it may be concluded that the use of U-RANS remains questionable and that more validation is required, while LES still appears as the most reliable approach, at least at moderate Reynolds numbers.

Validation of computer codes for simulation of thermal stripping is limited by the fact that suitable experimental data are scarce, although new data have recently been produced, for velocity measurements (e.g. Vattenfall [4, 5]). On real plants, temperatures (or deformations) of the solid walls are measured predominantly at the outer surfaces of conduits. Temperature fluctuations are damped by wall conduction as demonstrated analytically by Kashahara [2], so the measured amplitudes are small, which can lead to large uncertainties.

Ref. [3] makes the following recommendations based on solution of a benchmark problem (T-junction of a Liquid Metal Fast Breeder Reactor (LMFBR) secondary circuit):

- The range of the damaging frequencies from the wall thickness should be determined first (frequencies lower than this band do not produce sufficient ΔT across the wall, and frequencies higher than this band cannot penetrate the wall).
- The duration of the transient simulation should be deduced from the lower bound of the range, considering that the transient duration should cover at least ten periods of this low frequency (after statistical convergence).
- The time step of the computation must be small enough to resolve oscillations at the higher bound of damaging frequencies (at least half of the period corresponding to the highest frequency).
- Since realistic boundary conditions should be used and there are some limitations such as the size of the computational domain, the boundary conditions should include possible secondary flows (e.g. swirl flow) and low-frequency variations of temperature and/or velocity (boundary condition sensitivity analyses are a good practice).
- Transient simulations using a large eddy simulation model are recommended, with properly designed unsteady inlet conditions.
- The discretisation schemes must be at least of second order in space and in time.
- Care must be taken when applying the transient heat transfer coefficient to the computational mesh adjacent to the wall. The heat transfer coefficient links high-frequency fluid temperatures with solid temperatures that have been subjected to an induced filter of the high.

References

1. Chapuliot S. et al. (2005), “Hydro-thermal-mechanical analysis of thermal fatigue in a mixing tee”, *Nuclear Engineering Design*, Vol. 235, pp. 575-596.
2. Kasahara N. (2002), “Thermomechanical and fracture mechanics analysis on a Tee junction of LMFBR secondary circuit due to thermal striping phenomena”, IAEA-TECDOC-1318, pp. 89-116, November.
3. IAEA (2002), “Validation of fast reactor thermomechanical and thermohydraulic codes”, IAEA-TECDOC-1318, p. 13, November.
4. Westin, J., et al. (2006), “Experiments and unsteady CFD-calculations of thermal mixing in a T-Junction”, *Proceedings of the Benchmarking of CFD Codes for Application to Nuclear Reactor Safety (CFD4NRS),* Garching, Munich, Germany, 5-7 September 2006 (CD-ROM).
5. Odemark, Y., T. Green, K. Angele, J. Westin, F. Alavyoon and S. Lundström (2009), “High-cycle thermal fatigue in mixing tees: New large-eddy simulations validated against new data obtained by PIV in the Vattenfall experiment”, *Proceedings of ICONE 17*, Brussels, 12-16 July 2009.

3.3.4. Hydrogen explosion

The hydrogen-air reaction has the potential to threaten containment integrity or any other equipment in a nuclear power plant. Hydrogen becomes an issue during severe accidents with considerable gas releases mainly by oxidation of fuel cladding. Under design basis accident conditions, releases of hydrogen are considerably lower. During normal operation,

radiolysis of water produces some hydrogen as a stoichiometric mixture with oxygen. To preserve containment integrity under all conditions or to avoid hydrogen combustion at all, several mitigation strategies were developed. These include inertisation (BWR), dilution, installation of catalytic recombiners or the use of igniters. Underlying physical and chemical processes of hydrogen combustion including modelling approaches are rather complex and are dealt with in detail in reference [1].

Hydrogen combustion

The nature of hydrogen production and release determines the possible forms of hydrogen combustion. Hydrogen mostly appears in lean (under-stoichiometric) mixtures together with air and steam and may accumulate non-uniformly in clouds (premixed combustion) in the containment. The dimensions of a containment are too big and too complicated to investigate hydrogen combustion experimentally in full scale. All known experimental facilities have either much smaller dimensions or they address only selected aspects of hydrogen combustion. In the nuclear context, any modelling approach must pay special attention to scaling aspects from experiments at reduced scale, to full size, and to give geometric complexity.

Hydrogen combustion can occur as deflagration or detonation including a transitional process called DDT (deflagration to detonation transition). Deflagrations are the most common combustion mode and may range from slow deflagrations (flame speeds below 100 m/s) to fully accelerated turbulent combustion with flame speeds up to 1 000 m/s. The release of hydrogen may be continuous with occasional combustion events. In this case a standing flame close to the gas release source can also develop.

For assessment of containment integrity, temperature and pressure loads including pressure differences between compartments are of primary interest. Most models concentrate therefore on these parameters. This requires the correct prediction of flame propagation mechanisms (branching) and flame speeds. For deflagrations it can be shown that reaction kinetics is much faster than the mixing processes bringing reaction partners together. The most common CFD modelling approach simply addresses the mixing process and assumes infinitely fast chemical kinetics. This concept is called the Eddy break-up model and was introduced by Magnussen and Hjertager [2]. The reaction rate is defined by:

$$R = -\rho * \frac{\varepsilon}{k} * C * M_{\text{lim}} \quad (1)$$

with:

ρ - density

k,ε - turbulent energy and dissipation rate

C - numerical constant

M_{lim} describes the presence of fuel, oxidiser and products respectively, weighted by the stoichiometric relations within the reaction. The influence of products (water vapour) can be switched on or off by the factor B in eq. (2). The constant C must be fitted to experiments. There is a direct proportionality of the reaction rate to the inverse turbulent time scale defined by k/ε. This creates a mesh dependency of the reaction rate and calls for careful validation of the model. For the factor C, several modifications and extensions have been proposed. These are focused on local extinction of the reaction if turbulence becomes locally too high or on a reduction of the dependency on spatial resolution by introducing the laminar burning velocity [3]. Scaling of the Eddy break-up model from experimental

level to full-scale containment application must be made with great care. If possible, the mesh resolution relative to existing length scales should be preserved between experiment and application.

Recent commercial CFD codes also offer other modelling options for simulating premixed hydrogen deflagrations. Among these are flame front or pdf (probability density function) models. A promising approach is the combination of a flamelet pdf model with a turbulent burning speed closure. The numerical effort is however strongly increased compared with the Eddy break-up or Eddy dissipation formulation, which often prohibits their application to containment scale. A comparative application of several combustion models in a large simplified EPR containment can be found in [4] and in [5].

A general weakness of existing models is the completeness of combustion. Models consume all hydrogen, but this is in contradiction to experimental findings, which have always detected a low percentage of remaining unreacted hydrogen (about 0.5 to 0.8 vol.%).

Whatever the model, however, a general comment for the prediction of deflagration is that the CFD approaches for modelling turbulent combustion in this kind of application still need improvement and have a high degree of uncertainty. Hence, a careful analysis by experienced users is required for nuclear safety studies.

The transition from deflagration to detonation (DDT) cannot be predicted to date. But assuming a stable detonation is much easier to calculate and shows comparable loads. In the case of a detonation, it is not necessary to care about turbulence levels because the reaction is determined by the chemical reaction kinetics. Detonation algorithms are much simpler than for deflagration and computing times are rather short (about one order of magnitude shorter than for deflagrations).

For some applications it is enough to calculate AICC (adiabatic isochoric complete combustion) pressures, the potential of a mixture to create an accelerated deflagration (expansion ratio or sigma criterion) or the principal possibility of a detonation (7-lambda criterion). All these parameters are conservative and do not need much computational effort.

Mitigation strategies

There exist several options to reduce or avoid the potential consequences of hydrogen combustion [6]. Inertisation of possible release areas by either nitrogen or CO_2 makes any combustion impossible. Dilution is designed to avoid the transition to detonation. It needs less additional mass to be injected into the containment and produces hence less extra pressure built-up. Both options can be simulated by basic features of recent CFD codes. The choice of the turbulence model will be important. In view of the large geometric dimensions and long simulation times only two equation models have long been reported to be the only feasible approaches. Recent developments, however, demonstrate that second order models may be used as a standard option in complex geometries for single or two-phase flow approaches [7,8]. BPG for turbulence should be followed as much as possible to obtain predictable simulations.

Another option is the implementation of catalytic recombiners in the containment or in parts of the primary circuit to recombine hydrogen back to water in a smooth way. These have been installed or are planned for most PWR containments. These recombiner systems can be designed to cover hydrogen releases for design basis accidents or to reduce remaining loads in a severe accident.

A model of the processes ongoing in a catalytic recombiner needs to include the catalytic surface reactions (Arrhenius formulation), diffusion and convection of species, heat

conduction in solids and thermal radiation. An example of a CFD model can be found in [9]. If only the impact of recombiners in terms of hydrogen management in a containment has to be estimated, a much more simplified model can be used which can be easily implemented in any CFD code.

Finally, it is necessary to indicate the option relying on the use of spray systems that prevent overpressure in case of a steam break and enhance the gas mixing in case of the presence of hydrogen. In that case, the main phenomenon to deal with is not the turbulence created by natural convection but that resulting from the spray itself. The modelling still seems to be an open issue, regarding the influence of the droplets on the turbulence of the gas flow field, which is important since the thermodynamic effect of the spray system and the turbulence may have opposite effects on the Hydrogen combustion risk.

References

1. NEA (2000), *Flame Acceleration and Deflagration to Detonation Transition in Nuclear Safety*, SOAR, OECD Publishing, Paris, www.oecd-nea.org/jcms/pl_17424.
2. Magnussen, B.F. and B.H. Hjertager (1976), "On mathematical modelling of turbulent combustion with special emphasis on soot formation and combustion" *Sixteenth Symp. (Int.) on Combustion*, The Combustion Institute, p. 719.
3. Said, R., and R. Borghi (1988), "A simulation with a cellular automation for turbulent combustion modelling," *22nd Symposium (Int.) on Combustion*, University of Washington - Seattle, United States, pp. 569-577.
4. Baraldi, D., et al. (2003) "Application and assessment of hydrogen combustion models", *The 10th Int. Topical Meeting on Nuclear Reactor Thermal Hydraulics (NURETH-10),* Seoul, Korea, 2003.
5. Baraldi, D., M. Heitsch, and H. Wilkening (2005), "CFD investigation of hydrogen combustion in a simplified EPR containment with CFX and REACFLOW," *The 11th Int. Topical Meeting on Nuclear Reactor Thermalhydraulics (NURETH-11),* Paper 483, Avignon, France.
6. NEA (2014), *Status Report on Hydrogen Management and Related Computer Codes*, Nuclear Safety, OECD Publishing, Paris, www.oecd-nea.org/jcms/pl_17424.
7. Mimouni, S. et al. (2010), "A second order turbulence model based on a Reynolds stress approach for two-phase boiling and application to fuel assembly analysis", *Nucl. Eng. And Design*, Vol. 240.
8. Mimouni, S. et al. (2008), "Modelling of sprays in containment applications with a CMFD code", *Proceedings of the workshop on experiments and CFD code applications to nuclear reactor safety XCFD4NRS-2,* Grenoble, France, 10-12 September 2008, pp. 2260-2270.
9. Reinecke, E.-A. et al. (2016), "Validation and application of the REKO-DIREKT code for the simulation of passive autocatalytic recombiner operational behaviour", *Nuclear Technology,* Vol. 196, doi.org/10.13182/NT16-7.

3.3.5. Fire analysis

A variety of fire modelling tools employing different features are currently available. The most appropriate model for a specific application often depends on the objective for modelling and fire scenario conditions. Fire models have been applied in nuclear power

plants in the past to predict environmental conditions inside a compartment room of interest. The models typically try to estimate parameters such as temperature, hot smoke gas layer height, mass flow rate, toxic species concentration, heat flux to a target, and the potential for fire propagation in the pre-flashover stage compartment fire.

Fire models are generally limited by their intrinsic algorithms and by other factors impacting the range of applicability of a given model feature. These features are inherent in the model's development and should be taken into consideration to produce reliable results that will be useful in decision-making.

The engineer must bear in mind that most fire models were developed for general application and not specifically for the conditions and scenarios presented in nuclear power plants. A fire model's features and ability to address these conditions should be considered when selecting an appropriate fire model. These considerations affect the accuracy or appropriateness of the fire dynamics algorithms used for a unique analysis of a given space. The conditions can include but are not limited to the following:

- types of combustibles and heat release rates;
- types and location of ignition sources;
- the quantity of cables in cable trays and other in situ fire loads in compartments;
- location of fire sources with respect to targets in the compartments;
- high-energy electrical equipment;
- ventilation methods;
- concrete building construction, large metal equipment, and cable trays that will influence the amount of heat lost to the surroundings during fire;
- compartments that vary in size but typically have a large volume with high ceilings;
- transient combustibles associated with normal maintenance and operations activities.

Techniques used to model the transfer of energy, mass and momentum associated with fires in buildings fall into three major categories.

- Single equations: used to predict specific parameters of interest in nuclear power plant applications such as adiabatic flame temperature, heat of combustion of fuel mixtures, flame height, mass loss rate, and so forth. These equations can be steady state or time-dependent. The results of the single equation can be used either directly or as input data to more sophisticated fire modelling techniques.
- Zone models: assume a limited number of zones, typically two or three zones, in an enclosure. Each zone is assumed to have uniform properties such as temperature, gas concentration, and so forth. Zone models solve conservations equations for mass, momentum, energy, and in some examples, species. However, zone models usually adopt simplifying assumptions to the basic conservation equations to reduce the computational demand for solving these equations.
- Field models: field or computational fluid dynamics (CFD) models divide an enclosure into large number of cells and solve the Navier-Stokes equations in three dimensions of the flow field. CFD models also require the incorporation of sub-models for a wide variety of physical phenomena, including convection, conduction, turbulence, radiation and combustion. The resulting flows or exchange of mass, energy, and momentum between computational cells are determined so

that the three quantities are conserved. Accordingly, CFD models need intensive computational power, but these models can be run on high-end PC computers. The CFD models can provide detailed information on the fluid dynamics of an enclosure fire in terms of three-dimension field, pressure, temperature, enthalpy, radiation, and turbulent kinetic energy. These models have been used to model a variety of complex physical phenomena such as the impact of a suppression system (e.g. a sprinkler system or water mist system) on a specific type of fire, or smoke movement in a large compartment with complex details such that detection can be optimised. CFD models can provide a fundamental understanding of the flow field models for known compartment geometry, along with the physical phenomena that interact with the flow field.

Fire differs significantly in its behaviour from other fluids and gases due to its complex chemical, thermal and turbulent behaviour, and interaction. Because of this complexity, any simulation tool must be capable of handling the chemical reactions; the turbulent flows and radiative and convective heat transfer within the analysis. Fire suppression using mist-spray is an additional factor to consider when choosing a CFD tool to analyse fire.

FLUENT, STAR-CD and CFX are among the commercially available software that include modelling capabilities to deal with the complex nature of fire physics. Besides fireFOAM [1], Fire Dynamic Simulator (FDS) [2], developed, maintained, and freely distributed by the National Institute of Standards and Technology (NIST), is also capable of modelling fire growth and suppression. The drawback with FDS is its limited choice in the type of configuration it can deal with. FDS solves the conservation equation in rectilinear coordinates only and is not designed to handle geometries with curves. Also, the only available models to treat turbulence are LES with the Smagorinsky family SGS models (standard, dynamic, WALE) and DNS. For chemical reactions FDS uses a mixture fraction combustion model. The model assumes that combustion is mixing-controlled, and that the reaction of fuel and oxygen is infinitely fast, regardless of the temperature. If the fire is underventilated, fuel and oxygen may mix but may not burn. Also, the user must provide the products of the reaction that are difficult to estimate. For most cases, the user assumes complete combustion and relies on yield ratios for smoke and other constituents which are usually unavailable especially if one is dealing with incomplete reaction which is the case in most fire simulations. In the calculation of surface heat flux combined with LES, FDS uses ad hoc correlations of both natural and forced convection. This approximation will have a major effect on the prediction of heat flux to the walls and targets which are important parameters to the fire analysis. For more information on this model, visit www.nist.gov.

To evaluate the capabilities of fire models for nuclear power plant applications, the International Collaborative Fire Modeling Project (ICFMP) was organised. The objective of the project is to share the knowledge and resources of various organisations to evaluate and improve the state of the art of fire models for use in nuclear power plant fire safety and fire hazards analysis. The project is divided into two phases. The objective of the first phase is to evaluate the capabilities of current fire models for fire safety in nuclear power plants. The second phase will implement beneficial improvements to current fire models that are identified in the first phase and extend the validation database of those models. Currently, 22 organisations from 6 countries are represented in the collaborative project.

So far, this organisation has formulated five benchmark exercises. These were intended to simulate a basic scenario defined in sufficient detail to allow evaluation of the physics modelled in the fire computer codes. An assessment of appropriate input parameters and assumptions, interpretation of results, and determination of the adequacy of the physical sub-models in the codes for specific scenarios will establish useful technical information

regarding the capabilities and limitations of the fire computer code. Uncertainties in the predictions based on validations of each code will provide a basis for the confidence on the set of results developed in the exercise.

As with any flow simulation, guidelines must be followed to choose the grid to correspond to the appropriate chosen turbulence model. Additionally, the grid must satisfy a grid-independent solution to obtain the correct heat flux and temperature to the targets.

The right reaction model must be chosen to correctly simulate the oxidation kinetics of the fuel and the inclusion of the effect of turbulence. A lower oxygen limit (LOL) is used in many of the models to simulate the under-ventilation and extinction of the fire. The specification of LOL has a large effect on the prediction of the extinction and could be a large source of user effects.

Ventilation systems should be modelled correctly, as the flow pattern from mechanical ventilation systems will affect the temperature in local areas and will be a source of uncertainty.

A correct and robust radiation model is required to assess heat flux to the walls and targets from fire.

[1] OpenFOAM: User Guide: fireFoam, www.openfoam.com/documentation/guides/latest/doc/guide-applications-solvers-combustion-fireFoam.html, last accessed 13 June 2024.

[2] McGrattan, K., R. Mc Dermott, M. Vanella and E. Mueller (2024), *Fire Dynamics Simulator, User's Guide*, National Institute of Standards and Technology, United States, http://dx.doi.org/10.6028/NIST.SP.1019.

3.3.6. Water hammer

There is a long history of water hammer analysis, beginning with simple back-of-the-envelope calculations, which do a reasonable job estimating peak pressures. One-dimensional analysis generally provides quite good simulation of the initial pressure wave propagation, and usually works well for checking equipment against peak loads. Classic thermal-hydraulic safety codes have been successfully used for such analysis. However, one-dimensional analysis tends to under-predict decay of the peak pressure over relatively long transients (very long piping runs and/or multiple wave reflections). One major reason is the development of asymmetric flow instabilities [1, 2], which must be captured with multidimensional (CFD) flow simulations. A recent summary of water hammer analysis and experiments has been provided by Ghidaoui et al [3].

Unfortunately, because of the practical success of 1-D analysis, and the expense of full CFD calculations, there is insufficient CFD experience to provide specific user guidelines for those wishing to perform detailed water hammer simulations. The best general advice is to start with a good nodalisation for 3-D flow in a pipe, and to use the data provided by Brunone et al [1] for initial validation.

References

1. Brunone, B. et al. (2000), "Velocity profiles and unsteady pipe friction in transient flow", *Water Resources Planning and Management*, Vol. 126, pp. 236-244.

2. Das, D. and J.H. Arakeri (1998), "Transition of unsteady velocity profiles with reverse flow", *Journal of Fluid Mechanics*, Vol. 374, pp. 251-283.

3. Ghidaoui, M.S. et al. (2005), "A review of water hammer theory and practice", *Applied Mechanics Reviews*, Vol. 58, pp. 49-76.

3.3.7. Liquid metal systems

As the primary coolant of liquid metal-cooled fast reactors (LMFRs), liquid metal has the advantages of high boiling point, good neutron economy, strong heat carrying capacity and natural circulation ability. Lead-cooled fast reactors (LFRs) and sodium-cooled fast reactors (SFRs) are two of the six reactor technologies selected by the Generation IV International Forum (GIF) in 2001. This has led to significant research in LMFRs with most of the LMFR designs under development using a "pool type" conceptual layout. Some of the thermal-hydraulic phenomena of specific interest to LMFRs include:

- Fuel assembly and core: Spacer grids, wire-wraps and inter-wrapper flow.
- Above core: Jet interaction, thermal striping, free surface movement and gas entrainment.
- Pool regions: Natural and mixed convection and stratification.

However, due to the special thermophysical properties of liquid metal, such as high thermal conductivity and low Prandtl number, the heat transfer characteristics of liquid metal are very different from that of common fluids, such as water and air. The Reynolds analogy is commonly used to relate the transfer of momentum, mass and heat through a fluid and relies on similarity between the hydrodynamic, concentration and thermal flow fields[1]. Since this similarity cannot be assumed for liquid metals, the analogy is invalid. Unfortunately, extensive use is made of this analogy and its underlying assumptions in many RANS turbulence models. LES models are largely unaffected by this issue, as they resolve the larger (more energetic) turbulent eddies in the flow.

Specifically, the thermal boundary layer of liquid metal is much thicker than the momentum boundary layer. Therefore, when carrying out a CFD simulation of liquid metal, such as the flow and heat transfer of liquid metal in the rod bundle/coolant pool/primary side of a heat exchanger, the common turbulent heat transfer models that use a constant turbulent Prandtl[2] number may cause some non-negligible deviation in the estimation of heat transfer.

The methods that have been developed for RANS turbulence models to improve the modelling of turbulent heat transfer for liquid metals can generally be divided into three categories [1]:

- Mixed law-of-the-wall.
- Turbulent Prandtl number look-up tables and correlations.
- Turbulent heat flux models, such as algebraic heat flux models (AHFMs).

1. It is not always valid even for Pr of the order of unity.

2. Again, this is not true avec for Pr~1, in particular with mixed and natural convection.

Among them, both the mixed law-of-the-wall and turbulent Prandtl number modifications present the turbulent Prandtl number as a function of local/global flow variables (such as turbulent viscosity). Thus, they are relatively easy to implement in CFD codes. AHFMs are more theoretical but a little complex[3]. The combination of AHFM with some turbulence models is usually introduced to solve the turbulent thermal diffusivity, but this may cause a few additional problems:

- Difficulty in model implementation, equation closure and convergence.
- Complex boundary conditions for new variables.
- Longer computation time.
- Validity issue when combined with an eddy viscosity model whereas it should be with a Reynolds stress model.

These issues need to be considered in the actual model selection when the simulation is carried out. In addition, validation between the CFD codes and experimental data is also significant for the development and improvement of advanced turbulent heat transfer models. In recent years, some flow and heat transfer experiments of liquid metal have been carried out by the Karlsruhe Institute of Technology (KIT) [2], European Nuclear Energy Agency (ENEA) [3], Xi'an Jiaotong University (XJTU) [4] and other institutions [5]. Valuable experimental results such as coolant temperature, heat transfer coefficient, and Nusselt number were provided and the validation between CFD codes and experimental data is in progress. LES and DNS data from several teams collected within the Sesame European project are also of interest [6].

There are several sources of data for the thermophysical material properties of liquid metals [7]. However, there is a smaller body of data available than for more conventional engineering fluids, with less independent duplication of experiments. Users should, therefore, be cautious regarding the level of confidence and uncertainty associated with the published data.

The current state of the art and challenges associated with the thermal hydraulics of liquid metals has been published in a textbook as part of the recent European Commission funded SESAME (Simulations and Experiments for the Safety Assessment of Metal cooled reactors) project [6]. Further information and guidance on thermal-hydraulic modelling of liquid metals is provided in a technical volume that was funded under the UK Nuclear Innovation Programme [8].

References

1. Roelofs, F. et al. (2015), “Status and perspective of turbulence heat transfer modelling for the industrial application of liquid metal flows[J]”, *Nuclear Engineering and Design*, Vol. 290, pp. 99-106.
2. Pacio, J. et al. (2014), “Heavy-liquid metal heat transfer experiment in a 19-rod bundle with grid spacers[J]”, *Nuclear Engineering and Design*, Vol. 273, pp. 33-46.
3. Di Piazza, I. et al. (2016), “Heat transfer on HLM cooled wire-spaced fuel pin bundle simulator in the NACIE-UP facility[J]”, *Nuclear Engineering and Design*, Vol. 300, pp. 256-267.

3. With buoyancy an equation for the temperature variance must be solved.

4. Hou, Y. et al. (2019), "Experimental study of liquid sodium flow and heat transfer characteristics along a hexagonal 7-rod bundle[J]", *Applied Thermal Engineering*, Vol. 49, pp. 578-587.
5. Underhill, R. (2019), *Project FORTE - Nuclear Thermal Hydraulics Research & Development, Review of Thermal Hydraulic Test Facilities*, FNC 53798/46969R Issue 1, Frazer-Nash Consultancy.
6. Roelofs, F. (2019), Thermal Hydraulics Aspects of Liquid Metal Cooled Nuclear Reactors. Woodhead, SESAME – Thermal-hydraulics Simulations and Experiments for the Safety Assessment of MEtal cooled reactors, Woodhead Publishing (www.sciencedirect.com/book/9780081019801/thermal-hydraulics-aspects-of-liquid-metal-cooled-nuclear-reactors).
7. Sobolev, V. (2011), *Database of Thermophysical Properties of Liquid Metal Coolants for GEN-IV*, SCK-CEN-BLG-1069, Belgian Nuclear Research Centre SCK CEN.
8. Frazer-Nash Consultancy (2021), *Nuclear Heat Transfer and Passive Cooling,* Volume 5: Liquid Metal Thermal Hydraulics.

3.3.8. Molten salt systems

The use of molten salts in a nuclear reactor has a number of advantages and features from a thermal-hydraulic perspective: as a coolant, salts have high boiling points, so reactors do not need to be pressurised (unlike water cooled reactors); they can operate at high temperatures, giving high thermal efficiency and the possibility of hydrogen production; they do not exhibit violent chemical reactivity with, for example, water (unlike sodium) and they have a high volumetric heat capacity, reducing plant size.

However, it is not principally for thermal-hydraulic reasons that salts receive attention as part of reactor design. Certain salts containing dissolved fissile materials can be used as a liquid fuel, for example in a fast or thermal spectrum breeder configuration, providing efficiency in fissile resource utilisation and waste minimisation. A wide variety of salt compositions have been proposed for use as:

- Primary coolant for designs with solid fuels.
- Fissile and fertile material carriers for liquid fuelled designs, where salts of uranium, plutonium, thorium, or minor actinides (for transmutation) are dissolved within the mixture.
- Secondary and tertiary heat transport loops.

From a thermal-hydraulic modelling aspect, there is nothing particularly different about modelling molten salts compared to other working fluids, but how they are employed does require that any analysis is considered from the perspective of fundamental understanding of the heat transfer processes. Further information and guidance on thermal-hydraulic modelling of molten salts is provided in a technical volume that was funded under the UK Nuclear Innovation Programme [1].

Some of the thermal-hydraulic phenomena that need to be considered in a molten salt reactor analysis have been summarised in a PIRT exercise for solid [2] and liquid [3] fuelled designs. The main challenges and considerations in an analysis include:

- Low Reynolds number flow - The flow in the core, primary circuit, and decay heat removal circuits could be laminar, or in the laminar-turbulent transition region in some designs. This is caused by the relatively high viscosity of some salts, which

also leads to moderately high Prandtl numbers, influencing convective heat transfer from surfaces.

- Participative radiative heat transfer - Molten salts can be transparent and emit and absorb thermal radiation. Therefore, it is important to consider and include radiative heat transfer (Section 5.2.1).
- Coupled thermal-reactivity effects - Temperature effects on reactivity are particularly important because there is a strong negative reactivity feedback from increasing fuel temperature. For liquid fuelled reactors, this coupling is stronger because the fuel itself is a mobile heat generating fluid, so reactivity changes are immediate, and an increase in temperature also reduces the fluid density, including reducing the quantity of fissile material in the core in some designs.
- Freezing and melting of coolant or fuel salts may play a role in normal operation (via "freeze valves") or in fault conditions.
- Dissolved gases (tritium or fission products) can be present in molten salts, and their transport and removal need to be understood.
- Material properties - There is significant variation in the thermophysical properties of a salt mixture due to both the variation of properties for a given salt composition with temperature and the variation of the properties with the salt composition. There are several review papers and reports that collate and assess the available thermophysical properties for relevant salts, such as [4], [5] and [6].

References

1. Frazer-Nash Consultancy (2021), *Nuclear Heat Transfer and Passive Cooling*, Volume 6: Molten Salt Thermal Hydraulics.
2. Lin, H-C. et al. (2019), "Phenomena identification and ranking table study for thermal hydraulics for advanced high temperature reactor", *Annals of Nuclear Energy*, Vol. 124, pp. 257.
3. Diamond D. J. et al. (2018), *Phenomena Important in Modelling and Simulation of Molten Salt Reactors*, *Technical Report* BNL-114869-2018-IR, Brookhaven National Laboratory.
4. Romatoski R. and L. Hu (2017), "Fluoride salt coolant properties for nuclear reactor applications: a review", *Annals of Nuclear Energy*, Vol. 109, pp. 635.
5. Beneš O. and R. J.M. Konings (2012), "Molten salt reactor fuel and coolant. in comprehensive nuclear materials", Chapter 3.13, pp. 359-389.
6. Williams D. (2006), *Assessment of Candidate Molten Salt Coolants for the Advanced High Temperature Reactor (AHTR)*, ORNL/TM-2006/12, Oak Ridge National Laboratory.

3.3.9. Natural convection

Natural convection is caused by density differences in a fluid or by mixing fluids of different density. The density differences can be caused by concentration differences, and heating from internal or external sources. Natural convection can be used as a passive mechanism of heat removal as in the case of the small modular reactor (SMR) concepts. Buoyancy-driven flow can also occur in the case of mixing of fluids of different densities, (e.g. steam and nitrogen, liquid regions with different solute concentrations, bubbly plumes in a liquid pool). This case is relevant for boron dilution scenarios in PWRs. Also, high

Rayleigh number flows (Ra 10^15 to 16) can occur during an accidental scenario of an SMR submerged in a pool.

RANS modelling of temperature stratification for higher Rayleigh numbers of the system shows deficiencies. Classical turbulence models assume the isotropic approach of the Reynolds stresses and the Boussinesq approximation for the dependency of the density on the temperature. Possible solutions, listed below in order of increasing computational effort, are:

- consideration of RANS or URANS with additional sources in the turbulence;
- application of a Reynolds stress turbulence model combined with a generalised gradient diffusion for turbulent heat fluxes, which consider the anisotropy of the Reynolds stresses and of the turbulent heat fluxes respectively, possibly an algebraic flux model (AFM); and
- using a hybrid RANS/LES, which solves for the large-scale fluctuating flows and uses subgrid scale turbulence models for the small-scale motion (this is applicable to low/moderate Rayleigh numbers).

When using a method with transport equations for turbulent kinetic energy, or components of the Reynolds stress tensor, analysts should look for options to include special source terms for creation of turbulence from buoyancy. The work of Hanjalić [1] is a good source of discussion on this topic.

References

1. Hanjalić, K. and B. Launder (2011), *Modelling Turbulence in Engineering and the Environment: Second Moment Routes to Closure*, Cambridge University Press, 1st edition (20 October 2011).

4. Selection of appropriate simulation tool

The aim of this section is to provide guidance for the selection of an appropriate simulation tool among the commonly known approaches, from "classical thermal-hydraulic system code" to "component code" and "CFD code". Considering that the recommendation will be based both on the underlying theoretical hypotheses that have led to the corresponding models and on the supposed validation state of each tool, this selection approach may be valid for both single- and two-phase applications.

Beyond the standard use of each code within its usual application field, the possible complementary use of the different tools to deal with a given issue will also be explored, either independently or in a more integrated way that will lead to coupled approaches. The underlying framework is a multi-scale description of the reactor coolant circuit, each of the following approaches clearly referring to an appropriate "scale description".

4.1. Classic thermal-hydraulic system code

Thermal-hydraulic (TH) system codes have evolved over many decades to provide simulation of the response of full nuclear power plants to a wide range of accident scenarios. Each has been designed to perform simulations of a wide range of reactor plant designs and a full range of relevant experimental facilities. They must be able to model 1-D two-phase flow through any configuration of piping, and normally have provisions for some classes of 3-D regions.

Typically, over half of the source code in a system code is devoted to managing this flexibility. Most of this is associated with input processing required to define the system configuration and set initial and boundary conditions. Other significant functions associated with general flow topology are initialisation and management of flexible data structures, full system restart dumps, and output of graphical information.

The input processing capabilities built into current system codes are combinations of ASCII input files and binary restart information. Although powerful modelling capabilities are provided via this route, development of an ASCII input model for a reactor transient can require months for even a very experienced analyst. As a result, the standard TH system codes are now operating as computational engines within a broader suite of software tools, which provide a graphical user interface (GUI) for model construction, execution of the simulation, and display/output of results. In the United States, the Symbolic Nuclear Analysis Programme (SNAP) provides the interfaces to TRACE or RELAP5 (along with other packages for analysis of the containment and neutron kinetics). In France, CATHARE is supported by a similar interface. These GUIs are designed for intuitive assembly of complex systems, and radically reduce time for model creation and analysis of results. They also significantly reduce the possibilities for user errors in the creation of the initial model.

4.1.1. Underlying hypotheses and main outcomes

The hypotheses that lead to the equations solved in system codes allow the complete description of the whole primary circuit through a blending of a one-dimensional approach for the tubes; a zero-dimensional approach for some technological objects (lower and upper plenum; water box, pump, etc.), and coarse 3D discretisation within homogenised approaches for some other parts (the core; the vessel, etc.).

The fluid equations are solved in conjunction with wall conduction equations (including radiation effects), a transient simulation of the plant control system, and even with a solution of the neutron kinetics equations.

A key hypothesis in these codes is that turbulent diffusion terms are not important as direct contributions to the flow equations. Euler rather than Navier-Stokes equations are used. Within the standard range of mesh sizes employed with TH system codes, numerical diffusion is substantially larger than actual turbulent diffusion, so this assumption is justified. Turbulence is considered in correlations for heat transfer and friction (wall and interfacial) coefficients.

Physical models associated with two-phase flow and heat transfer are limited by various assumptions. Quantities used for interfacial terms such as flow regimes, bubble diameter, or droplet diameter are normally based on local conditions and not on the flow history. Heat transfer coefficients are based on data for fully developed flow and normally do not account for entrance effects. One exception is the occasional inclusion of grid spacer effects in rod bundle heat transfer correlations.

The main outcomes are fluid and solid domain variables representing averages over substantial volumes. This is especially true of 0-D models, but it is also important to notice that 1-D volumes frequently represent an average over a wide cross-sectional flow area and that even 3-D volumes are huge compared to those used in a CFD analysis (see Section 4.2). These codes do a credible job predicting quantities with relatively slow spatial variation but should not be expected to capture local phenomena with safety consequences such as hot spots on a fuel rod.

4.1.2. Classical validation process

The physical modelling of two-phase flows relies on numerous closure laws that have been tuned to obey to known correlations or for complex situations to follow experimental results obtained from some “as close as possible to real world” experiments. The resulting simulation tool can therefore be considered as a spatial-temporal interpolator between these results, with the capability of being used for new reactor concepts. Flow maps and transitions between different flow patterns are a key issue of the validation.

The validation process has always followed a standard tiered approach. To the extent possible, individual physical models (e.g. film boiling heat transfer coefficient) are evaluated through comparison against separate effects test (SET) data. The next level of complexity consists of component tests (e.g. reactor core, upper plenum). Finally, the full system capabilities of the code are evaluated against integral systems tests, which may be scaled facilities such as ROSA [1], or full nuclear plants such as Ringhals. Typically, analyses of separate effects and integral systems dominate the validation process.

As with all other general purpose simulation codes, validation must be tied to specific applications. Limited resources generally require careful focus of the validation process, which can be guided by the PIRT process (see Section 3.2).

4.1.3. Circumstances of standard use (recommended use)

The use of a TH system code is recommended for two main safety issues:

- to provide the main information relative to some nuclear reactor safety (NRS) related events that involve a system effect (in the sense that they result from an equilibrium that develops over the whole circuit or at least over circuit parts that cannot be investigated with other approaches);
- to provide proper boundary conditions (inlet and outlet condition) to other approaches usually finer.

These codes are appropriate for a full range of two-phase flow regimes. They are limited in the range of geometries that can be well modelled by the lack of turbulent diffusion terms. They are not suitable for large open regions of a system containing circulating flows (e.g. containment), as the circulation patterns will be controlled by numerical rather than turbulent diffusion.

In addition to safety analysis, the relatively fast run times for most TH system codes, make them good candidates for use in real-time training simulators. This speed compared to standard CFD codes is simply a result of the smaller number of finite volumes in spatial discretisations. Where the number of elements in a CFD spatial mesh are counted in the millions or for some applications in billions, the number of volumes in a real-time TH systems simulation are counted in the hundreds. The most complex TH systems simulations tend to still be on the order of ten thousand volumes. This advantage is only slightly offset by the fact that TH codes typically compute and store somewhat over an order of magnitude more state variables.

Over the 30-year course of evolution for most TH codes, the primary source of run-time improvement has been the radical increase in computer CPU speed. As in any field of computer-based simulation, problems that would not have been considered for real-time simulation a few years ago are now feasible in this context. In recent years, some of these codes have also taken advantage of parallel processing to improve wall clock execution times. A secondary source of speed improvement has been a steady improvement in robustness as various adverse peculiarities of numerical solutions have been fixed.

The best example of real-time TH simulation is the SCAR project in France. This tool is a version of CATHARE adapted for coarse grain parallelism (typically eight processors). In the United States, TRACE was designed to support distributed parallel calculations and is currently used by Knolls Atomic Power Laboratory for real-time simulation of naval nuclear power plants.

4.1.4. Main scales involved

Scales vary with the location in the system and the transient being modelled. However, the typical size of mesh is on the order of a metre. In a core volume, heights are seldom less than a third of a metre. In some sections of piping, the volume lengths may be many metres.

References

1. Kukita, Y. et al. (1996), “ROSA/AP600 testing: facility modifications and initial test results”, *Journal of Nuclear Science and Technology,* Vol. 33, pp. 259-265.

4.2. Component code (porous CFD)

Although 3-D modelling within system codes such as TRACE and CATHARE can be regarded as porous media models, in this section more special purpose codes utilising a porous media approach, such as COBRA-TF, are discussed [1].

4.2.1. Underlying hypotheses and main outcomes

The equations are derived after averaging the solid and the fluid, i.e. resulting in a homogeneous or porous media. The solids are not simulated but modelled through the closure laws such as wall friction coefficient. The heat conduction is solved in fuel elements to provide the heat flux to the fluid (source term in energy balance equation). The closure

laws are devoted to rod bundles geometry, typical of LWR reactor cores or Steam Generators. The validation covers steady-state and transient conditions that are used for design, optimisation and safety analysis. The boundary conditions are provided by the system scale (off- or on-line coupling). For core applications, coupling with neutronics is also necessary to provide an accurate power distribution.

4.2.2. Classical validation process

The validation process is based on experimental data obtained in rod bundles mock-up for a specific range of application (geometry, pressure, mass flow, etc.). These data are used either to derive specific closure laws (e.g. critical heat flux) or to optimise/tune existing models from the literature.

4.2.3. Circumstances of standard use (recommended use)

The use of component code is recommended to provide a multidimensional response within the component, i.e. reactor core, steam generator or heat exchanger, both for steady-state and transient conditions.

4.2.4. Main scales involved

For reactor cores, there are classically two levels of application: the so-called "sub-channel" level and the fuel assembly level. The sub-channel level is mostly used to assess the critical heat flux (CHF) margin, using local parameters such as mass flow and quality. A one-way coupling (zoom) between fuel assembly level and sub-channel level is necessary to provide the boundary conditions.

References

1. Thurgood, M.J. et al. (1980), "COBRA-TF, a three-field two fluid model for reactor safety analysis", *19th National Heat Transfer Conference,* Orlando, 27-30 November 1980.

4.3. CFD code

Computational fluid dynamics (CFD) has developed over the last 35 years into a reliable tool for analysing complex flow situations and has become an invaluable aid to design practice in, e.g. the automotive, aerospace and turbo-machinery industries. However, CFD is not as mature a technology as seen in commercial codes available for thermal and stress analysis in solid structures. The main difficulty is that standard CFD is highly non-linear, and resolution of flow structures spanning a wide range of scales (e.g. boundary and free shear layers, vertical structures, recirculation zones, impinging jets, rotations) is required.

Though universities and government laboratories may continue to pursue in-house CFD development, this activity is strictly limited to departmental specialities, and the major steps forward in CFD technology from an industrial standpoint are now being undertaken by commercial vendors of CFD software. The major players in this league are CFX, FLUENT (both now owned by ANSYS) and STARCD. Other relevant open-source developments include OpenFOAM, code_saturne and TrioCFD. Worldwide, the current estimate of regular users of commercial CFD codes is 25 000 to 30 000, and the number has been growing steadily by 15% to 20% annually for some years. This growth has enabled the major CFD vendors to sponsor, and more generally to become actively involved in, the development of innovative numerical modelling techniques, which they hope will convert into profit-based growth in the future. Vendors have, for example, provided direct funding

for master and doctoral programmes at universities and participated in EU-funded framework programmes.

The general picture is that CFD is rapidly expanding, with a large database of proven capability. The driving force for program development is generally not the nuclear community (e.g. aeronautics), as it was for the classical thermal-hydraulic system codes (see Section 4.1), except for several recent initiatives (e.g. the SESAME Euratom project). Nonetheless, many of the application areas overlap with those associated with NRS: flows in complex geometries, mixing in stratified fluids, flow separation and reattachment, turbulence, multiphase phenomena, chemical species interaction and combustion. Consequently, practitioners in NRS-related areas can indirectly benefit from the advancements in the technology taking place elsewhere. However, because of the complexity of modern commercial CFD packages, great care is needed in input preparation and equation solving to avoid errors. Some of these points are expanded in this report.

4.3.1. Underlying hypotheses and main outcomes

CFD is now a well-established methodology and is generally accepted as describing the broad topic encompassing the numerical solution, by computational methods, of the governing set of equations that describe fluid flow, i.e. the Navier-Stokes equations, mass continuity and additional conservation equations such as for heat and species concentration. This is done on scales down to those of the largest turbulence eddies and boundary layer widths, in marked contrast to those of the system codes described above.

It is an intrinsic assumption in CFD that the details of the geometry are important to the flow and must be represented accurately. Most CFD codes therefore employ body-fitted meshes, in which the faces of the mesh cells coincide with the physical boundaries of the problem (walls, inlets, outlets). For complex geometric, this means that careful and time-consuming mesh generation, with mesh refinement in regions of strong gradients, is an important precursor to any complex CFD simulation. The application of CFD to complex flow problems requires considerable experience, and critical interpretation of the results must be undertaken from a position of fundamental knowledge of fluid dynamics and heat transfer.

Nonetheless, the codes are only as good as the physical models programmed into them: in particular, for single-phase applications, the turbulence model must be scrutinised to determine whether it is appropriate to the situation being modelled. In addition, because of the complexity of modern commercial CFD packages, great care is needed in input preparation and equation solving to avoid errors.

A typical Reynolds number encountered in NRS applications will be of the order 10^5 to 10^6 and up to 10^8 in some accidental conditions. Consequently, turbulent flow conditions are to be expected. Industrial CFD simulations generally incorporate Reynolds-averaged Navier-Stokes or RANS turbulence models (usually the High Reynolds Number k-ε model or the K-omega SST), which return only mean values for the velocities and temperatures. However, turbulence is not only a small-scale phenomenon. For the Reynolds number quoted above, the ratio of the largest to smallest turbulent eddies is 10^6 to 10^8. RANS models average over all these length scales to produce estimates of the mean quantities. Most of the information related to the scale of variation (turbulent flows are highly irregular and unsteady) is lost in this process, though the mean turbulent kinetic energy and its dissipation rate do provide a measure of the average size of the velocity fluctuations. In addition, it has been recognised that some NRS applications (e.g. flow in Tee-junctions) require the use of more sophisticated turbulence modelling approaches, such as large eddy simulation (LES), in which the largest turbulence scales are computed explicitly, while

smaller ones are modelled, or even direct numerical simulation (DNS), in which all turbulence scales, down to Kolmogorov scales are computed, with no modelling assumptions. Such calculations are naturally three-dimensional and time-dependent. Hence, they are computationally expensive.

The k-ε model, though now over 50 years old, is still regarded as the industrial standard turbulence model, simply because it is robust and cheap. This is not to say that industry is fully satisfied with the results given by the model, only that a huge extra effort is required to moderately improve predictions, and therefore in the industrial context could not be justified. Basically, the model could be considered as satisfactory for momentum transfer (except for a few special flow types such as impinging-jet heat transfer) and extra issues with transfer are not due to basic deficiencies in the model but result from treating turbulent heat transfer in accordance with the Reynolds analogy (which relates the turbulent heat flux to the mean temperature gradient via a turbulent Prandtl number). The Reynolds-analogy choice is a balance between accuracy and the need for computational speed. At some point in the future, computer speeds and storage will be high enough for more detailed treatment of turbulent heat transfer. Nonetheless, the model also has rather well-known deficiencies regarding certain flow types (swirling flows, spreading of jets). This means that, for most CFD applications to NRS, there is a definite and crucial need to benchmark various simulations being undertaken and validate the predictions against experimental data (or high-fidelity numerical simulations), where available.

CFD is not a quick-and-easy methodology and should not be employed in NRS problems unless the precision of the data to be extracted justifies the computational effort needed to obtain it. It is recommended to take the instrument that is most appropriate for the job and can deliver the level of accuracy required at the minimum effort. In other terms: “Do not use a pair of scissors to cut the grass on a football field. On the other hand, do not cut your hair with a lawn mower”. The principal outcome from a CFD calculation is meso-scale fluid dynamic and heat transfer data.

4.3.2. Classical validation process

Today, CFD is an accurate methodology. However, like any precision instrument, a state-of-the-art, general purpose CFD package is a complex entity, and demands careful considerations in its application. The widespread use of such codes in industry, and the increasing reliance which is now placed on the predictions from the codes, has prompted several recent initiatives to produce a documented “code of conduct” or “best practice guidelines”. The objective of the present report is to provide such guidelines for applications to NRS. Nonetheless, quality assurance regarding CFD is best achieved by means of benchmarking and validation.

Validation examines whether the physical models used in computer simulations agree with real world observations. It is a process that addresses the question: “Have we solved the right equations?” Validation is one of the two fundamental tiers upon which the credibility of numerical simulations is built: the other is verification. The basic validation strategy is to identify and quantify both error and uncertainty through comparison of simulation results with experimental data. See Chapter 9 for a more detailed discussion of validation.

Validation bases for CFD (many of them with on-line access) exist for a variety of specialist application areas. The document produced by the NEA Writing Group on the “Assessment of CFD Codes for Nuclear Reactor Safety Problems” [4], lists the existing databases, and makes proposals for extending the concept to NRS issues.

The remarkable growth in the computing power (high-performance computing or HPC) from PC-cluster systems to massively parallel supercomputers has had a dramatic impact

on engineering research by enabling large-scale simulations of previously intractable phenomena. PC-cluster growth has been mirrored by the global number of emerging companies investing in hardware, software, support and training. As a result, numerous companies are now turning to clusters to expand their computational resources.

4.3.3. Circumstances of standard use (recommended use)

The use of CFD codes is recommended if there are important 3-D aspects of the system's thermal hydraulics that need resolving at scales smaller than that can be handled by standard containment and system codes. Typical instances in NRS problems include flow-induced vibration of structures; surface erosion; boron dilution; mixing and stratification; heterogeneous flow situations; pressurised thermal shock; hydrogen distribution, chemical reactions, and detonation in containments; and many other situations.

The choice of code is often made based on familiarity, convenience, tradition (or obligation?) or cost, or a combination. At least for the widely used commercial codes, it is only seldom that the final choice is influenced by code capabilities, since all contain similar models. Exceptions may include situations where a fluid/structure interaction problem needs to be solved and the CFD software maintainer has an agreement (and more importantly a user-friendly interface) with one of the important stress-analysis programs, or where the situation demands the use of an advanced turbulence modelling capability, such as LES. Most commercial CFD codes have interfaces to standard mesh-generation and post-processing software. However, the most critical consideration is correct use of the selected CFD code, and the present report aims to provide information on how to do this.

4.3.4. Main scales involved

In principle, CFD can be used to obtain fluid dynamics and thermal data at all meso-scales. Thus, the flow around individual fuel rod spacer grids can be computed, as can be the main flow in the hot and cold legs, the downcomer, and upper and lower plenums of a PWR. In practice, such an undertaking would be grossly over-ambitious, for the foreseeable future. Even with geometry data supplied by a CAD/CAM/CAE package, mesh generation, utilising unstructured grids and automatic mesh generation options, would be a major undertaking. The number of meshes needed would be staggering, and CPU times for running transient safety cases unattainable.

Thus, from a purely practical viewpoint, the CFD problem must be isolated (see the discussion in Section 3.1). For the example given here, the gross flow and heat distribution phenomena in the RPV and attached piping could be handled, but the core and perhaps the core-support structure would need to be modelled using a porous-medium approach to obtain a tractable CFD problem. Likewise, a detailed description of the flow in a small number of sub-channels could be attempted, with appropriate inlet and outlet boundary conditions supplied by external means.

In summary, the main scales for NRS simulations using CFD codes could be from millimetres to centimetres, and perhaps tens of centimetres, depending on the specific application. In many circumstances, a combination of each of these scales is included in different places in the fluid domain.

4.4. The 1D-3D multiscale coupling

System codes are widely applied to simulate the physical phenomenon inside the whole nuclear power plant. System codes have the advantages of fast execution and robust numeric methods in the design basis accidents analysis. However, the 1D or 3D coarse

meshes used in system codes cannot describe the detailed spatial effect of phenomena taking place at component scale or meso-scale. The accurate prediction of local phenomenon is beneficial from the development of CFD tools [1]. But the CFD simulation for the whole system scale is impractical and so the multiscale simulation is developed. The simulations are typically classified into three scales: system scale, component scale and meso-scale. Therefore, three coupling strategies are developed, which link system/CFD and component scale. However, many new questions must be addressed, and old ones revisited when linking is performed to the more complex mesh geometry associated with CFD. Some of them are given below.

- What should be the temporal nature of the coupling (implicit or explicit)?
- What should be the spatial nature of the coupling: should system code and CFD domains be separated (interfacial coupling) or partially or totally overlapping?
- What should be the features for interpolation of variables (if required), with a system code being based on staggered grid whereas CFD codes may be based on finite element or co-located finite volume grid?
- What are the quantities that should be conserved at the discrete levels when coming from one code to another?
- How to treat the restriction (in the 3D =>1D sense) and the prolongation, reconstruction (in the 1D =>3D) of the variable profiles?
- How to treat the coupling of codes using different variables and different numbers of field equations?
- What are the consequences of a possible inconsistency in the equations of state and other closure models?

4.4.1. Classification of coupling approaches

To answer the above questions, the coupling approaches are classified into seven characteristics. The characteristics can be divided into three levels [2], [3]. The coupling approaches are given below.

- The architecture levels.
  - Code integration: external and internal coupling (monolithic and partitioned solution).
- The operative level
  - Coupling execution: in-line and off-line (one-way and two-way coupling).
  - Code synchronisation: identical time steps and subcycling.
  - Information exchange type: parallel and sequential (parallel and serial).
- The numerical level
  - Spatial domain: overlapping and decomposition.
  - Field mapping: user-manual, user-subroutine and third-party libs.
  - Temporal coupling: explicit, semi-implicit and implicit.

4.4.2. General guidelines

The choice of coupling approaches depends on the simulation problems. A partitioned, off-line, sequential coupling considering the decomposition approach and an explicit time discretisation are particularly suitable for the simulations of some newly recognised

phenomena. A monolithic, in-line, parallel coupling considering identical time steps is particularly suitable for the simulation of some well-defined issues.

Also, the quantitative assessment could be carried out for different coupling methods for a specific problem. The performance indexes of coupling codes including efficiency, flexibility, scalability, simplicity, maintainability, realisability, accuracy and robustness in each coupling approach are assigned different weights. Then a score could be achieved, with a higher score meaning a better performance of the coupling codes.

References

1. Mingjun, W. et al. (2021), "Recent progress of CFD applications in PWR thermal hydraulics study and future directions", *Annals of Nuclear Energy*, Vol. 150.
2. Pucciarelli, A. et al. ((2020), "Coupled system thermal Hydraulics/CFD models: General guidelines and applications to heavy liquid metals", *Annals of Nuclear Energy,* Vol. 153.
3. Zhang, K. (2020), "The multiscale thermal-hydraulic simulation for nuclear reactors: A classification of the coupling approaches and a review of the coupled codes", *International Journal of Energy Research*, Vol. 44, pp. 3295-3315.
4. NEA (2023), Extension of CFD Codes Application to Two-Phase Flow Safety Problems – Phase 3, OECD Publishing, Paris, www.oecd-nea.org/jcms/pl_19560.

5. User selection of physical models

Nuclear reactor applications generally involve complex and full-scale geometries. CFD simulations are often a compromise between the execution times and solution fidelity obtained from optimal physical models and adequate discretisation of the spatial domain. In striking a balance it is also important to follow verification procedures outlined in Chapter 8, to ensure that the influence of models described in this chapter is not degraded by discretisation errors.

After identifying whether a problem is independent of the phenomenological scale (i.e. do Reynolds or Grashoff numbers appear as key parameters?), the user should follow the provided methodology to select the most appropriate turbulence modelling and associated wall functions.

Most reactor thermal-hydraulic phenomena include local effects and global effects such as thermal stratification (buoyancy effects), impinging jets, level swelling, counter-current flows, thermal conductivity, etc., which are considered by user selection of models for such things as the Boussinesq approximation, heat transfer, free surfaces, and fluid-structure interaction.

5.1. Guidelines for turbulence modelling in NRS applications

This section begins with a summary of its goals and limitations, briefly surveys related documents, and provides an overview of the current modelling approaches (e.g. RANS, LES, DES) [1].

5.1.1. Limitations and objectives of the present section

Most NRS flows are time-dependent (at least unsteady and/or transitional). This means that their main features are fluctuating in time and space and that their main effects and "properties" are far from the laminar steady case. This has a crucial influence on at least three items:

- the flow topology;
- the momentum and heat exchange capabilities between the flow and the surroundings;
- the ability of the scientific community to model these flows (i.e. to derive reliable ways to quantitatively predict their effects).

This has been the starting point for many attempts to provide theoretical, mathematical and practical modelling of turbulence phenomena. However, due to the long history and continuing efforts to propose such models, the collection of available models is very large and producing complete and exhaustive guidelines for all of them is far beyond the scope of this section.

This section provides a brief classification of turbulence models and a survey of their limitations. However, the focus is on providing a non-expert reader with a methodology for selecting the most appropriate turbulence model for an application. In consequence, this section is organised as follows. First a brief bibliography of existing related documents is provided. Next some insights are provided into turbulence modelling and some modelling procedures to help the user understand the modelling framework and therefore the information they need to provide. The following section deals with turbulence model classification and limitations associated with each class. Attention is then paid to the difficult question of the wall treatment before an attempt is made to provide a methodology

to select the best available model. The discussion of each type of turbulence model is closed with specific recommendations related to its use.

Reference

1. Benhamadouche, S. (2017), "On the use of (U)RANS and LES approaches for turbulent incompressible single-phase flows in nuclear engineering applications", *Nuclear Engineering and Design*, 312, pp. 2-11.

5.1.2. Related documents

Related existing documents may be divided into two types:

1. Documents that follow the same objective as the present section, to provide "guidelines" for use of turbulence models in numerical simulation. The main interesting document is the "Best Practice Guidelines" of the special interest group on "Quality and Trust in Industrial CFD" produced by ERCOFTAC [1]. Additional similar documents have been provided by the ECORA project [2], MARNET-CFD [3], and the QNET network (see [4]).
2. Documents that may provide direct validation of a given modelling (or most of the time of a family of models) against a specific configuration or topic. These documents fall into two categories:
   - Documents that deal with the validation of a model against a specific flow configuration that may be understood as an isolated effect (separate effects tests). Typical documents are the ERCOFTAC database [5], and specific tests of modelling such as found in References [2, 3, 4, 6, 7].
   - Documents that deal with a complete realisation that validate a modelling against combined effects and for which the validation goes beyond the simple model validation (integral effects tests). The best methodology in this case may be to look for a relevant experiment and to identify the modelling that has led to success. The CSNI Writing Group report on assessment of CFD codes [8] provides a review of existing data and pays particular attention to the papers related to specific nuclear applications [9].

5.1.3. Insights into the turbulence phenomena and modelling procedures

One basic definition of the phenomena is [10] that turbulence may occur as soon as a region of the flow is dominated by inertia (i.e. as soon as the Reynolds number is high enough). This is nearly always the case in flows related to NRS issues (see Section 11.3 for a notable exception). From a phenomenological point of view, turbulence is felt through the temporal and spatial unsteadiness of the flow features (velocity, thermodynamic state variables), leading to increased flow mixing. These features are general ones and weakly depend on the driving forces like imposed flow rate, gravity, pressure differences and flow separation. Even if it is difficult, a distinction should be made (at least for a modelling purpose) between unsteadiness and turbulence in flows. The latter concerns the flows for which development has been "sufficient" so that turbulence can be considered as mature. Turbulent flows contain a very large extent of spatial and temporal scales (see [10] for an explanation about the Kolmogorov cascade).

Mathematical modelling

From a mathematical point of view turbulence results from the non-linearity of the Navier-Stokes (NS) equations, whose expressions are known but cannot lead to a direct numerical resolution in all configurations (in terms of numerical equation integration) for CPU cost

reasons. The numerical resolution thus requires a modelling process for which the key issues are:

1. choosing a modelling context between direct (DNS), statistical (RANS), or a hybridisation between both (LES, DES, SAS);
2. deriving an adapted model (through theoretical and/or empirical considerations); and
3. validating it in dedicated situations.

Turbulent flow classifications

There are many ways to classify turbulent flows for turbulence modelling validation issues. One choice may be to consider the issue both for single and global effects. Indeed, the rather complex configurations arising in industrial situations [1] have led people to consider "canonical" situations that may be identified in industrial flows.

1. The first level of complexity consists of flows dominated by a single and identified phenomenon, and a single and identified regime for a given identified geometry. Usual isolated effects lead to consideration of wall shear flows (boundary layers, wall jets), free shear flows (mixing layers; wakes; plumes, jets), and impinging flows. Geometries are simple and may refer to "canonical configurations" including plane walls and tubes. The related flows are driven by a nearly two-dimensional strain.
2. The second level of complexity includes configurations with secondary flows, and configurations with a strong coupling between turbulence and another physical phenomenon like flow rotation, buoyancy or stratifications where a tensorial representation of turbulence is recommended.
3. More complex flows involve strongly unsteady flows for which the timescale of variations is of the order of the turbulence timescale. Unsteadiness may originate from unsteady boundary conditions, from flow separations, from coupling between turbulence and other phenomena (e.g. acoustics or material vibrations). These circumstances are not always compatible with the hypotheses of turbulence modelling and the predictive capacity of such flows is difficult to assess.

The mathematical tools applied to the derivation of practical models have led to two different approaches: scale-resolving and statistical modelling.

The only deterministic approach is direct numerical simulation (DNS is not "a model"). This technique achieves the direct resolution of all temporal and spatial scales of a flow through the direct solution of the Navier-Stokes equations. This has been performed for many simple, low to moderate Reynolds number flows (single or two-phase, sometimes reactive flows), leading to the knowledge that the complete unsteady Navier-Stokes equations are able to describe all turbulence phenomena. Unfortunately, turbulence theory tells us that the smallest persistent eddy diameter is roughly proportional to the turbulent Reynolds number to the minus three-quarters power ($1/Re_t^{3/4}$). This means that the number of mesh points in DNS scales like $Re_t^{9/4}$, and only a very limited range of problems can be solved with DNS on current computers. The range of problems amenable to this approach will expand gradually with the increase in computer speed and memory. However, foreseeable future application of DNS to NRS will be restricted to calculations that improve the understanding of local phenomena.

The LES framework is not deterministic (see discussion in Pope "Turbulent Flows" p 613 and note[4]). It refers to the numerical resolution of the space and time low-pass filtered Navier-Stokes equations with the resulting turbulence motion to be composed of scales between the largest down to the filter size. The description of the motion on the resolved spectral band (containing the most energetic scales) is, as with DNS, a direct result of the solution of the three-dimensional unsteady Navier-Stokes equations. The effects of the filtered on the resolved scales are modelled through different procedures (phenomenological, formal, structural, statistical, etc.). Two main motivations governing this type of modelling are worth mentioning: first the phenomena that must be modelled take place at very small scales and exhibit a rather universal behaviour; and second the explicit simulation of the most energetic scales is sufficient to capture the main features of the flow. The resulting modelling is therefore potentially powerful, provided that the filter (which size is generally linked to the mesh size) can take place at sufficiently small scales. Unfortunately, unless wall functions are not being used, LES may not be affordable for high Reynolds number flows[5]. This limitation may be mitigated by selective use of LES within hybrid methods, as discussed later in this section.

Statistical modelling corresponds to the use of the Reynolds-averaged Navier-Stokes (RANS) equations, resulting from the application of a statistical averaging procedure to the Navier-Stokes equations. All turbulence effects are modelled in a statistical way, leading to an averaged solution as a statistical result. This derivation concerns both the steady (RANS) and unsteady (U-RANS or T-RANS [Refs 12-16]) modelling. The corresponding modelling has historically been the first developed because of limits on computer resources. Special closures must be provided (e.g. k-ε, k-ω or SST) to describe the effects of turbulence over all the physical scales. This approach allows a larger minimum mesh size than required for DNS or LES and explains the lower simulation costs. Unfortunately, this modelling approach has suffered from recurrent difficulties as physicists have tried to develop models covering a large range of applications.

Figure 5.1 illustrates the underlying modelling framework as far as the turbulence spectrum is concerned. It shows turbulence frequencies resolved by the solution of the Navier-Stokes equations on the left, and those covered by special models on the right.

About footnote 5: This is rare but possible. It means that no dissipation is being solved.

4. LES is a statistical modelling approach. It makes no sense to compare a DNS, filtered a posteriori, with a LES started from the same filtered initial field. The two simulations will rapidly be de-correlated and only statistics from the DNS can be compared to statistics from the DNS. The LES subgrid scale model reproduces the correct level of dissipation "on average", but the Smagorinky model compared to the real instantaneous subgrid stress extracted from a DNS field will show a very poor correlation.

5. Most LES computations of free flows (jets) or atmospheric boundary layers does not even need the specification of the molecular viscosity, because viscosity is negligible in front of eddy viscosity.

Figure 5.1. Part of the turbulent spectrum that is explicitly simulated (Left) and modelled (Right) for DNS A); steady RANS (B); U-RANS (C) and LES (D); from [17].

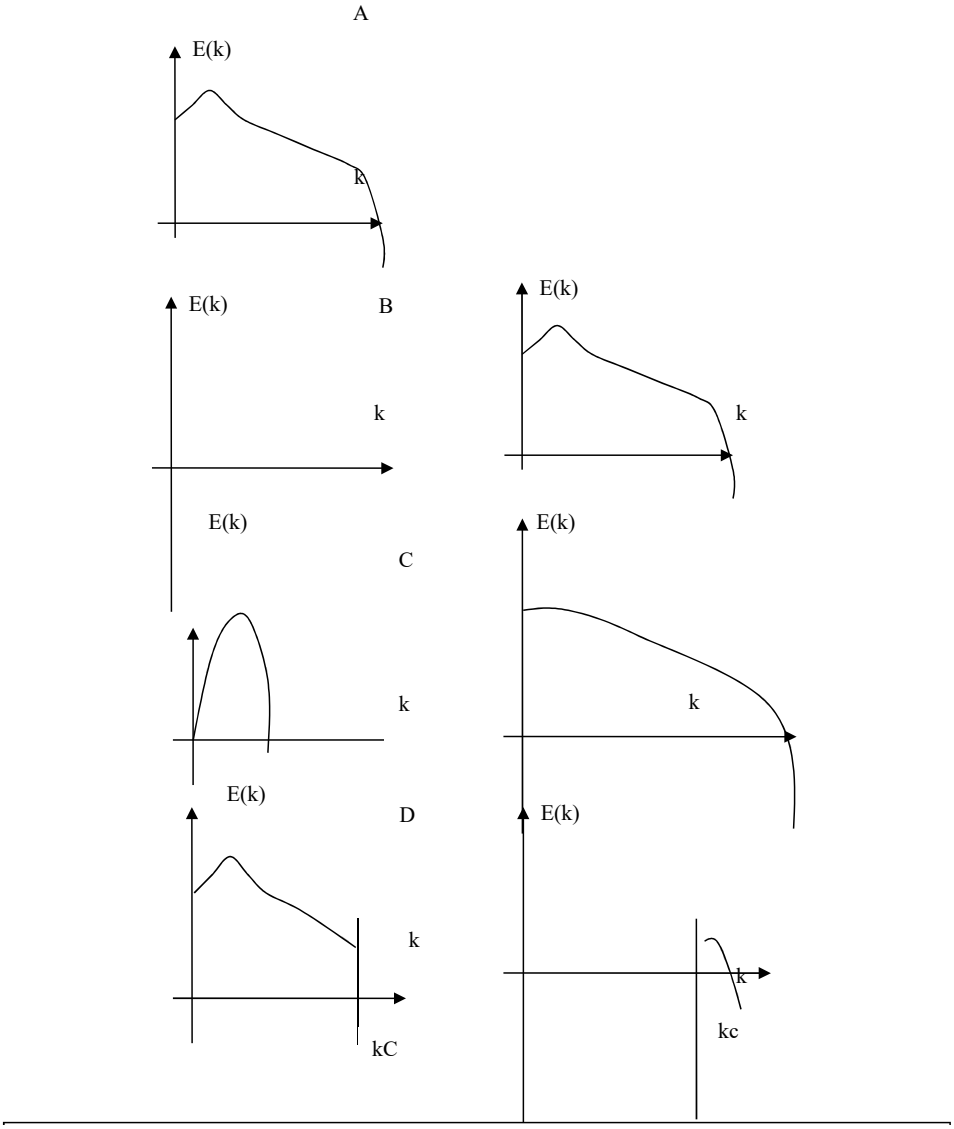

5.1.4. Turbulence model classification and limitations

Turbulence models are classified first by whether they are purely statistical over the full range of turbulence scales (e.g. RANS) or use the three-dimensional unsteady Navier-Stokes equations to deterministically model turbulence over at least a portion of the eddy spectrum (e.g. LES).

RANS and U- or (T-) RANS Turbulence Models

RANS methods are the most widely used approach for CFD simulations of industrial flows and as such have received the most modelling support from vendors of commercial CFD codes. The simplest modelling is linear, expressing a direct proportionality between the unknown Reynolds stresses or other second moments (e.g. $\langle u'\varphi \rangle$ with φ standing for u, T, Y_k) and the averaged dependent variables. Additional models must be provided for the associated eddy coefficients α_t (turbulent viscosity for momentum and turbulent diffusivity

for temperature and species). This is the Boussinesq hypothesis that relates to the eddy viscosity models (EVMs). The eddy viscosity hypothesis assumes that the Reynolds stresses can be related to the mean velocity gradients in a manner analogous to the relationship between the stress and strain tensors in laminar Newtonian flow. The eddy coefficient is proportional to the product uL of a turbulent length scale L and a turbulent velocity scale u, or to the product kT of a turbulent energy scale k and a turbulent time scale T.

Early methods made use of algebraic formulations (also called zero-equation model see [17] and [18]). These models were all directly designed for a given type of flow. Most of them are based on the description of a canonical configuration such as boundary layer, mixing layer, etc., and are therefore not suited to a large range of applications (see e.g. [19]). According to the classification of this report, the range of application is limited to a few cases of flow of first level complexity. The use of algebraic models is not recommended for general flow simulations, due to their limitations in generality and their geometric restrictions.

Algebraic models have been largely replaced by more general transport equation models for both implementation and accuracy considerations. These transport models are the lowest level of turbulence models, which offer sufficient generality and flexibility for general use. The simplest of them rely on a one-equation turbulence model, transporting turbulent kinetic energy (k). Although the range of flows that can be treated is wider than that for algebraic models, it is not considered sufficient for general purpose application. The Spalart-Almaras model [20] is one of the most famous of these models and has a transport equation for the turbulent viscosity, which is not a physical quantity.

The most popular modelling approach over the last 30 years uses two transport equations to model the behaviour of turbulence. They are based on the description of the dominant length and time scale by two independent variables. The most famous model of this family is the k-ε model [21]. Here in addition to an equation transporting the turbulence kinetic energy (k), a second equation transports the rate at which turbulence kinetic energy is dissipated (ε). The second most common two equation model is k-ω, where ω is a specific frequency of turbulence, obtained from solution of the second transport equation. In both cases, results of the transport equations are used in a simple algebraic expression to obtain a turbulent viscosity, and often Reynolds analogy is then applied to obtain thermal diffusivities. A hybrid of these approaches [22] takes advantage of the superior k-ω performance near walls, and transitions to a k-ε model away from walls while also introducing a limiter on the turbulent viscosity to ensure that the shear stress is proportional to the turbulent kinetic energy in the wake of the boundary layer.

Since k-ε is a common first choice, it is useful to list some of its shortcomings and behaviour of the basic version relative to other turbulence models. This model and its close relatives cannot be expected to perform well in the cases listed below. Reynolds stress models or an LES (or hybrid RANS/LES) approach should be explored in these situations. Look for degraded results from k-ε within:

- impinging jets;
- reattachment regions;
- flow separation in a strong adverse pressure gradient;
- regions with strongly swirling flows or other sources of high curvature in the streamlines;
- buoyancy driven flows such as a thermal plume;

- secondary flows;
- round jets

However, for flat plate transition the k-ε Jones Launder 1972 [60] is still one of the best models, while some more recent models (e.g. SST [55]) produce poor results. Some variations of the k-ε model have been created to overcome some of these problems, (non-linear models, curvature corrections, linear production etc.) but they are not as widely available in commercial software.

The k-ε model behaves well for most configurations at the first level of complexity. In addition, the family of the first order turbulence closure involving transport equations is very wide and real improvements have been achieved beyond standard k-ε models such as Durbin's k-ε-v2 [61] or Menter's SST [55], for some cases of separation and buoyancy-dominated flows. These advanced models behave well for most configurations at the first level of complexity and for some at the second level complexity.

Models that are more complex have been developed and offer more general platforms for the inclusion of physical effects. They are based on transport equations for the second moments, and the most complex RANS model used in industrial CFD applications are second moment closure (SMC) models, also called Reynolds stress models (RSM) (see [23] and [24]). These models do not use the eddy viscosity hypothesis. Instead of two equations for the two main turbulent scales, this approach requires the solution of seven transport equations for the independent Reynolds stresses and the length of time scale. Algebraic Reynolds stress models solve algebraic equations for the Reynolds stresses, whereas differential Reynolds stress models solve differential transport equations individually for each Reynolds stress component. The exact production term and the inherent modelling of stress anisotropies theoretically make Reynolds stress models more suited to complex flows, including non-equilibrium flows. The range of application of these models covers the first, second and some configurations of third level complexity. However, these models may lead to time-dependent solutions and require finer meshes or more advanced numerical approaches as they are less dissipative (this has in the past been wrongly interpreted as a numerical stability issue).

RANS responds well to the mesh sensitivity studies described in Section 8.5 as part of verification activities necessary before attempting to validate an application. The mesh convergence can be reached when the models resolved the near-wall regions. This feature is not satisfied in the same manner for U-RANS methodologies: some of them exhibiting inconsistencies.

When using RANS or its transient implementations it is important to understand limitations of the available turbulence models. Because there are so many variations on the two-equation approaches (k-ε, k-ω, SST, k-ε-V2, non-linear k-ε, etc.) the user should read and understand the documentation of these models provided for the specific code being used. Many modifications of the original models have been created with a specific application in mind or with the aim at improving a specific aspect where a model fails (for example ensuring the linearity of the production term or improvement for rotating flows). When questions arise on the optimal choice for a given flow configuration, validation tests should be run and compared for several candidate models. It is important, however, to keep in mind that some models are similar and therefore obtaining similar results might not be enough to declare that results for a given case are not dependent on the turbulence model. When testing the influence of the turbulence model in each case, different "families" of models should be used such as EVMs and RSMs or elliptic relaxation models.

Recommendations for RANS and U-RANS

So-called buoyancy driven boron dilution transients (BDT) and pressurised thermal shock (PTS) scenarios have been analysed using transient statistical modelling (U-RANS or T-RANS) in the ECORA and FLOMIX-R projects. These projects have demonstrated that T-RANS CFD modelling has indeed some shortcomings in situations when the time scale of the main flow is of the same order of magnitude as the time scale of the large turbulent eddies in the downcomer of the RPV [25] and [26]. Obviously, more advanced scale resolving CFD methods [16] [18] based on LES, DES, or SAS (scale adaptive simulation) may be tested for such cases.

Large eddy simulation (LES)

This modelling approach is based on the concept of filtering the velocity and pressure fields to separate the large scales from the small ones[6]. The idea being that the large scales can be resolved, and the small ones (or subgrid) modelled. This makes it easier from the modelling point of view since only a portion of the spectrum needs to be modelled. The main LES models are usually based on the Boussinesq hypothesis (the subgrid tensor $\langle u\phi\rangle - \langle u\rangle\langle\phi\rangle$ is considered as proportional to the resolved gradient of $\langle\phi\rangle$, where $\langle\phi\rangle$ is the low-pass filtered part of the whole field ϕ). The previous limitations arising from this statement in the context of RANS are restricted to the unresolved small scales for LES, which have led people to consider this approach as very promising. The first model was proposed by Smagorinsky for meteorological purposes (see [27]). The last 30 years have led to a very large collection of new models that can be classified into several families (see [28] and [29] for a complete review):

- Algebraic models providing an eddy diffusivity based on a given operator including a proportionality fixed constant (Smagorinsky model [27] or the structure function model family [10], WALE [30]) or with a constant evaluated through a local evolution of the flow state (Dynamic modelling [31]). These models are globally dissipative.
- More specialised models based on formal analytical evaluation of the subgrid scale tensor from the resolved scales: this includes the scale similarity model [33, 32] and all the modelling based on deconvolution procedures [32].
- Models based on the subgrid scale energy transport equation. These models may be attractive because they allow the introduction of more physics and are easy to introduce in codes already having RANS models.
- Models based on the numerical dissipation inherent in the discrete approximations of differential operators. These approaches are referred to as monotonic integrated for LES (MILES) and are very tempting when an appropriate dissipative numerical scheme is available in a solver (see [29] and [48]). In effect a numerical viscosity (or diffusion coefficient) replaces the use a specific subgrid model at filtered length scales.

Combinations of previous modelling

Recent modelling and dynamic modelling have been shown to behave well over a very large range of canonical configurations listed above as troublesome for RANS, including rotation, curvature, separation and transitional flows. Due to its formulation, LES is the only model able to simulate high-frequency events or events where the timescale of the

6. The filter in practice (for standard finite volume approaches) is implicit and depends on the space/time discretisation and the model.

main flow is of the same order of magnitude as the timescale of the large turbulent structures.

Recent LES developments have started to extend the application domain of LES to real gas and reacting flows (see [34] and [36] for a review), to particle-laden flows [35], and to two-phase flows. These models potentially cover all the flow configuration complexity levels previously defined. However, these successes are moderated by the fact that they have usually required rather fine meshes and are very expensive simulations when compared to their RANS counterparts. The fact that LES in naturally 3D and unsteady means that symmetry conditions are not compatible and to have meaningful quantities a long-time averaging procedure is required, thus increasing further the computational resources.

One common problem observed with LES is lack of intrinsic convergence in mesh refinement studies (also true for DES). This can be caused by intrinsic inconsistencies between turbulence resolved by the detailed Navier-Stokes solution, and small-scale turbulence covered by a subgrid model. When solutions on successive meshes are viewed closely, the lack of convergence can also be associated with the fundamentally chaotic nature of the Navier-Stokes equations. Studying convergence of instantaneous values for local state variables will normally not be profitable in these situations. The key to sensitivity studies for LES (and convergence in DNS) is selection of target variables that represent averaged flow behaviour important to the goals of the analysis (e.g. mean flow velocities, friction coefficients, turbulence spectrum).

When performing convergence studies with LES, it is also important to not put too much weight on experience from such studies using RANS or U-RANS. The mesh structure required for a given level of discretisation error will be different, and the degradation of results as mesh is coarsened can be more pronounced with LES.

Recommendations for LES

LES is currently available in some commercial solvers as well as in many specialised codes developed at universities and government laboratories. It should be used in conjunction with no diffusive high-order schemes (centred or stabilised centred schemes) for space discretisation of convection and with high-order time integration methods. This recommendation does not hold in case of the MILES approach, but this latter type of modelling must be considered with care because numerical diffusion can vary significantly more from the physical diffusion terms than is reasonable.

For most applications, the space filter applied in generating the LES equations is directly connected with the local mesh size and is a key-point of the modelling procedure. As a rule of thumb, the user should ensure that four to five mesh cells[7] are available to span (in each direction) the smallest eddies resolved by the Navier-Stokes solution. This can be done by comparing the filter size with the turbulent length scale, Lt. In all situations of course, the mesh must be three-dimensional and isotropic (except near walls) as eddies have no preferred direction (in opposition to RANS simulations).

In “wall resolving” LES, the mesh should be able to describe not only the main flow gradient as for a RANS simulation but also the turbulent mechanisms, including low and high-speed streaks[8]. However, wall function approaches are compatible with LES in many

7. Beware that most commercial code manuals and publications issued by non-expert users now erroneously define the filter width as one mesh cell only.

8. E.g. dy+=1, dx+=30-40 and dz+=10-20 depending on the subgrid scale model.

cases (non-separating pipe flows, bluff bodies, etc.) and it is not necessary to resolve down to y+=1.

Because LES is based on the explicit description of the main energy containing scales, numerical solution of transient behaviour also requires caution. The time filter introduced by the selection of time step size should not mask the space filter for turbulence modelling. An eddy moving more than one mesh cell in one time step will not be adequately resolved. Protection from this problem is guaranteed for solutions using explicit time integration, where the restriction of CFL number less than one based on local velocities is tighter than a restriction on eddy motion based on mean flow velocity. If an implicit method is employed in the transient solution, the user needs to be certain that maximum time steps continue to resolve eddy motion (see [56]). The time step size also needs to be substantially less than the smallest eddy decay time, but this is normally less restrictive than a CFL test.

When large CPU resources are available, wall-resolved LES can be used with success for moderate Reynolds numbers flows (such as the ones involving natural or mixed convection, for these phenomena, the flow is better characterised by Grashof and Richardson numbers rather than Reynolds number) in very complex geometries (see for example [40], [41]) and for rather high Reynolds number flows for simulation of local effects. High Reynolds number flow within a complex and large geometry requires an unaffordable CPU effort today, unless wall function can be used. LES is the only practical tool available for situations where high unsteadiness is to be described. In research from the THERFAT FP5 EU project, it was concluded that LES is required instead of T-RANS for the prediction of the high cycle thermal loading in T-junctions [43]. Lately, more wall-resolved simulations have been carried out in nuclear reactor components but limited to simple geometries such as tube bundles, pipe junctions or heat exchanges and at moderate Reynolds numbers [62, 63, 64]. These almost always require the use of high-performance machines and are not done on a day-to-day basis.

Wall-resolved or wall-approximated turbulence modelling

The near-wall region is usually governed by the velocity shear and energy transfer and is very important for most NRS applications. This region is very complex regarding the physics of turbulence because it contains the main turbulence production and dissipation areas. This modifies the turbulence structure beyond the assumptions of standard turbulence models. Describing carefully what happens in this region is theoretically possible for all the previously described turbulence models, but it requires their extension and for numerical simulations this usually requires a very fine mesh near the wall, which requires very large mesh numbers. This difficulty is treated using wall functions avoiding the expense of the wall resolution. RANS models were first developed with approximate wall boundary conditions. This has opened a large area of additional models for the law of the walls. The spirit of this modelling was to replace the complex flow simulation near the wall by empirical closure laws. These are generally based on the assumption that the flow in this region is close to an incompressible, turbulent, attached, and fully developed boundary layer at zero pressure gradient, which can be basically considered as an extension of the RANS concept. One looks for an algebraic relation between parietal transfer of momentum or energy and the resolved unknowns where they are available “far” from the wall, leading to the “log law”. Many models have been used in practice (logarithmic laws, Werner and Wengle modelling; Schuman laws, etc.), having the same physical bases. Additional closures concern the turbulence modelling itself. An overview of wall laws guidelines for RANS is provided in Ref [1]. The range of validity of this modelling depends on the behaviour of the flow within the boundary layer [2]. Strong compressible flows or flows strongly heated may be not accurately described. Impinging and separating regions are also poorly described through these wall functions. The validation of LES use with

standard wall functions is less complete than for the RANS counterparts: some drawbacks have been identified concerning very high Reynolds number flows (see [46]). This also leads to constraints in the meshing itself. For RANS, U-RANS and LES, the limitations of standard wall functions have led to consideration of fully wall-resolved solutions. Some examples of the use of wall-resolved LES have been becoming more available due to the increase in computer power available worldwide but are still limited to low or medium Reynolds numbers, see for example [62].

Section 6.2 provides a discussion of nodalisation requirements when wall functions are in use.

Information on hybrid methods

While today's CFD simulations are mainly based on RANS turbulence models, it becomes obvious that certain flows could be represented more adequately with models in which all or a part of the turbulence spectrum is resolved in at least a portion of the computational domain. Such methods are termed scale-resolving (SRS) models. These provide additional information that cannot be obtained from the RANS or U-RANS simulation. Examples are acoustics simulations where the turbulence generates noise sources, unsteady heating in unsteady mixing zones of flow streams at different temperatures, impinging jets, massively separated flows (Menter, 2015), etc. Recently, the utilisation of SRS received attention for the simulation of multi-physics phenomena such as flow-induced vibrations. The eddies in the flow are the ones that induce the structural vibration, and therefore, these need to be resolved or modelled with great care.

SRS models comprise LES as well as the hybrid U-RANS/ZLES turbulence modelling approaches. Today, there are many different hybrid models available not only in the commercial codes, but also in the open-source CFD software. A typical hybrid model is the SAS (scale adaptive simulation). In SAS, LES is used for the simulation of unstable flow regions, while the stable flow regions are solved by U-RANS. In ZLES (zonal large eddy simulation) and ELES (embedded large eddy simulation) the user defines in advance the zones where either LES or U-RANS solutions should be applied. DES (detached eddy simulation) switches between LES and U-RANS based on the grid resolution. There are also other turbulence models from the DES family such as DDES (Delayed-DES), SDES (Shielded-DES), PITM (partially integrated transport modelling), etc.

LES modelling has been used with wall laws coming from the RANS modelling but adapted in for unsteady flows [45]. This can be considered as the first RANS/LES coupling method and has opened the field of hybrid modelling. Unsteady flows requiring a time evolving solution in situations where standard RANS solutions fail have therefore been treated in many ways. The main underlying ideas in the hybrid approaches being:

- to promote the use of an attached U-RANS solution in the near-wall region;
- to switch from this U-RANS framework in the near-wall region towards a LES concept in the core of the flow.

This is a kind of extension of the use of wall functions for LES. The expected gain of this methodology is the gain in capability of describing all the unsteadiness in the core of the flow without paying for a complete LES resolution in the near-wall region, which would be too expensive.

The main motivation for the utilisation of hybrid turbulence models is the combination of improved accuracy, compared to U-RANS, while at the same time the computational effort is still acceptable and lower than for a pure LES. In SRS the important part of the computational domain is solved with high-resolution LES methods, while the rest of it is treated with URANS in an efficient way. For example, the idea behind the ZLES or ELES

is to predefine different zones in the computational domain with different treatments of turbulence already in the pre-processing stage. The domain is divided into U-RANS and LES zones before the simulation. Between the different regions, the turbulence model is switched from U-RANS to LES/WMLES (wall-modelled LES). To maintain consistency, synthetic turbulence is generated at the U-RANS/LES interfaces. ZLES and ELES are not new models, but rather an infrastructure that combines existing elements of technology in a zonal fashion. The recommendations for each zone are therefore the same as those applicable to the individual models (Menter, 2015).

Detached eddy simulation (DES) was first formulated by Spalart (Spalart et al., 1997). The main idea was to propose a hybrid formulation that switches between RANS and LES according to the grid resolution in the computational domain. Thus, the wall boundary layers are treated with the U-RANS model, while far from walls the free shear flows are usually computed with LES. Detached eddy simulations (DES, see [47]) have been applied to the flow and thermal mixing in an experimentally investigated T-junction [49, 50]. The DES-calculations were compared with results of time-dependent RANS calculations using the RNG k-ε model. Both simulation techniques were used on two different grids. The RANS turbulence models showed discrepancies as compared to data, and the disparities could not be reduced by grid refinement or by using unsteady inlet boundary conditions. On this specific case, the DES results showed more realistic fluctuations with strong temperature and velocity gradients, caused by vortex shedding behind the incoming branch flow and the instabilities due to the separation zone. The predicted mixing was clearly influenced by the secondary flows caused by upstream bends in the piping system. Although there were quantitative differences between experiments and DES computations, the results clearly showed the importance of using a scale-resolving simulation technique such as DES or LES for this type of flow situation.

One hybrid implementation is scale-adaptive simulation (SAS), a recently developed methodology designed to better predict unsteady-state flows [51, 52, 53]. Although it still requires qualification and must be used with care, SAS is described here in some detail as an example.

SAS involves the introduction of an additional production term in the transport equation for the turbulent velocity scale which allows the model to adjust to resolved scales in a simulation. Essentially, SAS is an improved U-RANS approach, which avoids the occurrence of unphysical single-mode unsteady flow features, as observed in classical U-RANS methods. As a result, unsteady regions display a breakdown of the large turbulent structures to smaller and smaller scales as typical for turbulent flows. The method by itself distinguishes between stable and unstable regions of the flow. In stable regions, the model operates in classical U-RANS mode, whereas in unstable regions, the model displays a LES-like behaviour. As the SAS model formulation does not explicitly involve the grid spacing, it avoids the undefined model regimes of DES. In case of overly coarse grids or too large time steps, the model reverts to the underlying U-RANS formulation.

The SAS model is based on a re-evaluation of the k-L model proposed by Rotta [54]. It was shown that some of the arguments used in the derivation of that model have been overly restrictive. As a result, the Rotta model features a length scale based on the third velocity derivative, which is not attractive in CFD simulations. The re-formulation of the model results in the use of the second derivative, leading to the von Karman length scale as the natural length scale.

The SAS term has also been transformed into the SST turbulence model [55]. It gives an additional term in the k-equation, which can be implemented with relative ease.

Recommendations for hybrid methods

There are no general recommendations yet for these methodologies and the reader is asked to refer to the latest publications in this field. However, it is important to be particularly cautious with this type of hybrid model. Gant [39] demonstrates that DES and SAS error may increase when the mesh is refined whereas the RANS error decreases.

Nevertheless, before performing a hybrid analysis the user should be at least aware of the following:

- The choice of the hybrid turbulence model should consider the flow problem to be investigated. Some hybrid models like SAS, SBES are more suitable for globally unstable flows (flows with strong swirling instabilities, impinging jets), while others (ZLES. ELES) provide good results for locally unstable flows (flows with large separation zones, flows with weak swirl instabilities).
- When using ZLES or ELES models, the user should carefully analyse the domain geometry and the zone of particular interest, where the LES model will be activated. Based on this analysis, the LES zone will be explicitly specified in the input of the CFD programme. It is important to position the interfaces between U-RANS and LES up- and downstream the zone of particular interest. At the interface, synthetic turbulence is generated, for example with harmonic functions.
- The central differencing (CD) advection scheme is the best choice, because of its higher accuracy, but in cases with complex geometry and not very high mesh quality it might become unstable and produce unphysical solution (wiggles, overshoots). In such cases the bounded central differencing (BCD) scheme proposed by Jasak et al (1999) could help. There are also advection schemes that switch between second order high-resolution and CD schemes.
- The time integration should be performed with second order schemes. The time steps should be selected to achieve CFL≈1 in the LES part of the CFD domain. The problem time calculated should be sufficient for at least 10-20 flow through times. The more statistics is available from the transient run, the higher the accuracy of the results will be. This is important for the averaging procedure for the calculated variables and quantities during the post -processing phase.
- Simulations with hybrid turbulence models can be initialised with RANS or U-RANS solutions. During the first-time step of a ZLES or ELES simulation, synthetic turbulence at the U-RANS/LES interface is generated.
- The post-processing of simulations with hybrid turbulence models is also very important. Visual inspection already during the run will help the user to identify potential issues. With the help of an isosurface and the Q-criterion the turbulence structures might be inspected. Their size and form will depend on the turbulence model applied. Furthermore, the turbulence structures will show if turbulence is generated in the expected regions of the CFD domain. The user should verify that the synthetic turbulence at the U-RANS/ZLES interface does not decay or disrupt downstream.

For further information, the interested reader is advised to have a look in the document *Best Practice: Scale Resolving Simulations in ANSYS CFD* from F. Menter (Menter, 2015). It contains a detailed and useful guidance on the CFD analysis with hybrid turbulence approaches.

Inlet boundary conditions

The turbulent state of the incoming flow has an influence on the downstream flow development. The implication on the turbulence modelling is twofold:

- Some models directly require the knowledge of the incoming turbulence state (k and ε profiles for the k-ε model should be prescribed for example). There are no directly available data to universally prescribe such quantities. The code thus generally contains specific internal treatment allowing a synthetic state of the turbulence at the inlet, which relies on hypotheses that are not always valid. As one form of remediation, the user may need to consider extension of the computational domain in the upstream direction far enough to capture all significant influences on the flow behaviour in the region of interest (for example if the investigation concerns a region downstream of an elbow, then the elbow must be considered).
- For LES, specific treatments in the upstream direction have been derived but require further development (see [57], [58], and [59]).

5.1.5. Methodology to select an appropriate turbulence model

NRS applications usually encompass a large collection of the complexities described in Section 5.1.3. Three key steps in assembling the best set of CFD modelling options are:

1. Analyse the flow regimes to identify the main features (complexity) of the flow to be reproduced to assess a "correct" flow representation and those that can be omitted with acceptable physical realism and preserved predictive capabilities.
2. Select the most appropriate framework of modelling that is pertinent for the flow and reasonable as far as the CPU cost/precision of the whole simulation is concerned. DNS is currently used mostly on simple geometries because of its computational cost associated to the very fine meshes required. The choice for industrial studies is to be done between LES RANS or U-RANS; research and validation are still in progress on hybrid methods, DES, SAS or RANS/LES coupling.
3. Select a model within a given context that is compatible with the chosen framework and for which there is validation assessing its capability to take account of the required flow features; this step addresses the choice of wall-resolved or wall-modelled strategies.

When selecting a turbulence model, it is important to be aware of the shortcomings of a given approach. As a starting point, an EVM model can be used and further comparison with RSMs should give an insight on how the turbulence model is affecting the quantities of interest. The use of RANS models will be a first step in any simulation and LES should be performed when there are specific reasons for concern. When performing LES, a different mesh strategy is required, and details of the flow need to be known. It is therefore almost always necessary to have a RANS simulation before being able to know the mesh requirements for good quality LES. Whether using RANS or LES special attention needs to be paid to the way the near-wall effects are considered; the turbulence model will need to be consistent with the near-wall treatment. In instances when heat transfer, friction or other such near-wall quantities are highly important, the use of wall function might not be desirable.

To end this section, it is noted that the choice of a turbulence model is a matter of compromise between the accuracy of the global model and its costs and feasibility. For NRS applications, one may prefer a given solution falling within accepted uncertainties than the use of the "best" model for a given situation. In that respect it should be noted that

current uncertainty methodologies will probably require a prohibitive amount of computing resources to estimate error bounds associated with a turbulence model for three-dimensional unsteady situations. When uncertainty analysis is not feasible, a CFD user should at least:

- use "new" or "marginally known model" with care;
- compare the results coming from different modelling to access the sensitivity of the results to a given model and reconsider the first choice in case of inconsistencies.

References

1. Casey, M. and T. Wintergerste (ed.) (2000), *Special Interest Group on 'Quality and Trust in Industrial CFD' Best Practice Guidelines, Version 1*, ERCOFTAC Report.
2. Menter, F. (2002), *CFD Best Practice Guidelines for CFD Code Validation for Reactor-Safety Applications*, European Commission, 5th EURATOM Framework Programme, Report, EVOL-ECORA-D1.
3. WS Atkins Consultants (2002), *Best Practices Guidelines for Marine Applications of CFD*, MARNET-CFD Report.
4. QNET https://kbwiki.ercoftac.org/w/index.php/Main_Page_/ (last accessed June 2024).
5. ERCOFTAC website, www.ercoftac.org/ (last accessed June 2024).
6. Tzanos, C.T. (2001), "Performance of k-eps turbulence models in the simulation of LWR fuel bundles fuel", ANS/ENS Annual Meeting.
7. Menter, F. (2015), *Best Practice: Scale Resolving Simulations in ANSYS CFD, Version 2.0*, ANSYS, November.
8. Willemsen, S.M. and E.M.J. Komen (2005), "Assessment of RANS CFD modelling for pressurised thermal shock analysis", *Proceedings of the 11th International Topical Meeting on Nuclear Reactor Thermal-Hydraulics (NURETH-11),* 2-6 October 2005.
9. NEA (2005), *Assessment of CFD Codes for Nuclear Reactor Safety Problem's*, OECD/Nuclear Energy Agency Report. NEA/SEN/SIN/AMA(2005)3 www.oecd-nea.org/science/wprs/egrsltb/BFBT/participants/sen-sin-ama2005-3.pdf
10. NEA and IAEA (2006), "Benchmarking of CFD codes for applications to nuclear reactor safety"; CFD4NRS NEA International & International Atomic Energy Agency (IAEA) Workshop, 5-7 September 2006.
11. Lesieur, M. (1997), *Turbulence in Fluids*, Kluwer Academic Publishers.
12. Ducros, F. (2003) "Modélisation et Simulation des Écoulements Turbulents (Modeling and Simulation of Turbulent Flows)", "CLEFS" CEA internal Journal No47, Winter 2002-2003 issue.
13. Kenjeres, S. and K. Hanjalic (2006), "LES, T-RANS and hybrid simulations for thermal convection at high Ra numbers", *International Journal of Heat and Fluid Flow,* Vol.27, pp. 800-810.
14. Kenjeres, S. et al. (2002), "A T-RANS/VLES approach to indoor climate simulations", *Proceedings of the ASME 2002 Joint US-European Fluids Engineering Division Conference*, pp.1-9.

15. Kenjeres, S. and K. Hanjalic (2002), "Combined effects of terrain orography and thermal stratification on pollutant dispersion in a town valley: a T-RANS simulation", *Journal of Turbulence*, Vol.3 (26), pp.1-25.

16. Hanjalic, K. and S. Kenjeres (2001), "T-RANS simulation of deterministic eddy structure in flows driven by thermal buoyancy and Lorentz force", *Flow, Turbulence and Combustion,* Vol. 66, pp.427-451.

17. Kenjeres, S. and K. Hanjalic (1999), "Identification and visualisation of coherent structures in Rayleigh-Benard convection with a time-dependent RANS", *Journal of Visualisation,* Vol.2 (2), pp.169-176. 4.

18. Baldwin, W.S. and H. Lomax (1978), "Thin-layer approximation and algebraic model for separated turbulent flows", paper of the American Institute of Aeronautics and Astronautics, Inc.

19. Cebecci, T. and A.M.O. Smith (1974), *Analysis of Turbulent Boundary Layers*, Series in Appl. Math. & Mech., Vol. XV, Academic Press.

20. Rodi, W. (1993), *Turbulence Models and their Application in Hydraulics,* IAHR Monograph, Taylor & Francis, ISBN 90-5410-150-4.

21. Spalart, P. and S.R. Almaras (1992), "A one-equation turbulence model for aerodynamic flows", paper of the American Institute of Aeronautics and Astronautics, Inc.

22. Launder, B.E. and D.B. Spalding (1974), "The numerical computation of turbulent flows", *Computer Methods in Applied Mechanics and Engineering*, Vol. 3 pp. 269-289.

23. Menter, F.R. (1994), "Two-equation eddy-viscosity turbulence models for engineering applications", *AIAA Journal, Vol. 32*, pp.1598-1605.

24. Launder, B. E., G. J. Reece and W. Rodi, (1975), "Progress in the development of a Reynolds-stress turbulent closure", *Journal of Fluid Mechanics*, Vol. 68(3), pp. 537-566.

25. Hanjalic, K. and B. E. Launder (1972), "A Reynolds stress model of turbulence and its application to thin shear flows". *Journal of Fluid Mechanics Digital Archive,* Vol. 52, Issue 04, pp. 609-638, DOI: 10.1017/S002211207200268X

26. Scheuerer, M. et al. (2005), *Condensed Final Summary Report*, ECORA Deliverable D17, March 2005.

27. Rohde, U., T. Höhne, S. Kliem, M. Scheuerer, B. Hemström, T. Toppila, T. Dury, J. Klepac, J. Remis, P. Mühlbauer, L. Vyskocil, I. Farkas, A. Aszodi, I. Boros and Y. Bezrukov (2003), "FLOMIX-R: Fluid mixing and flow distribution in the primary circuit - Final summary report", 5th Euratom Framework programme 1998-2002.

28. Smagorinsky, J. (1963), "General circulation experiments with the primitive equations", *Month. Weath. Rev.*, Vol. 93, pp. 99-165.

29. Sagaut, P. (2001), "Large eddy simulation for incompressible flows", (1st edition), Springer Ed.

30. Nicoud, F. and F. Ducros (1999), "Subgrid-scale stress modelling based on the square of the velocity gradient tensor", *Flow, Turbulence and Combustion*, Vol. 62, pp. 183-200.

31. Moin, P. et al. (1991), "A dynamic subgrid scale modelling for compressible turbulence and scalar transport", *Phys. of Fluids*, Vol. 3, p. 2746-2757.
32. Stolz, S., N.A. Adams and L. Kleiser (2001), "The approximated deconvolution model for LES of compressible flows and its applications to shock-turbulent-boundary layer interaction", *Physics of Fluids*, Vol. 13., pp. 2985-3001.
33. Bardina, J., J.H. Ferziger and W.C. Reynolds (1980), "Improved subgrid-scale models for large eddy simulation", AIAA Paper 80-1357, 13th AIAA Fluid and Plasma Dynamics Conference.
34. Lartigue, G. (2004), *Simulation des Grandes Echelles et Instabilities de Combustion*, PhD thesis of the National Polytechnique Institute of Toulouse.
35. Kaufmann, A. (2004), *Vers la Simulation des Grandes Echelles en Formulation Euler-Euler des Ecoulements Réactifs Diphasiques*, PhD thesis of the National Polytechnique Institute of Toulouse.
36. Poinsot, T. and Veynante, D. (2001), "Theoretical and Numerical combustion", R.T. Edwards Inc. publishers, Philadelphia, PA, United States.
37. Benarafa, Y. (2005), *Application du Couplage RANS-LES aux Ecoulements Turbulents à Haut Nombre de Reynolds de l'Industrie Nucléaire*, PhD thesis, Paris 6 université, https://theses.hal.science/tel-00011371/.
38. QNET-CFD (2002), "Turbulence modelling: Part 2, Limitations of the k-epsilon models" (not publicly available).
39. Gant, S. (2010), "Reliability issues of LES-related approaches in an industrial context", *Flow, Turbulence and Combustion,* Vol. 84, pp. 325-335.
40. Höhne, T. and U. Bieder (2006), "Modelling of a bouancy-driven flow experiment at the ROCOM test facility using the CFD-codes CFX-5 and Trio_U", *Nuclear Engineering and Design*, Vol. 236, pp. 1309-1325.
41. Bieder, U., G. Fauchet, S. Bétin, N. Kolev and D. Popov (2007), "Simulation of mixing effect in a VVER-1 000 reactor", *Nuclear Engineering and Design*, Vol. 237, pp. 1718-1728.
42. Rohde, U. (2005), *Final Summary Report*, Flomix-R (FIKS-CT-2001-00197), 2001.
43. Schippers, M. (2005), "D10: Numerical Analysis of thermo-hydraulic tests", European project: Thermal Fatigue Evaluation of Piping System "Tee"-Connection, deliverable No THERFAT R (13)/D10/2003 (not publicly available).
44. Scheuerer, M. (2005), *Condensed Final Summary Report*, EVOL-ECORA-D18.
45. Deadorff, J.W. (1970), "A numerical study of three-dimensional turbulent channel flow at large Reynolds numbers", *Journal of Fluid Mech*, Vol. 41, pp. 453-465.
46. Nikitin, N.W. et al. (2000), "An approach to wall modelling in large eddy simulations", *Physics of Fluids*, Vol. 12, pp. 1629-1632.
47. Spalart, P.R. et al. (1997), "Comments on the feasibility of LES for wings and on a hybrid RANS/LES approach", in *Advances in DENS/LES*, Z. Liu Ed., pp. 137-147, Greyden Press.
48. Grinstein, F. F., C. Fureby and C.R. DeVore (2005), "On MILES based on flux-limiting algorithms", *International Journal for Numerical Methods in Fluids*, Vol. 47, pp. 1043-1051.

49. Veber, P. and L. Andersson (2004), "CFD calculation of flow and thermal mixing in a T-junction – time-dependent calculation part 2 (BG-project)", *Teknisk not 2004/21, Rev 0*, Onsala Ingenjörsbyrå.

50. Henriksson, M., U. Andersson and J. Jungstedt (2002), *Termisk Blandning i T-Stycke – Resultatrapportm*, Report U02:134, Vattenfall Utveckling AB.

51. Menter F.R. and Y. Egorov (2004), "Re-visiting the turbulent scale equation", *Proc. IUTAM Symposium; One Hundred Years of Boundary Layer Research*, Göttingen.

52. Menter F.R. and Y. Egorov (2005), "A Scale-adaptive simulation model using two-equation models", *AIAA paper 2005-1095*, Reno/NV.

53. Menter F.R. and Y. Egorov (2005), "Turbulence models based on the length-scale equation", *Fourth International Symposium on Turbulent Shear Flow Phenomena,* Williamsburg, 2004, Paper TSFP4-268.

54. Rotta, J.C. (1972), *Turbulente Strömungen (Turbulent flows),* Teubner Verlag, Stuttgart.

55. Menter, F.R. (1994), "Two-equation eddy-viscosity turbulence models for engineering applications", *AIAA Journal, 32(8)*, pp. 269-289.

56. Weber C, F. Ducros and A. Corjon (2005), "Assessment of implicit time integration for LES", AIAA Paper 99-3355.

57. Sergent, E. (2002), *Vers une Méthodologie de Couplage entre la Simulation des Grandes Echelles et les Modèles Statistiques*, PhD thesis of Ecole Centrale de Lyon.

58. Schluter, J.U., H. Pitsch and P. Moin (2004), "Large eddy simulation inflow conditions for coupling with Reynolds-averaged flow solvers", *AIAA Journal*, Vol. 42(3), pp. 478-484.

59. Jarrin, N. et al. (2006), "A synthetic-eddy-method for generating inflow conditions for large-eddy simulations", *International Journal of Heat and Fluid Flow*, Vol. 27(4), pp. 585-593.

60. Jones, W.P. and B.E. Launder (1972), "The prediction of laminarisation with a two-equation model of turbulence", *International Journal of Heat and Mass Transfer*, Vol. 15, pp. 301-314.

61. Parneix, S., P.A. Durbin and M. Behnia (1998), *Computation of 3-D Turbulent Boundary Layers Using the V2F Model, - Flow, Turbulence and Combustion*, Springer.

62. Benhamadouche, S. and C. Le-Maitre (2009), "Large eddy simulation of the flow along four sub-channels downstream a mixing grid in a PWR", *NURETH-13: Proceedings of the 13th International Topical Meeting on Nuclear Reactor Thermal Hydraulics,* Atomic Energy Society of Japan.

63. Yuan, H. et al. (2017), "Flow-induced vibration analysis of a helical coil steam generator experiment using large eddy simulation", *Nuclear Engineering and Design.,* Vol. 322, pp. 547-562.

64. Merzari, E. et al. (2017), "Large-scale large eddy simulation of nuclear reactor flows: Issues and perspectives", *Nuclear Engineering and Design,* Vol. 312, pp. 86-98.

65. Spalart, P.R. et al. (1997), "Comments on the feasibility of LES for wings, and on a hybrid RANS/LES approach", In: Advances in DNS/LES, *1st AFOSR Int. Conf. on DNS/LES.*

66. Jasak, H., H.G. Weller and A.D. Gosman, (1999), "High resolution differencing scheme for arbitrarily unstructured meshes", *Int. J. Numer. Meth. Fluids*, Vol. 31, pp. 431-449.

5.2. Heat transfer modelling

Heat transfer via convection, conduction and thermal radiation is one of the key phenomena for reactor thermal hydraulics. The evaluation of heat transfer in reactor cores is of particular importance for the design of economical and safe reactors. Characteristics of heat and fluid flows should be correctly predicted under operational and accidental conditions to maintain the coolability and the structural integrity of the core. The same applies for the analysis of pressurised thermal shock (PTS) in the RPV of PWRs and for fatigue analysis in pipe networks and components such as heat exchangers. Heat transfer and coupled flow effects must also be resolved in containment analyses under operational and accidental conditions for different purposes ranging from HVAC simulations to hydrogen-risk analyses. Single-phase heat transfer is important in fast reactors, gas reactors and in many applications in water reactors, while two-phase heat transfer dominates accident analysis in water reactors. Given the single-phase flow focus of this report, two-phase heat transfer is not discussed.

In pool type fast reactors the temperature difference between the core inlet and exit is more than 100 K in normal operation. Several heat transfer phenomena need to be considered in thermal-hydraulic analyses of these reactor vessels, including thermal stratification, non-uniform flow, stagnation and thermal striping. Thermal stratification is seen in reactor transients such as shutdown. In this case, core exit temperatures and flow rates decrease rapidly, and the mixing with high-temperature coolant is reduced in the upper plenum. The temperature difference can exceed 100 K in the vertical direction, and the effects on core structures is large. Non-uniform flows are caused by complex shapes such as above and below core structures. Thermal striping refers to temperature fluctuations in the mixing process, such as the hot coolant from the fuel bundle and cold coolant from the control rod bundle and T-junction mixing [1].

Non-uniform flows and incomplete mixing are also important in high-temperature plenums in gas-cooled reactors. Thermal stratification is significant in water reactors during ECCS water injection. For instance, in the case of an accident with ECCS actuation cold water is injected into cold legs. The temperature difference between the primary coolant and ECCS water can be more than 200 K, and the effects on piping would be significant when the flow rate of primary coolant is small (see Section 11.2).

These examples of heat transfer phenomena are three-dimensional and closely related to single-phase turbulent flows. Accurate predictions of these phenomena are difficult when using conventional reactor safety analysis codes based on one-dimensional modelling that employ empirical correlations. CFD codes based on continuum equations and using turbulence models could simulate complex geometries and are often used to simulate these phenomena.

Heat transfer in fluids is governed by conservation equations for mass, momentum and energy. For turbulent flows, which are widely encountered in nuclear applications, the dependent variables in the conservation equations are usually divided into average and fluctuating parts, and Reynolds or ensemble averaging is used to obtain equations for the mean flow variables. The mass and momentum equations are solved for the averaged

velocity and pressure fields. The Reynolds stresses, $\rho\overline{u_i u_j}$, appear as additional unknowns in the momentum equations. The turbulent heat fluxes, which are made up of velocity and temperature fluctuations, $\rho\overline{u_i t}$, are included in the averaged energy conservation equation. The turbulent heat fluxes are strongly related to turbulent flow models, and thus the temperature field is substantially affected by the flow field and vice versa if buoyancy is important or material properties change significantly with temperature.

The purpose of the models described in Section 5.1.4 is to obtain the eddy viscosity, which in turn is needed to calculate the Reynolds stresses. The equivalent for energy is the eddy thermal diffusivity, which can be obtained by dividing the eddy viscosity by a turbulent Prandtl number (by applying Reynolds analogy, usually called simple gradient diffusion hypothesis (SGDH)). This model for turbulent heat flux is widely used in combination with most standard RANS models. This is considered appropriate for forced convection, thermal mixing, and heat transfer in most fluids (water and gases, where Prandtl number is in the order of O~1 or higher).

The behaviour of the boundary layer in high Prandtl number fluids, such as molten salts (Section 3.3.8) is well understood [2]. The high Prandtl number means that the thermal boundary layer will be thinner (or gradients higher) than the momentum boundary layer in laminar flows and steeper in the near-wall (sublayer) region of turbulent boundary layers. The effect of the high Prandtl number should be taken into account in the near-wall treatment ($T^+ = Pr\ y^+$ in the viscous sublayer, so y^+ should be ~1/Pr for wall-resolved methods), but otherwise the same modelling approach can be employed, and the implications of using a simple turbulent heat flux model are not as systemic and important as they are for low Prandtl number fluids (as long as forced convection is the dominant transport process).

For low Prandtl number fluids, such as liquid metals (Section 3.3.7), the thermal boundary layer is much larger than the momentum boundary layer. It may be necessary to use a more complex treatment, such as a turbulent heat flux model to separately evaluate turbulent thermal intensity, defined as the variance of the temperature fluctuation. this latter and its dissipation, can be calculated using two additional transport equations. Turbulent heat flux models are more appropriate when the similarity between the momentum transport and energy transport is not as good, for some buoyancy driven flows or for low Prandtl number fluids (such as liquid metals).

Immediately next to a surface (or "at the wall"), the velocity and temperature of the flow are normally considered to be the same as those at the wall itself (no slip and no temperature jump), so heat transfer at the fluid-solid interface is entirely due to conduction. Further into the fluid, the wall-parallel fluid motion and turbulent mixing enhances the transfer of thermal energy, which makes the temperature profile in the fluid layers away from the wall flatter and the temperature gradient at the wall stronger. Since the convective heat transfer at the wall is strongly influenced by the temperature gradient and detailed near-wall flow field, a wall-resolved method (y^+~1 or 1/Pr for high Prandtl number fluids) is recommended for accurate heat transfer predictions.

Buoyancy driven flows are inherently unsteady, so it is recommended to adopt a transient solution scheme to capture the time varying velocity and temperature variations. In addition, it is often important to include the variation in fluid properties with temperature, and careful consideration needs to be given to the appropriateness of the external model boundary conditions i.e. adiabatic, constant heat flux, constant temperature, or applied heat transfer coefficient (HTC) and ambient temperature.

In most cases, an equation of state is required to account for the density variation with temperature and pressure. When using transport equations to calculate the eddy viscosity

and the eddy thermal diffusivity for buoyant flows, some modifications are necessary. The transport equations for the turbulent kinetic energy and its dissipation rate contain production terms due to buoyancy.

In some instances, Reynolds stress models (RSMs) as described in Sections 3.3.9 and 5.1.4, may be more suited to modelling buoyant flows, as they contain fewer simplifying assumptions. In addition, LES models that resolve the larger (more energetic) eddies can explicitly simulate all buoyancy effects, provided the use of LES is recommended for the considered flow (see Section 5.1.4).

5.2.1. Thermal radiation

All surfaces continuously emit, reflect and absorb electromagnetic radiation; the intensity and spectrum of wavelengths of the emitted photons depends on the temperature of the surface. Any medium between surfaces, except a vacuum, can also "participate" in thermal radiation exchange (i.e. absorb, emit, and scatter radiation passing through it), although in many cases this is minimal (as in air). Surface-to-surface radiation is important when the radiant heat flux is of the same order of magnitude or larger compared to the heat transfer rate due to convection or conduction. Gas radiation in participating media is important e.g. if the flow has stagnant zones which are not involved in the convection. Furthermore, radiation transports heat directly (at the speed of light), which can be relevant in transient flows.

The emitted radiant heat flux is proportional to the temperature to the power of four, so radiation is typically considered important at high temperatures. Thermal radiation is therefore important in high-temperature gas reactors (HTGRs), molten salt reactors (MSRs) and external heat loss calculations across gaps between vessels and to the surrounding environment. Additionally, it is relevant in situations with low temperature differences and where the convection and conduction heat fluxes are low, for example in situations of stable stratifications [3]. For example, in containment flows ($\Delta T<100K$), thermal radiation affects the gas temperature field and thus the pressurisation [4], introduces local buoyancy effects, and thereby affects the mixing process. Furthermore, condensation rates are affected by a change in gas saturation conditions or structure surface temperatures [5]. Thus, gas radiation affects the water-steam balance and associated effects like aerosol transport or flammability. Consequently, neglecting radiative heat transfer is not conservative.

Dealing with the full details of thermal radiation is complex and the models must compromise between exact photon or ray tracing (directionally exact, but computationally expensive for a high number of photons/rays to include radiation from all points in space to all other visible points in space) and solving diffusive transport equations (not directionally exact but ensure conservation of radiative heat transfer). Thus, simplifying assumptions are often used:

- Surfaces are considered "diffuse" (i.e. emission or absorption are independent of direction), "gray" (i.e. properties are independent of radiation wavelength) and "opaque" (i.e. no transmission of thermal radiation occurs through the surface).
- The medium between surfaces is non-participating.

These simplifications allow the heat transfer between surfaces to be calculated, based on the Stefan-Boltzmann law for the emitted heat flux due to thermal radiation from a surface ($E = \varepsilon\sigma T^4$). The absorptivity of a surface (α) defines how much incident radiation is absorbed (with 1-α reflected). Kirchoff's law states that $\alpha = \varepsilon$ at each wavelength. This means that highly reflective surfaces also do not emit significantly and thus (if not heated otherwise) remain cooler under irradiation than highly absorptive surfaces. For gray

surfaces, this is simplified to be the case across the entire spectrum, which is a sufficiently accurate approximation for most applications, except for semi-transparent media and when solar radiation (insolation) is important.

Further information and guidance on thermal radiation modelling is provided for example in [6]. A more complete description of the concepts and governing equations for thermal radiation and typical engineering approximations can be found in [7] and [8].

The non-linearity of thermal radiation with temperature usually requires numerical or iterative solution. Possibly for this reason, thermal radiation is often neglected from heat transfer calculations as a simplification. However, this may introduce substantial inaccuracy (even at moderate temperatures) so omitting thermal radiation from heat transfer analysis should be considered carefully. This is particularly true in passive cooling situations where thermal radiation can become significant to a point where it can provide a dominant part of the cooling mechanism. In buoyant flows, thermal radiation can always play a role: Warmer media (thinking of warm air, possibly also with water vapour content in containment analysis) accumulates at the top of rooms, heating up the top-room surfaces which themselves radiate heat to the colder surfaces at lower elevations of the rooms. In case of water-vapour content, the warm cloud itself radiates, too. Without modelling radiation, these effects would not be represented, and the floor surfaces would remain cold with direct impact on buoyancy.

The type of thermal radiation modelling required depends on the properties of the fluid (i.e. participating, or non-participating media):

- Air and most simple gases (e.g. helium and argon): Radiative heat transfer occurs between surfaces, and they are considered non-participating media (neither absorb, emit, or scatter thermal radiation at the IR wavelengths of interest), and variations of surface properties with temperature and wavelength are usually ignored.
- Water vapour, CO_2, and particles (such as soot or droplets): These constituents emit, absorb, and scatter thermal radiation, and where they are present in significant concentrations, and long optical path lengths exist, a fluid may need to be considered as a participating medium.
- Molten salts: Depending on salt composition, these can be semi-transparent media that absorb and emit radiation significantly, and potentially non-uniformly, over the spectrum of wavelengths emitted from a hot surface.

There are several standard thermal radiation models available in most CFD software with different levels of complexity and medium participation. The most common models include:

- P-1 radiation model: The radiative transfer equation (RTE) for the P-1 model is a diffusion equation that is easy and fast to solve, although this means it is only appropriate for optically thick applications and is not recommended for complex geometry with non-participating media. However, in many situations it might be better to switch on the P-1 model rather than excluding thermal radiation at all. There is no directional dependency in the model, it solves for spherical waves. An advantage of the model is that a transport equation for radiation is solved which should ensure conservation of radiative heat transfer. The P-1 model can include the effect of absorption and particulates within the medium with properties that can vary with radiation wavelength, i.e. non-gray and gray radiation. It assumes that the reflection of incident radiation at a surface is isotropic (diffuse).

- Surface-to-surface (S2S) radiation model: The S2S radiation model is a good choice for modelling radiative heat transfer within an enclosure without participating media. It calculates the view factor between each wall face (or cluster of faces) to determine the energy transfer between two surfaces based on their size, separation distance and orientation. This usually assumes gray radiation and that all surfaces are diffuse. This means that the S2S model is not applicable for participating media. An advantage of this model is that the view factor calculation is usually performed as a pre-processing step which makes the model fast during the solution process.
- Discrete ordinates (DO) radiation model: The DO model has the capability to solve radiative heat transfer for participating and non-participating media, including semi-transparent walls [9]. Therefore, it can include the effect of absorption, scattering and particulates within the medium for gray and non-gray radiation. It solves the RTE as a transport equation for radiation intensity for a finite number of discrete solid angles, and so the accuracy of the solution depends on the angular discretisation. If the discretisation is too coarse, it can lead to physically unrealistic bumps and oscillations in the incident radiation field, the so-called "ray effect". Furthermore, it is known to suffer from false scattering, which is numerical diffusion resulting from the non-orthogonality between ray and cell faces [10]. The main disadvantage of the DO model is that it can be computationally expensive, and so increases the solution time [11].
- The discrete transfer method (DTM)/method of characteristics (MoC) solves the integral form of the RTE along representative rays of radiation starting from known wall boundary conditions and subsequent computation of the radiation sources in the participating media [12]. As the rays are only computed once at the beginning of a simulation, the method can be comparably fast but becomes expensive on large meshes and when applied with non-gray models.
- The Monte Carlo (MC) method [13] is a statistical method that simulates radiative heat transfer by tracking a large number N of photon bundles (histories) through the system. It is a very general purpose method and allows considering gray/non-gray, scattering, emission, and absorption. It always contains a statistical error E~1/sqrt(1/N), which can be reduced by increasing the number of photon histories but makes the method computationally expensive.

In case of participating media, there is an exponential increase in the computational effort resulting from the number of cells, each emitting several angles/rays which each represent several bands to be computed. In such cases, e.g. large complex 3D geometries and application of multi-band models, the Monte Carlo method quickly becomes more efficient [13]. Concluding, the method is computationally intensive, but as it allows considering complex 3D geometric configurations it can be the most attractive solution technique for practical applications [14].

Gas radiation

The spectral properties of the medium have a highly irregular dependence on the wavelength as depicted in Figure 5.2 (data from HITRAN database, processed with HAPI [15]).

Figure 5.2. Spectral absorption coefficient of H_2O, CO and CO_2 (data from HITRAN database)

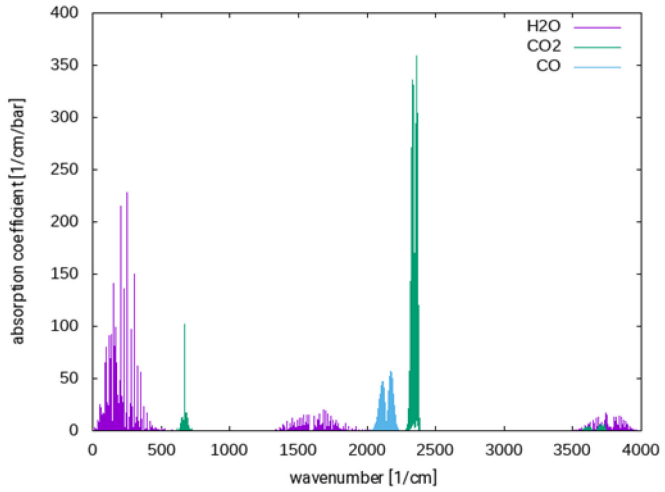

Consequently, gas thermal radiation emission and absorption are both a function of the local gas temperature and mixture composition as well as the present radiation spectrum. A comprehensive overview of various modelling approaches is given by [16]:

- The simplest model is a gray medium, which considers the absorption coefficient to be wavelength independent or simply temperature dependent (e.g. Planck mean absorption coefficient).
- The weighted-sum-of-gray-gases model (WSGG) proposed by [17] replaces the entire spectrum by a few bands of gray gases and transparent windows with uniform absorption coefficients. The weighting coefficients that account for the contribution of each gray gas correspond to the fraction of the blackbody energy in the spectrum region where the gray gas is located. These coefficients are typically obtained by fitting data of the total emittance for different temperatures and pressure path lengths. The main limitation of most of the published sets of coefficients is that they consider only a fixed molar ratio of H_2O and CO_2 of one or two, which can hardly be expected for typical containment atmospheres. To overcome this limitation, [18] proposed a new approach to derive the coefficients of the WSGG model for a gas mixture composed of arbitrary concentrations of H_2O, CO_2 and soot. This method is based on generating WSGG correlations for the individual species, which are then superposed to form correlations for the mixture. Still, obtaining suitable model coefficients for typical containment conditions is difficult and often demands the user input of a mean free radiation path.
- More detailed non-gray models are the "full spectrum correlated k" (FSCK) model [19] or the "statistical narrow band correlated k" (SNBCK) model [20] which subdivide the spectrum into 10 to 100 bands.

The most accurate approach is the line-by-line (LBL) integration of spectral characteristics related to the absorption and emission behaviour of molecules e.g. within the HITRAN or HITEMP databases. It is prohibitively demanding for practical applications, however there are several benchmark solutions available (e.g. [21]).

The choice of the spectral model clearly depends on the application and the expected overall impact of gas radiation. Nevertheless, considering the spectral properties depicted in Figure 5.2, one can easily conclude that a gray (i.e. averaged) treatment of a medium

with few distinct absorption lines like CO_2, will yield a significantly higher error than for a medium with a broader absorption spectrum like steam.

Besides the physical modelling aspects, there are also several numerical considerations required to limit the additional computational effort for solving the RTE. These depend on the model (e.g. number of quadrature angles or photon histories) but can also be highly specific to the implementation of the models into a specific code. For example, the computational effort can be reduced by assuming that:

- Radiation-turbulence interaction is negligible (this may not be the case for combustion applications), i.e. the radiation source terms need to be updated only once per time step.
- The transient progression is slow so radiation source terms can be updated only every Nth time step or physical period (e.g. 1s).
- The gradients in the radiative flux are less steep than in the fluid fields so that radiative transport can be computed on a coarser mesh and source terms can be mapped onto the fluid mesh.

Conclusions and recommendations

Radiation heat transfer can be modelled accurately using the advanced methods and physical models described before. However, there is still a considerable lack in documented modelling experience and dedicated validation cases except for combustion modelling, where most of the approaches were developed for. It must be noted that besides very simple approaches like P-1, there is no general comparability of the methods among the different CFD codes that can be stated e.g. for turbulence models.

Radiation heat transfer is implicitly involved in many NRS validation experiments. On the one hand its modelling simplifications add uncertainty to the assessment of the other physical models, on the other hand it does not allow for a separate validation of RTE solver and spectral model. To estimate the global effect of radiative heat, transfer a simple model (P-1, S2S, gray media) may be employed and compared to a no radiation solution. However, if radiation turns out to be relevant in terms of the figures of merit, the results obtained need to be confirmed by a ray tracing approach. Furthermore, independence of the numerical parameters needs to be demonstrated.

There are large uncertainties related to the knowledge and modelling of the material spectral properties of fluid and structures. While for gases there is e.g. the HITRAN database, the specification of the emissivity of steel depends on many aspects, e.g. surface roughness, material history, paint, temperature, spectrum of the radiation etc., which can hardly be determined generically or in situ. The only, but demanding, possibility to quantify the effect on validation results is an uncertainty analysis.

5.2.2. Conjugate heat transfer

Conjugate heat transfer (CHT) is the coupling of stored thermal energy and heat conduction in solids with convective and radiative heat transfer in neighbouring fluids. The ability to predict the variation in temperature of solid components, such as the fuel cladding, pipe networks, vessels and structures, because of heating or cooling by a fluid is important for all nuclear power plants.

CHT analysis is required when it is not sufficient to simply consider heat transport in the fluid, with an idealised thermal boundary condition applied at the fluid and wall interface.

In these cases, the coupled problem, including heat conduction in the solid wall adjacent to the fluid, must be considered. Further information and guidance on CHT modelling are available, for example in [2].

The accurate prediction of fluid and solid temperatures is used to support performance assessments and structural integrity calculations as part of the design and safety of all nuclear power plants. Detailed predictions of the fluid and solid temperatures within the primary circuit are required under normal operation, start-up, and shut-down transients, as well as during fault scenarios. These are used to determine the operating envelope and safety margins for the reactor design, including peak fuel cladding temperatures and rate of reactor cooldown during station blackout events.

CHT analysis is a key input into structural integrity calculations to demonstrate the integrity of structures, systems and components and predict component life. Failures in components may be caused by situations such as large thermal shocks causing fracture (e.g. emergency cooling in pressurised thermal shock scenarios), temperature fluctuations over a long period causing fatigue or temperatures that lead to enhanced corrosion.

5.2.2.1 Coupling level for conjugate heat transfer

Common approaches to CHT analysis include uncoupled and coupled methods using a resolved solid, shell conduction or porous media zones. A key reason for performing CHT analysis is to support structural integrity assessments. Usually, CFD software can predict CHT alone within a coupled approach to calculate fluid and solid temperatures in one simulation. A solid mechanics (FEM) software is additionally needed when not only the solid temperatures are of interest, but also the thermal stresses. Therefore, CHT analysis is often used to generate inputs for FEA models, enabling solid deformations, internal stresses, and thermal fatigue to be predicted by structural engineers. In most of the nuclear applications this one-way loose coupling is sufficient for the desired analysis goals and a backward coupling from the FEM to the CFD analysis is not needed. Two-way coupling is necessary only in cases where the structures move in such a way that the CFD solution is affected, for example due to strong deformations or oscillations.

- Uncoupled: In this approach, the flow and fluid temperatures are predicted in a CFD model and the temperatures within solids are predicted in a separate thermal-structural FEA model. Information is passed one-way (from the CFD model to the FEA model) using data extracted from the flow solution, usually a combination of near-wall fluid temperatures and heat transfer coefficients (HTCs) to allow recalculation of the local heat fluxes in the FEA model. Care should be taken that the HTCs are derived using the local and not bulk flow conditions if local near-wall fluid temperatures are provided. This method is generally only appropriate for situations where the thermal environment is changing so slowly that the fluids and solids can be in a quasi-steady state, or the HTC is effectively independent of the solid temperatures (which may occur in forced convection flow). An uncoupled approach may be the simplest and computationally cheapest method for calculating the temperatures and stresses within components over long fault scenarios (hours or days).
- Coupled using resolved solid: In a fully coupled CHT approach, the energy equation for temperature needs to be solved in both the fluid and solid domains. The physical processes and solutions of the governing equations can be either solved in a single model (monolithic approach) or in separate fluid and solid models (partitioned approach). In both CHT approaches, the solid domain needs to be properly modelled and meshed, which significantly adds to the complexity and time

required to build the model. A fully coupled approach is suitable for any combination of fluid and solid regions, including complex conduction paths and inter-connected fluid-solid regions. It also enables time-varying temperatures to be calculated when the fluid and solid temperatures are strongly dependent on each other (e.g. mixed, and natural convection, complex conduction paths, large Biot number or large thermal mass). To analyse thermal stresses in addition, the solid temperatures from the CFD solution can be mapped to a FEA model.

- Coupled using shell conduction: Creating full meshes for solids to resolve the temperature gradients within them can be onerous, but in many geometries (such as pipes or ducting) the conduction behaviour is relatively simple. Therefore, some CFD software enables thin-wall or shell conduction to be modelled in the solver, by predicting the temperature variation within solids using a virtual (pseudo-mesh) that is generated by the CFD solver with the prescribed wall thickness. In addition to non-meshed thick walls that are also available in some CFD codes and only conduct in the direction normal to the wall face, in shell-conduction walls a three-dimensional conduction is possible. Usually, no control on the wall mesh is foreseen, though. Additional restrictions may apply, and the model should be used with care. Heat transfer in corners, for example, where two shell-conduction walls meet, might be impossible from one wall to the other. The thermal resistance of the solid is accounted for by assigning appropriate material properties, although the spatial temperature variation within the solid is not recorded as part of the solution.
- Coupled using porous zones: Most CFD solvers offer the ability to specify and use porous zones. These can be applied to a wide variety of problems, including perforated plates, tube banks and pebble beds. This applies an additional pressure loss to the flow that is usually based on a user specified anisotropic loss coefficient. In most cases, the superficial velocity, based on the volumetric flow rate, is solved to ensure continuity of momentum and mass flow. Sometimes, however, the use of a free volume fraction in the porous medium, the porosity, can be used to solve for the (faster) physical velocity in the fluid fraction of the porous zone. Therefore, care is needed to ensure that the loss coefficient is appropriately derived, and the treatment of turbulence within the porous zone is understood (by default, the turbulence generation and dissipation rate is often assumed to be unaffected by the solid component). The thermal equations can be solved using an equilibrium model (where the solid and fluid are locally assumed to be at the same temperature and are represented using effective material properties combining solid and fluid contributions, based on porosity of medium) or a non-equilibrium model (separate temperatures are modelled for solid and fluid zones with heat transfer between them). The non-equilibrium model is more appropriate for transient calculations because it enables changes in the solid temperature to "lag" changes in the fluid temperature, because of its representation of thermal mass and the finite rate of heat transfer. Additionally, in transient cases, the effect of porosity on the transport velocity for energy and species in the flow can be included, even if the superficial velocity is solved for. This might be different from code to code. Then, the resistance coefficients are still based on superficial velocity for the pressure losses, but the unsteady transport of species and energy is modelled using the physical velocity in the porous media.

5.2.2.2 Mesh requirements for conjugate heat transfer

This section highlights that for unsteady CHT with varying temperatures in the fluid, the solid mesh needs fine mesh layers at the surface to adequately resolve the temperature in

the solid and accurately calculate the convective heat flux. An example application is the CFD simulation of a thermal transient in a component like a heat exchanger or the gas distribution calculation in a nuclear containment under accidental scenarios.

As for other CFD tasks, the CHT meshes also must be generated to resolve the expected gradients in the solution fields with the desired accuracy. For the fluid side of the CHT wall, and assuming turbulent flow, this means that the mesh generation follows the requirements for the selected turbulence model and, if used, other fluid-side models like wall condensation. Using two-equation turbulence models, either a mesh for turbulent wall functions or a finer mesh for turbulent near-wall treatment is needed.

For the solid side of the CHT wall, this is different and application dependent. In a steady state simulation, the final temperature distribution through a planar wall between a warmer side and a colder side with given area and thickness is linear and the heat flux is only dependent on the thermal conductivity of the wall material according to Fourier's law. To resolve the linear temperature field, theoretically one cell over the thickness of the wall would be sufficient. For more complex shapes of solids in steady state and more than two adjacent temperatures, the required mesh resolution is finer and shape dependent.

In unsteady simulations the density and the specific heat capacity in addition to the thermal conductivity are responsible for the temperature field as a function of time in the solid. These three material properties determine the temporal storage and distribution of heat and the resulting solid temperatures. In the heat conduction equation, they form the thermal diffusivity, often denoted as $\alpha = k/\rho c_p$. Like the Courant-Friedrichs-Lewy number, one can define a thermal diffusion number $\Delta x^2 / (\alpha\ \Delta t)$, which links solid mesh resolution and simulation time step.

In CHT simulations with given solid material, temperature fluctuations from the fluid side like a hot streak of water or air must be resolved in the solid correctly, as the solid surface temperature as a function of time is an input parameter for the heat flux into the wall as a function of time. With a thick first cell in the solid behind the wall surface, the heat flux from the hot fluid streak only results in a small temperature rise, as the initially colder wall-material temperature dominates the average temperature in the solid cell. The heat flux at subsequent times will be too high because the temperature gradient between fluid and solid is overpredicted.

The same initial heat flux assigned to a thin first cell layer in the solid results in a larger temperature rise in the solid, and the heat flux at subsequent times will be realistic. A similar consideration can be applied to the transition from the first cell layer to the second cell layer in the solid. Here, the temperature changes in the first cell of the solid are not as fast as the temperature changes in the fluid, because the first cell of solid acts as a buffer material. All these thoughts have the consequence for the meshing of the solid, that the region neighbouring the fluid needs a fine mesh resolution, starting with a fine first cell layer. Subsequent layers into the solid can become thicker, which can be realised with a growth factor for the inflation layer in the meshing software.

CFD users can perform a mesh sensitivity analysis on a heat-up transient close to the intended application of a solid heated from one side, other walls set to adiabatic to check different meshes. A mesh with very thin layers can serve as the accurate solution if no analytic solution or another scientific code for solving the heat conduction equation is available. A fine resolution of the solid surface is not only important for the correct heat flux. All fluid-side models that need a correct solid surface temperature, such as wall condensation or thermal radiation, profit from it. To this extend, special caution must be paid regarding the solid and fluid resolution time steps to ensure the continuity of temperature and normal fluxes.

5.2.3. CHT analyses of rod bundle flows using polyhedral cells

This section discusses the application of polyhedral meshing to CHT analyses of rod bundle geometries. Rod bundle configurations are ubiquitous to the industry (including existing fleet and advanced concepts), and accurate predictions of temperature and flow distribution are of paramount importance to the safety of the nuclear reactor. The geometries of rod bundles can also contain complex intricate details that need to be adequately resolved to be able to model the turbulent flow and heat transfer. The key physics that needs to be accurately predicted for rod bundles includes non-uniform temperature distribution in and around the cladding; an important parameter for ensuring integrity of the core and safety of the reactor. For all rod bundle configurations and pitch-to-diameter ratios (P/D), it is recommended that CHT between the fluid region and solid cladding is used in the CFD model to accurately predict the wall temperatures of the heated rods.

A well-organised mesh predominantly based on hexahedral cells is often desired to ensure the numerical stability and accuracy for CHT simulations of rod bundles in 3D. However, due to the nature of the complex geometry of rod bundles especially at the spacers (e.g. appendages in PHWRs, wire-wrapped bundles, mixing vanes in LWRs), it is often challenging to use block-structured or other hexahedral meshing methods. For such scenarios, polyhedral cells are preferable to tetrahedral cells because they are bounded by more neighbouring faces that result in improved estimation of gradients, result in lower numerical diffusion and aid towards improvement of numerical stability.

In addition, for complex spacer arrangements such as vanes, wire-wrapped rod bundles, and in geometry configurations that feature tight P/D ratios (e.g. LMFRs and PHWRs), polyhedrons are more efficient in filling the space with fewer elements. Meshes based on polyhedral cells can also be stretched (i.e. elongated) and can be continuously graded in size. These attributes are advantageous in resolving the geometry while achieving a computationally economical cell count for rod bundle configurations. Furthermore, conformal meshes (one-to-one contact) at the interfaces that reduces interpolation efforts and contributes to enhanced numerical stability for CHT problems is generally ensured with the use of polyhedral schemes.

Other factors that generally need to be given consideration for CHT analyses and development of high-quality meshes are:

- Solid region(s) need to be explicitly modelled to the extent practicable instead of adopting a simplistic approach, such as shell conduction.
- Sharp growth in the cell size in the vicinity of the fluid-solid interface should be avoided.
- Depending on the thickness of the cladding, at least three to five solid layers are recommended within the solid region.
- A wall-resolved method ($y^+ < 5$) should be used to resolve the viscous sublayer and appropriately predict the convective heat transfer, and a prismatic (layered) mesh should be applied normal to solid surfaces before changing to a polyhedral topology, to resolve the boundary layer.
- Variation of thermophysical properties of solid material with temperature should be used.
- Anisotropic turbulence models based on non-linear eddy viscosity models can provide better results than isotropic models for the flow distribution.

References

1. NEA (2011), *Report of the OECD/NEA-Vattenfall T-Junction Benchmark Exercise*, OECD Publishing, Paris, www.oecd-nea.org/jcms/pl_19022.
2. Kays, W.M. (1994), "Turbulent prandt l number-where are we?" *Journal of Heat Transfer*, Vol. 116(2), pp. 284.
3. Kelm, S., H. Müller and H. Allelein (2016), "Importance of thermal radiation heat transfer modelling in containment typical flows" in *Proc. OECD/NEA and IAEA Workshop on Experiments and CFD Codes Application to Nuclear Reactor Safety (CFD4NRS)*, pp. 9-13.
4. Filippov, A.S., S. Grigoryev and O.V. Tarasov (2016), "On the possible role of thermal radiation in containment thermal-hydraulics experiments by the example of CFD analysis of TOSQAN T114 air-He test", *Nucl. Eng. Des.*, Vol. 310, pp. 175-186.
5. Dehbi, A., S. Kelm, J. Kalilainen and H. Mueller, "The influence of thermal radiation on the free convection inside enclosures", *Nucl. Eng. Des.*, Vol. 341, pp. 176-185, doi: 10.1016/j.nucengdes.2018.10.025.
6. Frazer-Nash Consultancy (2021), *Nuclear Heat Transfer and Passive Cooling, Volume 2: Convection, Radiation and Conjugate Heat Transfer*, funded under the UK Nuclear Innovation Programme.
7. Incropera, F.P. (2011), *Fundamentals of Heat and Mass Transfer*, Seventh edition, John Wiley & Sons.
8. Howell, J.R., M. P. Mengüç, R. Siegel (2016), *Thermal Radiation Heat Transfer,* Sixth edition, CRC Press.
9. Murthy, J.Y. and S.R. Mathur (1998), "Finite volume method for radiative heat transfer using unstructured meshes", *Journal of Thermophysics and Heat Transfer*, Vol. 12(3), pp. 313-321.
10. Chai, J. C., H. S. Lee and S. V. Patankar (1993), "Ray effect and false scattering in the discrete ordinates method" *Numer. Heat Transf. Part B Fundam*., Vol. 24, no. 4, pp. 373-389.
11. Balsara, D. (2001), "Fast and accurate discrete ordinates methods for multidimensional radiative transfer. Part I, basic methods" *J. Quant. Spectrosc. Radiat. Transf.,* Vol. 69, no. 6, pp. 671-707.
12. Lockwood, F. C. and N. G. Shah (1981), "A new radiation solution method for incorporation in general combustion prediction procedures", *Symposium (International) on Combustion*, Vol. 18, no. 1, pp. 1405-1414.
13. Modest, M. F. (2013), *Radiative Heat Transfer*, Academic Press.
14. Maurente, A., H. A. Vielmo and F. H. R. França (2007), "A Monte Carlo implementation to solve radiation heat transfer in non-uniform media with spectrally dependent properties", *J. Quant. Spectrosc. Radiat. Transf.*, Vol. 108, no. 2, pp. 295-307.
15. Kochanov, R. V. et al. (2016), "HITRAN application programming interface (HAPI): A comprehensive approach to working with spectroscopic data", *J. Quant. Spectrosc. Radiat. Transf.*, Vol. 177, pp. 15-30.
16. Siegel, R. (2001), *Thermal Radiation Heat Transfer*, CRC press.

17. Smith, T. F., Z. F. Shen and J. N. Friedman (1982), "Evaluation of coefficients for the weighted sum of gray gases model", *Journal of Heat Transfer,* Vol. 104(4), pp. 602-608.

18. Cassol, F. et al. (2014), "Application of the weighted-sum-of-gray-gases model for media composed of arbitrary concentrations of H2O, CO2 and soot" *Int. J. Heat Mass Transf.*, Vol. 79, pp. 796-806.

19. Modest, M. F. and H. Zhang (2002), "The full-spectrum correlated-k distribution for thermal radiation from molecular gas-particulate mixtures", *J Heat Transf.*, Vol. 124, no. 1, pp. 30-38.

20. Soufiani, A. and J. Taine (1997), "High temperature gas radiative property parameters of statistical narrow-band model for H2O, CO2 and CO, and correlated-K model for H2O and CO2", *Int. J. Heat Mass Transf.*, vol. 40, no. 4, pp. 987-991.

21. Goutiere, V., F. Liu and A. Charette (2000), "An assessment of real-gas modelling in 2D enclosures", *J. Quant. Spectrosc. Radiat. Transf.*, Vol. 64, no. 3, pp. 299-326.

5.3. Free surface modelling

The discussion here will be restricted to incompressible, single-phase aspects of free surface modelling in which there is no phase change, but the physical properties (density, viscosity, thermal capacity, and thermal conductivity) of the single fluid change discontinuously across the interface. Even with this restriction, there remain several interesting application areas in NRS, including level swelling in BWR suppression pools, estimates of the free surface levels in accumulator tanks in PWRs, level-tracking in condenser units, and generally free surface behaviour under seismic loads.

An interface between a gas and liquid is often referred to as a free surface. The reason for the "free" designation arises from the fact that the location is not known a priori, but forms part of the solution procedure. Large differences in the densities of the gas and liquid can occur for example the ratio for water and air is about 1 000. A low gas density means that its inertia can generally be ignored compared to that of the liquid. In this sense, the liquid is the main driving force for the interface motion. Nevertheless, if there is a gas flow parallel to the surface, friction may create waves.

The presence of a free or moving boundary introduces serious complications for any type of analysis. Free surfaces require the introduction of special models to define their location, their movement and their influence on the flow. There are two types of free surface modelling methods. Conceptually, the simplest means of defining and tracking a free surface is to construct a Lagrangian grid that is imbedded in, and moves with, the fluid. This model is ideal for continuous free surfaces for which a very accurate interface prediction is required. Other free surface tracking methods use a fixed, Eulerian grid as the basis for computations, so that more complicated surface motions may be treated. This is well-suited for large deformation problems, such as filling, sloshing, droplet break-up and other discrete processes.

For the Lagrangian grid methods (examples are front-tracking [1] and boundary-integral [2] methods), the principal limitation is that they cannot track surfaces that break apart or intersect. Even large amplitude surface motions can be difficult to track without introducing regridding techniques such as for the Arbitrary Lagrangian-Eulerian (ALE) method [3]. On the other hand, since the proper boundary condition can be applied at the surface, the most precise evolution of the shape and location of a surface with time can be obtained. To avoid remeshing issues, other numerical methods without grids have been developed. For

example, the SPH [4] and MPS [5] schemes represent a fluid by many calculation points (particles) moving with flow. In these methods, the partial differential operators appearing in the Navier-Stokes equations are replaced by the appropriate interaction modelling between particles.

Modern examples of Eulerian approaches are the volume of fluid (VOF) method, level sets [6, 7], and phase field methods [8]. Historically, the earliest numerical method devised for time-dependent free surface flow problems was the marker-and-cell (MAC) method [9]. This scheme is based on a fixed, Eulerian grid of control volumes. The location of fluid within the grid is determined by a set of marker particles that move with the fluid, but otherwise have no volume, mass or other properties. A free surface is defined to exist in any grid cell that contains the markers and that also has at least one neighbouring grid cell that is void. The MAC method succeeded in solving a wide range of complicated free surface flow problems. One reason for this success is that the markers do not track surfaces directly, but instead track fluid volumes. Surfaces are simply the boundaries of the volumes, and in this sense, surfaces may appear, merge or disappear as volumes break apart or coalesce. The principal limitation of marker particles is that they do not do a very good job of following flow processes in regions involving converging/diverging flows. When fluid elements get pulled into long, convoluted strands, the markers may no longer be good indicators of the fluid configuration.

The volume of fluid (VOF) method [10], which is the method that has been used most frequently and widely so far, is based on the concept of a fluid volume fraction. If the fraction of fluid in each cell (control volume) is known, it is possible to locate surfaces, as well as determine surface slopes and surface curvatures. Surfaces are easy to locate because they lie in cells partially filled with fluid or between cells full of fluid and cells that have no fluid. Slopes and curvatures are computed by using the fluid volume fractions in neighbouring cells. The essential element in this process is to remember that the volume fraction should be a step function, i.e. having a value of either one or zero. In the original method, only the liquid governing equations are solved, and the free surface is considered as a boundary condition. The application of free surface boundary conditions consists of assigning the proper gas pressure (plus equivalent surface tension force) as well as determining what velocity components outside the surface should be used to satisfy a zero shear-stress condition at the surface. In practice, it is sometimes simpler to assign velocity gradients instead of velocity components at surfaces. In alternative methods [11], the free surface is considered as a discontinuity of the fluid properties, both fluids being seen as a single fluid. Accordingly, no boundary conditions are required at the free surface. Finally, to compute the time evolution of surfaces, a technique is needed to move volume fractions through a grid in such a way that the step-function nature of the fluid volume fractions is retained. A straightforward numerical approximation cannot be used because numerical diffusion and dispersion errors destroy the sharp, step-function nature of the distribution of the fluid volume fractions. Thus, numerical schemes dedicated to the advection of discontinuous functions in 3D must be used.

The level set (LS) technique [7] is also Eulerian in nature, and like VOF in principle, except that a continuous function is used to delineate the phase boundary. The level set function Φ is defined as the signed minimum distance to the interface, positive on one side and negative on the other. Thus, the sign of the function at any point defines in which phase the point lies, and its magnitude defines its distance from the interface. The interface itself is the surface $\Phi=0$. Clearly, Φ is continuous across the interface, and its normal gradient is unity at the interface. With Φ known throughout the flow field, the normal gradient and curvature of the interface can be determined in the same way as with VOF, using values in neighbouring cells. Again, as with VOF, the level set function Φ is advected with the flow field. The basic overhead of the method computationally is that it is necessary to re-

initialise Φ after each advection step to ensure that the isosurfaces of Φ remain locally parallel to the interface. This is necessary because of the "blending" procedures that need to be introduced for the discontinuous changes in the physical properties.

In summary, probably the most popular and successful method for free surface modelling is the VOF technique and its derivatives, mainly because of its simplicity and robustness. Research to improve the VOF method is still underway, and is focused on deriving better, more accurate, ways to move fluid fractions through the grid.

References

1. Unverdi, S.O. and G. Tryggvason (1992), "A front-tracking method for viscous, incompressible, multifluid flows", *J. Comput. Phys.,* Vol. 100, pp. 25-37.
2. Hou, T.Y., J.S. Lowengrub and M.J. Shelley (2001), "Boundary Integral Methods for Multicomponent Fluids and Multiphase Materials", *J. Comp. Phys.*, Vol.169, pp. 302-323.
3. Hirt, C.W., A.A. Amsden and J.L. Cook (1974), "An arbitrary lagrangian-eulerian computing method for all flow speeds", *J. Comp. Phys.*, Vol. 14, pp. 227-253.
4. Gingold, R.A. and J.J. Monaghan (1977), "Smoothed particle hydrodynamics: theory and application to non-spherical stars", *Mon. Not. R. Astron. Soc*., Vol. 181, pp. 375-389.
5. Koshizuka, S. and Y. Oka (1996), "Moving-particle semi-implicit method for fragmentation of incompressible fluid", *Nucl. Sci. Eng.,* Vol. 123, pp. 421-434.
6. Osher, S. and R.P. Fedkiw (2001), "Level Set Methods: an Overview and Some Recent Results", *J. Comp. Phys.*, Vol.169, pp.463-502.
7. Sethian, J.A. (2001), "Evolution, implementation, and application of level set and fast marching methods for advancing fronts", *J. Comp. Phys*., Vol.169, pp. 503-555.
8. Jacqmin, D. (1999) "Calculation of Two-Phase Navier-Stokes Flows Using Phase-Field Modeling", *J. Comp. Phys.*, Vol.155, pp. 96-127.
9. Harlow, F.H. and Welch, J.E. (1965), "Numerical Calculation of Time-Dependent Viscous Incompressible Flow", *Phys. Fluids,* Vol. 8, pp. 2182-2189.
10. Hirt, C.W. and B.D. Nichols (1981), "Volume of Fluid (VOF) Method for the Dynamics of Free Boundaries", *J. Comp. Phys.,* Vol. 39, pp. 201-225.
11. Lafaurie, B., C. Nardone, R. Scardovelli, S. Zaleski and G. Zanetti (1994), "Modelling merging and fragmentation in multiphase flows with SURFER", *J. Comput. Phys*, Vol. 113, pp. 134-147.

5.4. Fluid-structure interaction

5.4.1. Fluid-structure interaction methods and modelling

The interplay between fluid and adjacent structure is called fluid-structure interaction (FSI). The structure might be either immersed in the fluid or it could enclose the fluid. A pipe with a heated wall is an example for a simple FSI set-up. The fluid inside the pipe will influence the stress and temperature distribution in the pipe wall, while the thermal inertia of the latter and its heat transfer will have an impact on the temperature distribution inside the fluid in a transient process. More complex FSI involves structure displacements/deformations. For example, such might occur when highly energised flow

impinges on long, slender and flexible structures such as rods, tubes, etc., and thus deforms these structures. As a result, flow-induced vibrations occur. The best practice guidelines in this section are dedicated to the analysis of such phenomena. Nevertheless, some of these could be used also for other FSI types.

FSI is considered in the design process and the analysis of technical systems in many engineering disciplines such as nuclear, automotive, aerospace, energy, healthcare, construction, oil, and gas, etc. Neglecting the effects of the interaction between the structure and the flow might lead to serious damage to the structures, e.g. from accelerated fatigue up to catastrophic damage. Therefore, such phenomena need to be predicted and analysed with the help of simplified engineering estimations or numerical tools.

In the past, the issues with FSI phenomena were investigated with the help of empirical correlations [1, 2]. Today, modern 3D CFD programs can be coupled with computational structural mechanics (CSM) tools to allow an FSI analysis [3]. In the following sections, focus will be put on FSI with structure deformation. In each domain (solid and fluid), mathematical equations are solved to determine loads and mesh deformations. These equations are solved on discretised domains, represented with numerical meshes. In coupled FSI applications usually the CFD program calculates the forces on the common boundary interface (usually a wall) and provides these to the computational solid mechanics (CSM) code. The CSM code uses these as boundary conditions and then calculates the mesh deformation. With the deformed mesh as a boundary condition, the CFD performs the next iteration within the time step. This sequence repeats until all convergence criteria are met.

The choice of the FSI coupling between CFD and structural models is one of the main difficulties in FSI simulation. Depending on the analysed FSI phenomena and of the expected results from root cause analysis to quantitative evaluation of displacement of the structure or force on structure, different FSI methods may be applied. Thus, competences in both fluid and structural mechanics are needed to choose the appropriate CFD and CSM methods and models.

5.4.1.1 Coupling approach and data transfer

The level of coupling between the CFD and the CSM simulations required to obtain consistent results depends on the specific application. If the structure displacement is small enough to consider its influence on the fluid flow negligible, a sequential simulation approach could be retained: The structure is not included in the CFD simulation and the time history of the fluid forces, calculated by this stand-alone CFD simulation and acting on the structure, is provided as boundary condition to the CSM simulation. The CFD and CSM simulations are therefore performed separately, and this FSI simulation approach is generally referred to as one-way coupling. For moving structures with displacements large enough to alter the flow pattern, a real coupling approach is required: the CFD and the CSM calculations are performed along the same simulation, with a continue data transfer between the two blocks (CFD and CSM). This approach is generally referred to as two-way coupling.

Thus, according to the literature, three main FSI simulation approaches exist:

- Decoupled sequential approach: The whole analysis is first performed with one of the codes (CFD), and then the solution variables are provided as time-dependent boundary conditions in a table form to the second code (CSM). In this analysis two stand-alone simulations (CFD and CSM) are sequentially performed. This approach is referred to as one-way coupling.

- Partitioned approach: The equations governing the flow and the displacement of the structure are solved with two separate (CFD and CSM) solvers. Both solvers exchange data during the simulation. This approach is referred to as two-way coupling.
- Monolithic approach: The equations governing the flow and the equations describing the structural displacement are solved simultaneously in one single solver. This approach is referred to as two-way coupling.

5.4.1.2 Coupling approach vs application

The CFD code calculates the fluid pressure and viscous forces and the coupling software transfers and applies these on the structural walls. With these boundary conditions, the CSM code calculates the equation of motion and determines the new mesh displacement of the solid structure. The shape of the CFD domain is then modified correspondingly, and the balance equations in the CFD domain are solved again for the next iteration.

In the following, the coupling approaches introduced in the previous paragraph 5.4.1.1 are discussed in terms of their application to FSI phenomena:

- One-way coupling: In the one-way coupling the CFD code provides boundary data to the CSM code. The latter solves the designated physics equations, but its solution is not transferred back to the CFD programme. In this manner, the CSM feedback is neglected. This scheme is computationally cheaper than the one of the two-way couplings, but its application has certain limitations. It is used for problems, where the feedback from the second code does not have a significant influence on the FSI results. One-way coupling can be successfully applied to vibrations of steam pipes where the structural displacement will not perturb the steam pressure. Another application of one-way coupling is the fuel rod vibration under the core axial (or mainly axial) flow: these flow-induced vibration is in normal operation conditions) of very small amplitudes and have negligible influence on the turbulent scales of the flow, responsible for the fluid forces on the rods. In such conditions, a sequential FSI approach can generally predict consistent results in terms of vibration behaviour, provided that the fluid forces are consistently predicted by the CFD simulation. LES simulations are therefore often required to properly calculate the turbulent fluctuating pressure fluid forces acting on the structures. If such LES simulations are unfeasible (due to their high computational cost), hybrid LES/URANS approaches or URANS with turbulence models coupled to stochastic models, that generate fluctuations, might be used. Such pressure fluctuation model is proposed in [7] Once the fluid force time and space history on the walls is calculated by the CFD, it is applied as boundary condition for the CSM simulation to calculate the associated structure displacements/stresses.
- Two-way coupling: In the two-way coupling the CFD programme provides boundary data to the CSM code, and the CSM feedback is transferred back to the CFD programme. The CFD uses this data as boundary condition for the calculation of the next coupling iteration/time step. In this iterative process, the feedback from the CSM code is considered in the coupled code solution. This scheme is computationally expensive in comparison with the one-way coupling scheme, but provides some advantages over it (larger displacements, eigen frequency excitations, simulation of resonance vibrations, etc.). Many FSI configurations feature structure displacements/vibrations large enough to significantly deform the fluid-structure interfaces and, in turn, the flow pattern. Vibrations of slender structures in crossflow (tubes of U-tube SG, for example) generally feature

significant amplitudes, above all in case of resonances/instabilities. Self-excitation mechanisms leading to high vibration amplitudes can occur also for slender structures in axial flow. For all this type of configurations, a two-way coupled FSI simulation approach is required to predict consistent results.

5.4.1.2.1 Classification of the two-way partitioned approaches

In a two-way coupled approach, CFD and CSM calculations share data along the same transient simulation. Different levels of coupling can be retained. A first approach consists in sharing data only at the end of each numerical time step: once the CFD calculation is converged, the fluid forces are passed to the CSM tool as boundary conditions, which in turn calculates the structure displacement; the displacement is then applied to the CFD calculation as boundary condition for the next time step, and so on. This approach, referred to as two-way explicit (or weak) coupling, (weak coupling) can be consistent for problems where the fluid-structure coupling is weak, i.e. the coupling time scales and/or the structure displacements between two-time steps are small enough to consider that the fluid behaviour quickly adapts to the new deformed interface and is, therefore, correctly predicted after a single coupling iteration. The deformation of a plate, the opening of a valve are typical examples for which such partitioned approach should provide consistent results. of such configurations. Explicit coupling is considered as numerically least stable.

If the fluid flow and the structure displacement are strongly coupled, i.e. the structure displacement calculated during a time step has a large, instantaneous influence on the fluid flow (and vice versa), a two-way explicit coupling can lead to inconsistent results. Resonances between fluid and mechanical modes (vortex induced vibrations, for example) and fluid-elastic instabilities are examples for phenomena that need to be analysed with of such coupling approaches. For these configurations, convergence between the fluid flow and the structure displacement should be achieved within each time step: the CFD and CSM codes share data within each time step (and not only at the end, as for the two-way explicit approach), until convergence is reached. This approach is generally referred to as two-way implicit. Implicit couplings provide higher numerical stability but are also more costly.

One should also note that the smaller the numerical time step value is, the smaller the perturbation on the flow and the structure motion will be. Therefore, for very small (compared to the fluid and structure time scales) numerical time steps, one should expect that results calculated through a two-way explicit approach will tend to be identical with the ones calculated through a two-way implicit approach.

Fluid-structure resonance mechanisms usually feature coupling frequencies much smaller than turbulence scales: the fluid modes that URANS approaches can calculate can, in certain cases, be sufficient to predict the consistent fluid forces acting on the solid walls.

Simplified fluid models can be used in the two-way coupling approach. Linear (acoustic or potential based) fluid models are available in most CSM codes and are commonly used together with linear structures to perform fluid-structure interaction vibroacoustic analyses in both the time and frequency domains. These models have been used for simulation of the depressurisation wave following a pipe break in light water reactor i.e. LOCA (loss-of-coolant accident) [8]. The main load during a LOCA is due to the asymmetric pressure waves propagating in the vessel and internals. The simulation of the pressure waves does not require the resolution of the turbulent flow that could be neglected. A linear fluid model is the most appropriate choice to reduce the calculation time, as resolving the Navier-Stokes equations would require a factor ten or more in CPU time. Still, the most important phenomena for the structure integrity, the pressure wave propagation, is resolved in a much more efficient way.

5.4.1.2.2 Simulation parameters

5.4.1.2.2.1 Coupling interface

Numerical convergence at the coupling FSI interfaces is essential for the numerical stability and the accuracy of the FSI results. Therefore, convergence should be achieved in both codes and at the coupling interfaces. This convergence strongly depends on the numerical grids used.

In a two-way coupling approach, it is possible to consider two main options for the modelling of the fluid-structure interface:

- Methods with moving fluid grid and explicit representation of the fluid-structure interface: The structure is solved through a dedicated mesh, which deforms as a function of time, space, and the forces, provided by the CFD code. The CSM code then deforms the common CFD-CSM boundary. This approach is referred to as Arbitrary Lagrangian-Eulerian (ALE). The generation of conformal CFD and CSM meshes (node-to-node) at the coupling interface might be very challenging, sometimes even impossible. Therefore, methods such as General Grid Interface [4] allow the use of non-conformal grids at the interfaces, thus significantly increasing the flexibility of the mesh generation process for the FSI simulation.
- Methods with fixed fluid grid: Typical representative is the immersed boundary method, in which the Eulerian fluid grid is fixed, while Lagrangian structure nodes can move over it. The elastic forces, calculated by the CSM programme, are interpolated from the structural nodes to the surrounding fluid. The velocity is then interpolated from the CFD domain to the structural nodes.

There are further FSI methods like Chimera (moving and fixed fluid grid), particle methods (SPH), etc. A good overview on the different FSI methods can be found in [5].

5.4.1.2.2.2 Numerical time step

Special attention should be paid to fixing the numerical time step. Both fluid and structure parameters should be considered to estimate a consistent value of this parameter. On the fluid side, the choice of an appropriate time step is often driven by both physical (flow time scales) and numerical (CFL) considerations. The CFD time step is usually significantly lower than the structure time scale. Nevertheless, attention should be paid to always guarantee proper time discretisation of the structure motion: For example, enough time steps per natural motion period should be guaranteed.

5.4.1.2.2.3 Reduced order models

Since coupling of CFD and CSM programmes might become expensive concerning CPU time, reduced order model techniques can be used to provide reliable results at lower computational cost. Reduced order models are useful in settings where it is often unfeasible to perform numerical simulations with the complete full order model. This can be due to limitations in computational resources or the requirements of the simulation setting. On the other hand, the generation of the input for the reduced order model or its training may also require significant effort. In a coupled FSI run, reduced order models could substitute either the CFD or the CSM code to speed up the calculation. CFD simulation coupled to a mechanical reduced order model might reduce the overall wall-clock time of the FSI run almost down to the wall-clock time needed by the CFD stand-alone simulation.

5.4.2. Application in the nuclear reactor safety

Several examples of FSI applications in the field of nuclear reactor safety are listed below:

- evaluation of FIV in reactor cores, steam generators, and other components;
- evaluation of thermal fatigue in T-junctions, welds, etc.;
- detailed assessment of pressurised thermal shock (PTS) scenarios and their impacts on the nuclear reactor structural integrity;
- evaluation of neutron flux fluctuations in reactor cores;
- investigation of sloshing phenomena, resulting from seismic loads;
- fuel assembly bow;
- crack growth analysis;
- analysis of water hammer phenomena;
- evaluation of hydraulic forces and broken pipe motion as a consequence, for example, of a double ended LOCA (guillotine rupture).

Since the evaluation of the FIV is one important field of application of FSI methods in reactor safety, best practice guidelines are provided for such analysis.

5.4.3. Best practice guidelines for the numerical evaluation of FIV phenomena with FSI methods

The first step of a FSI analysis is to become acquainted with the scenario to be investigated. The assessment of the phenomena expected to occur will help you with the identification of the suitable FSI method for the study. For example, a URANS approach might be sufficient for the analysis of a scenario with structural vibrations, triggered by an external load, while this approach might provide inaccurate results for a scenario with structural vibrations induced by flowing fluid. In such cases, LES or hybrid URANS/LES turbulence approaches are expected to provide better results. In this initial phase of the analysis, empirical correlations and models might be used to have a rough estimation of the system's vibration characteristics. Usually, these correlations are derived from experiments with simple geometries (rods, tube arrays), and therefore, are subject to some limitations [1, 2].

In a next step, more information on the occurring phenomena in the investigated scenario could be gathered by performing stand-alone CFD and CSM simulations. Steady state or transient CFD calculation will provide important information on the flow field (fluid velocity, pressure and temperature distributions). The CFD analysis should consider the BPGs for CFD simulations, described in this report (influence of time step size, advection scheme, turbulence model, etc). On the structural side, a modal analysis, performed with the CSM code, will reveal the eigen frequencies and the mode shapes of the structure, providing valuable information on structure vibration behaviour.

The mesh quality needed for a FSI analysis is generally higher than for a pure CFD simulation. During the coupled calculation mesh deformation occurs. This directly affects the mesh quality during the simulation run by changing important mesh parameters (min. orthogonality angle, expansion factor, aspect ratio, skewness, etc). This might negatively affect the CFD solver convergence and lead to instability and other numerical issues. Furthermore, very small volumes in the vicinity of the moving boundary might also be deformed extremely because of the mesh displacement. The result might be negative volumes in the numerical mesh, which immediately lead to simulation crash. In such cases one can enlarge the volumes (coarsen the mesh) in the vicinity of the boundary region. The

price is lower accuracy. If the user cannot insist on the high accuracy, the appearance of negative volumes could be avoided by increasing the mesh stiffness around small volumes or FSI boundaries. Such options are available in advanced commercial CFD programmes.

The information from both CFD and CSM stand-alone calculations might then be used by the analyst to choose the appropriate FSI method. At this stage the analyst should decide if 1-way coupling will be sufficient, or two-way coupling will be needed to properly address the expected vibration phenomena. This decision might be preliminary, because detailed information on the real size of the vibration amplitudes will not be available. Furthermore, before carrying out the high-fidelity, expensive FSI simulations, reduced order models might be used. Although such approaches usually have some limitations, these provide valuable information on the vibration phenomena at comparatively low cost [6].

After analysing the whole information on the investigated FIV so far, the FSI analyst may proceed with the decision for the final FSI method to be used. At this point, it is important to mention, that if a two-way coupling is necessary, the results of the sensitivity analyses (time step size, advection scheme, etc.), performed previously with the CFD stand-alone simulation, might not be applicable for the coupled two-way FSI simulation. This is because of the present feedback from the CSM to the CFD domain. For example, using two different small time step sizes in a stand-alone CFD simulation might result in nearly the same velocity distribution in the computational domain. In a two-way CFD-CSM simulation these two-time step sizes might lead to nearly the same velocity distribution in the CFD domain as in the pure CFD simulation but predict two vibration amplitudes that differ by factors.

Therefore, although expensive, some sensitivity analyses need also to be performed with the coupled code. The Courant-Friedrichs-Lewy (CFL) number (mean and maximum) should be kept low throughout the whole simulation for numerical stability and high-quality results. The analyst should also estimate the length of the simulated problem time. He/she must ensure that at least several flow through times (relation between flow path length, flow velocity and simulated time) occur during the simulated problem time. It is also important to gain enough statistics for the post-processing of the results (FFT analyses, etc). The frequency resolution in the FFT analysis is directly proportional to the signal length and the sampling rate. Therefore, appropriate simulation time and time step size should be chosen to resolve the frequencies of interest. A rough estimation of the expected wall-clock time for the simulation should also be made. Sometimes, the strict following of all best practice guidelines might result in simulation times well beyond the time available for the whole FSI analysis.

Before performing the final FSI analysis, attention should be paid to the specified convergence criteria. Within each time step the CFD and CSM codes should reach internal convergence, and this applies also for the convergence of the quantities in the coupling interface. Therefore, the execution of sufficient number of code-to-code iterations within the time step should be ensured.

The post-processing of a FSI simulation should not be underestimated. The size of the generated data is usually large, not only because of the large numerical meshes, but also because of the large number of time steps performed. Most simulation tools will provide detailed information on the mesh displacement, but often velocities and accelerations of the deforming structures need to be provided. In such cases the first and second derivatives of the displacements must be calculated. Attention should also be paid to the FFT analysis (length, sampling frequency, window functions, etc.) that will make the transition of the results from the time domain into frequency domain.

References

1. Blevins, R.D. (1979), *Formulae for Natural Frequency and Mode Shapes*, Krieger Publishing Company, New York.

2. Blevins, R.D. (1979), "Flow-induced vibration in nuclear reactors: a review". In: *Progress in Nuclear Energy,* Pergamon Press, pp. 25-49.

3. Yuan, H., J. Solberg, E. Merzari, A. Kraus, I. Grindeanu (2017), "Flow-induced vibration analysis of a helical coil steam generator experiment using large eddy simulation"*, Nuclear Engineering and Design*, Vol. 322, pp. 547-562.

4. Ansys Inc. (2021), Ansys® FLUENT, Release 2021 R1, Help System, ANSYS FLUENT User's Guide.

5. Degroote, J., T. Demeester and N. Delaissé (2020), *Computational Methods for FSI/FIV, Fluid-Structure Interaction for Industrial Applications*, Von Karman Institute Lecture Series, Brussels, Belgium.

6. Papukchiev, A. (2019), "Numerical analysis of reactor relevant vibrations using advanced multiphysics CFD-CSM methods", *Nuclear Engineering and Design*, Vol. 350, pp. 21 -32.

7. De Santis, D., J. Chouchoulis and A. Shams (2019), "An innovative numerical framework for the simulation of flow induced vibration for nuclear applications", SESAME International Workshop*,* Petten, the Netherlands.

8. Nilsson, K. and F. Tornberg (2019), "On blowdown analysis with efficient and reliable direct time integration methods for wave propagation and fluid-structure-interaction response", *Computers & Structures*, Vol. 216, pp. 1-14.

6. User control of the numerical model

User control of numerical models comes primarily through selection of discretisation in space and time, and through care in selection of convergence criteria for any iterative solution procedures. These issues are addressed both here through guidance on initial choice, and in Section 8 where guidance is provided for checking of errors associated with these choices. Available options are discussed for numerical approximations to differential operators, as are other options such as surface tracking that can improve modelling fidelity.

6.1. Transient or steady model

The choice between transient and steady state is only an issue with RANS based simulations. More detailed simulations based on LES, DES and DNS are fundamentally transients. Most selections are based on common sense, and the only serious problems in making the choice arise in configurations that appear steady based upon imposed boundary conditions but may be shedding vortices (e.g. from a trailing edge) or contain fundamentally unstable macroscopic flow patterns.

The best option for questionable flows is to run a transient and inspect the flow patterns. If the user wishes to start the analysis running a CFD code in steady state mode, it is important to understand the code's algorithm for obtaining steady state. If the specific CFD code achieves steady state solutions through some pseudo-transient iteration procedure, it will generally not converge if the flow is fundamentally transient. However, if its algorithm is a direct solution of flow equations with no time derivative terms, it may provide a smooth answer that masks actual transient behaviour.

If vortex shedding is detected a more important question is level of detail required in simulating a flow. RANS does not do a particularly good job of resolving these vortices, and consideration should be given to use of a code with LES or DES options (see Section 5.1.4).

6.2. Grid requirements

The computational grid is a discretised representation of the geometry of interest. It should provide an adequate resolution of the geometry and the expected flow features. The grid's cells should be arranged in a way to minimise discretisation errors. Specific recommendations here follow closely those provided by ECORA and ECOFTAC [1, 2].

6.2.1. Geometry generation

Before the grid generation can start, the geometry must be created or imported from CAD data or other geometry representations. Attention should be given to:

- Use of correct coordinate systems.
- Use of correct units.
- Completeness of the geometry: if local geometrical features with dimensions below the local mesh size are not included in the geometrical model, for instance fuel element assemblies, they should be incorporated via a suitable empirical model.
- Oversimplification due to physical assumptions: problems can for instance arise when the geometry is over-simplified, or when symmetry conditions are used that are not appropriate for the physical situation.

- Location of boundary conditions: the extent of the computational domain has to capture relevant flow and geometrical features. A major problem can be the positioning of boundary conditions in regions of large gradients or geometry changes. If in doubt, the sensitivity of the calculation to the choice of computational domain should be checked.

When the geometry is imported from CAD data, these data should be checked thoroughly. Frequently, CAD data must be adapted (cleaned) before they can be used for mesh generation. For instance, some mesh generators require closed three-dimensional volumes (solids) for mesh generation, and these are not always directly obtained from CAD data. Therefore, the CAD data must be modified. However, care must be taken to ensure that these changes to the geometry do not influence the computed flow.

6.2.2. Grid design

In a CFD analysis, the flow domain is subdivided into many elements or control volumes. In each computational cell, the model equations are solved, yielding discrete distributions of mass, momentum and energy. The number of cells in the mesh should be sufficiently large to obtain an adequate resolution of the flow geometry and the flow phenomena in the domain. As the number of elements is proportional to storage requirements and computing time, many three-dimensional problems require a compromise between the desired accuracy of the numerical result and the number of cells. The available cells need to be distributed in a manner that minimises discretisation errors. This leads to the use of non-uniform grids, hybrid grids consisting of different element types, overset grids, and local grid refinement.

Modern CFD methods use body-fitted grids where the cell surfaces follow the curved solution domain. Different mesh topologies can be used for this purpose as follows:

- Structured grids consist of hexahedral elements. Cell edges form continuous mesh lines which start and end on opposite block faces. The control volumes are addressed by a triple of indices (i,j,k). The connectivity to adjacent cells is identified by these indices. Hexahedral elements are theoretically the most efficient elements and are very well-suited for the resolution of shear layers. The disadvantage of structured grids is that they do not adapt well to complex geometries, although this problem can be eliminated using an overset grid.
- Unstructured grids can be generated automatically by assembling cell by cell without considering continuity of mesh lines. Hence, the connectivity information for each cell face must be stored in a table. This results in an increase of storage requirements and calculation time. Often, tetrahedrons are used as mesh elements. Special types of unstructured grids are:
  - hybrid grids that combine different element types, i.e. tetrahedral, hexahedra, prisms and pyramids;
  - block-structured grids that are assembled in an unstructured manner from several structured mesh blocks.

6.2.3. Grid quality

A good mesh quality is essential for performing a good CFD analysis. Therefore, assessment of the mesh quality before performing large and complex CFD analyses is very important. Most of the mesh generators and CFD solvers offer the possibility to check the mesh parameters, such as grid angles, aspect ratios, face warpage, right-handedness, negative volumes, etc. The CFD user should check the guide of the applied mesh generators

and CFD solver for specific requirements. General recommendations for generating high-quality grids are to:

- Avoid grid angles below 20° and above 160°.
- Avoid jumps in grid density: growth factors between adjacent volumes should be smaller than 2.
- Avoid non-scalable grid topologies: non-scalable topologies can occur in block-structured grids and are characterised by a deterioration of grid quality under grid refinement.
- Avoid grid lines which are not aligned with the flow direction (e.g. tetrahedral meshes, in thin wall boundary layers). Computational cells that are not aligned with the flow direction can lead to significantly larger discretisation errors.
- Avoid high grid aspect ratios: this criterion depends on the flow solver. For standard iterative solvers, aspect ratios should not be larger than 10 to 50 to obtain convergent solutions. Solvers with multigrid acceleration can absorb higher aspect ratios.
- Use a finer and more regular grid in critical regions, e.g. regions with high gradients or large changes such as free surfaces.
- Avoid the presence of non-matching grid interfaces in critical regions. An arbitrary grid interface occurs when there is no one-to-one correspondence between the cell faces on both sides of a common geometry face.
- In areas where local details are needed, the local grid refinement can be used to capture fine geometrical details. If grid refinement is used, the additional grid points should lie on the original boundary geometry, and not simply be a linear interpolation of more grid points on the original coarse grid.

If the target variables of a turbulent flow simulation include wall values, like wall heat fluxes or wall temperatures, the choice of the wall model and the corresponding grid resolution can have a large effect on the results. Typical “wall functions” are:

- Calculation of the wall shear stresses, and wall heat fluxes based on logarithmic velocity and temperature profiles.
- Calculation of the wall shear stresses, and wall heat fluxes based on linear velocity and temperature profiles.
- Calculation of the wall shear stresses, and wall heat fluxes based on linear/logarithmic velocity and temperature profiles.

Wall functions of this kind are used for all RANS turbulence models, and for LES and DES simulations. The choice of the wall model has a direct influence on the mesh design. The following values are recommended for the distance of the first grid point away from the wall:

- Logarithmic wall functions: $30 < y^+ < 500$. The upper limit is Reynolds number dependent. The limit decreases for decreasing Reynolds numbers. A logarithmic near-wall region does not exist for very small Reynolds numbers.
- Linear wall functions: $y^+ < 5$. Linear wall functions can only be used in combination with special low-Re versions of the k-ε turbulence model. k-ω-type models usually do not need special modifications.

- Linear/logarithmic wall functions: $y^+ < 500$. Linear/logarithmic wall functions can only be used in combination with special low-Re versions of the k-ε turbulence model. k-ω type models usually do not need special modifications.

Here y^+ is the non-dimensional wall distance:

$$y+ = \frac{\rho u}{\mu} \quad y\tau = \frac{\sqrt{\rho \tau_w} y}{\mu}$$

The recommendations above are strictly only valid for two-dimensional attached flows. The logarithmic law is not valid for separated flows. Close to separation, the wall shear stress τ_w goes to zero, and with it the non-dimensional wall distance y^+, irrespective of the physical wall distance, y. In contrast, the linear near-wall law remains valid, but requires finer resolution. The combination of logarithmic and linear wall functions yields the best generality and robustness against small variations of the near-wall grid distance.

For two-dimensional flows, the following equation is valid:

$$u\ U\tau = {}_e\sqrt{c_f/2}$$

U_e is the velocity at the boundary layer edge or a characteristic reference velocity. The skin friction coefficient c_f for turbulent flows is typically in the interval from 0.003 … 0.005. With these two values, the friction velocity u_τ and the distance of the first grid point away from the wall can be a priori estimated as:

$$y = \frac{y+\mu}{\rho u_\tau}$$

Finally, some recommendations regarding the choice of element types are made:

- Hex elements are the most efficient elements from a numerical point of view. They require the least memory and computing time per elements. They can be well adapted to shear layers (long and thin), for instance in the vicinity of walls. However, generation of hex meshes in complex geometries often requires a large manual and cognitive effort.
- If this effort seems too high, use of tetrahedral meshes is a viable alternative. Tetrahedral elements require roughly 50 % more memory and computing time per element than hex elements. They are not very efficient for the resolution of shear layers: Either many tetrahedral elements must be used, or the grid angles become very small. If wall values are the target values of a calculation, pure tetrahedral meshes should either be avoided or used with great care.
- The combination of tetrahedral elements in the flow domain and prism elements close to walls is a *reasonable* alternative to the use of pure tetrahedral grids. The combination of tetrahedral elements in the flow domain, and hex elements close to walls (with pyramids as transition elements) is a *good* alternative to pure tetrahedral grids.
- Non-matching grid interfaces, which combine different grid types and/or mesh densities, should be avoided, if possible. They can have a negative impact on accuracy, robustness (convergence) and parallel scalability (depending on the numerical algorithm and the application).

Based on these observations, the following rules and priorities can be formulated to obtain the best accuracy and efficiency:

1. Use of pure hex element grids if the grid generation effort is manageable.
2. Use of hybrid grids with hex elements close to walls, and tetrahedral elements in the core of the domain.
3. Use of hybrid grids with prism elements close to walls, and tetrahedral elements in the core of the domain.
4. Use of pure tetrahedral element grids.

The order becomes reversed if the manual grid generation effort is the sorting parameter. The final decision and compromise which grid to use is up to the user. However, the reasoning which has led to the use of a particular grid and topology should be part of the final documentation of the analysis.

A grid dependence and sensitivity study should always be performed to analyse the suitability of the mesh and to provide an estimate of the numerical error of the results. At least two (better: three) grids with significantly different mesh sizes should be employed. If this is not feasible, results obtained with different discretisation schemes in time and space can be compared on the same mesh (see Section 8.5).

References

1. Menter, F. (2002), "CFD Best Practice Guidelines for CFD Code Validation for Reactor-Safety Applications", European Commission, *5th EURATOM Framework Programme,* Report, EVOL-ECORA-D1.
2. Casey, M. and T. Wintergerste (ed.) (2000), *ERCOFTAC Best Practice Guidelines: Special Interest Group on "Quality and Trust in Industrial CFD" (Version 1)*, ERCOFTAC, London.

6.3. Discretisation schemes

Ideally, selection of discretisation schemes should be automated within the CFD code and not a user option. Unfortunately, the current state of CFD presents the user with a list of potential discretisation schemes with some general advice on situations in which each is appropriate. Selection of temporal and spatial discretisation is a balancing act between too much numerical diffusion for low order schemes, and spatial wiggles (unphysical non-monotonic behaviour) in key state variables with higher order schemes.

The concept of numerical diffusion was quantified for first order numerical schemes by Tony Hirt in 1967 [1]. Consider a simple 1-D advection equation, approximated with backward Euler time (fully implicit) and first order upwind spatial discretisation. Applying Hirt's analysis, the numerical solution can be shown to closely approximate the analytic solution of an advection-diffusion equation.

$$\frac{\partial \rho}{\partial t} + \frac{\partial}{\partial x}(\rho V) = D\frac{\partial^2 \rho}{\partial x^2},$$

where the numerical diffusion coefficient D is

$$D = \frac{V}{2}(V\Delta t + \Delta x).$$

Anyone contemplating use of numerical methods that are first order accurate in time or space, should obtain typical values for turbulent diffusion coefficients (or molecular diffusion coefficients if the flow is laminar), and use the previous formula to estimate the time step and/or mesh size needed to make the numerical diffusion substantially less than the physical one. In the case that physical diffusion is unimportant to a problem, numerical diffusion should at least be limited to the point that it does not significantly distort the results of advection terms.

In general, the use of first order discretisation should be avoided. The one significant exception comes in steady flow solutions. In some cases, a CFD code will be unable to converge its steady state iteration when using an appropriate higher order spatial discretisation. In this situation an initial steady solution can usually be obtained with a first order spatial method, then this used as a starting point for iteration to steady state with the higher order method. However, even this approach does not always work, and the CFD code may be trying to tell you that vortex shedding is significant, and no steady solution exists.

Higher order methods remove second derivative terms from Taylor truncation error analysis that give rise to obvious numerical diffusion. However, they do not completely suppress numerical diffusion. A recent study by Vyskocil [2] is one of many examples of the numerical diffusion that can be introduced by higher order methods, particularly in problems involving continuity or shock waves. He was able to demonstrate degradation of results for several spatial discretisation's, propagating a thermal wave in a flow field. The problem for the analyst is in quantifying the magnitude of numerical diffusion relative to turbulent diffusion in each simulation.

The Richardson based error analysis described in Section 8.5 is a way to determine that errors introduced by numerical diffusion are bounded. However, Richardson analysis tends to break down in continuity or shock waves (particularly near the inflection point), and even when working well does not allow direct comparison of numerical and physical diffusion. Another approach is to perform numerical experiments with simple continuity waves as in Vyskocil's work and analyse the results with the "C-Curve" method originally developed to extract diffusion coefficients from experiments (see Levenspiel [3]). Application of this technique to a simple numerical problem was described by Macian and Mahaffy [4] as part of a study on limiting numerical diffusion in boron dilution problems. The method is basically 1-D, so is most useful for examining the behaviour of portions of a mesh after the nature of the flow field has been established. Boundary conditions must be used carefully to isolate the chosen section of the mesh and to drive a continuity wave along the direction of flow observed in the full calculation.

Higher order upwind methods are typically selected for use in RANS calculations. However, LES, DES and DNS calculations need the lower numerical diffusion associated with central-difference methods (typically 4^{th} order or higher). For methods operating on a logically rectangular mesh, performance is optimal when flow is aligned with a mesh direction. Results should be studied with particular care when flow is diagonal to the mesh lines. All higher order methods have the potential for cell-to-cell spatial oscillations in key state variables, and results, particularly near continuity or shock waves, should be watched carefully for this behaviour. When these oscillations are severe, they can be controlled by a flux correction method (available in any up-to-date CFD code). Such techniques are automatically applied to limited areas and reduce the spatial accuracy to first order in these regions.

Local application of flux correction prevents the type of numerical diffusion associated with global use of a first order upwind method. However, a user needs to be cautious of two potential side effects. Many flux correction algorithms can take a wave with a very

gradual rise on the leading edge, and artificially sharpen it to something with a very steep leading edge. If propagation of sound or continuity waves is an important phenomenon in each simulation (e.g. boron dilution), some simple numerical studies should be run to understand the impact of selected numerical methods on wave shape, and a decision made on the physical significance of any distortions. The second side effect of flux correction is propagation of the local reduction of accuracy to the global solution. This is particularly a concern if internal code criteria for engaging flux correction are too loose and can be checked using Richardson analysis on simplified test problems (see Section 8.5).

When evaluating tests of discretisation schemes, it is important to keep a proper prospective. Understand that the results of a Richardson error analysis will probably indicate lower effective order of accuracy than advertised for the selected discretisation scheme. The important goals are to demonstrate convergence of the solution as the mesh or time step is refined (see Section 6.4.1) and to achieve acceptably low numerical distortion of important physical phenomena at the discretisation used in the final analysis.

References

1. Hirt, C.W. (1967), "Heuristic stability theory for finite-difference", *J. Comp. Phys*., Vol 2. No. 2, pp. 339-355.
2. Vyskocil, L. (2005), "Numerical Diffusion in FLUENT 6", *Proceedings of the 11th FLUENT User's Conference*, pp. 117-127.
3. Levenspiel (1972), *Chemical Reaction Engineering*, 2nd Ed. New York, Wiley.
4. Macian, R. and J.H. Mahaffy (1998), "Numerical diffusion and the tracking of solute fields in system codes: Part I. one-dimensional flows", *Nuclear Engineering and Design*, Vol. 179, pp. 297- 319.

6.4. Convergence control

There are two meanings of *convergence* in common use in CFD. Both forms of convergence must be checked to understand the accuracy of a calculation.

6.4.1. Differential versus discretised equations

The first convergence refers to the formal process which brings the exact solution of the discretised equation set ever closer to the exact solution of the underlying partial differential equations, as each of the discretisation sizes for independent variables approaches zero. That is:

$$T_j^n \to T\left(x_j, t_n\right) \text{ as } \Delta x_j, \Delta t \to 0.$$

In practice, the definition is not very useful, since exact solutions of algebraic equations (with no round-off errors, for example) are generally difficult to obtain, and exact solutions of the partial differential equations even more so, except for a few over-simplified demonstration cases. However, in the case of linear equations, it is possible to link the concept of convergence with *consistency* and *stability*, which are easier to demonstrate.

A system of algebraic equations generated by a space and time discretisation process is said to be *consistent* with the partial differential equation if, in the limit of the grid spacing and the time step tending to zero, the algebraic equation is identical with the partial differential equation at each grid point, always. Consistency may be demonstrated by expressing the differences appearing in the discretised equations in terms of Taylor expansions in space

and time, and then collecting terms. For consistency, the resulting expression will be identical with the underlying partial differential equation, apart from a set of remainder terms, which should all tend to zero as Δx_j, $\Delta t \rightarrow 0$. In CFD, almost universally, the numerical schemes for solving the fluid flow and energy equations are consistent, due simply to the methodology employed in their development.

Numerical stability, however, is far more difficult to prove, and most of the formal procedures are limited to linear equations. In a strict sense, stability only applies to marching problems (i.e. to the solution of hyperbolic or parabolic equations) and will be defined here accordingly. A numerical scheme is *stable* if errors arising from any source (e.g. round-off or truncation) do not grow from one time step to the next. The most common example of instability arises from the use of explicit time differencing for convective problems in which the time step exceeds the Courant-Friedrich-Levy (CFL) criterion [1]. Physically, this corresponds to information being numerically transported within a time step faster than the physical communication process, either by sonic or fluid velocities. In practical terms, small disturbances grow until the solution is destroyed. There are classical methods available for determining the stability of numerical schemes, but most of the work refers to linear systems.

The Lax Equivalence Theorem states that, given a well-posed, linear, initial-value problem (well-posed means that the solution develops in a continuous manner from the initial conditions), and a finite difference approximation to it that satisfies the consistency condition, stability is a necessary and sufficient condition for convergence of the numerical result to the analytic solution as discretisation is refined. The theorem is powerful since, as noted, it is much easier to demonstrate consistency and stability than convergence directly, though convergence is the most useful property in the sense of quality and trust in the solution. Though the theorem is stated in terms of finite differences, it applies too to other discretisation schemes, such as finite volume and finite element. The theorem can only be rigorously applied to linear, initial-value problems, whereas with CFD the governing equations are non-linear, and of the boundary- or mixed initial/boundary-value type. In these circumstances, the Lax Equivalence Theorem should be regarded as a necessary, but not sufficient, condition, and used heuristically to provide a pragmatic solution strategy, i.e. one that is consistent and stable.

Although users have no iron-clad guarantee of convergence to the solution of the Navier-Stokes differential equations, they should use common sense to look for obvious signs of trouble. Frequently analysts assume that step to step oscillations associated with bounded numerical instabilities are oscillating about the correct mean solution to the problem. This may not be the case and isolated time step sensitivity studies should be performed on any such case to determine shift in mean behaviour with time step size. Error studies discussed in Sections 8.5 and 8.6 are also important in this respect. Although convergence of results as time step or mesh size are reduced towards zero is not a guarantee that the numerical solution is converging to the solution of the set of PDE's, it is a good indicator. If no convergence can be seen in these sensitivity analyses, there is no hope of converging to the PDE solution.

6.4.2. Termination of iterative solvers

The second meaning of convergence refers to the criterion adopted to terminate an iterative process. Such processes nearly always arise in CFD simulations, because of (1) implicit or semi-implicit time differencing, and (2) the non-linear nature of the governing equations.

For a fully coupled solver, all the governing equations are considered part of a single system and are solved together. This means that all variables are updated simultaneously, and there is just one overall iteration loop. For highly non-linear equations in three dimensions, as

occur in industrial CFD applications, this entails a large memory overhead, and until recently such approaches were considered impractical. However, with the advent of large-memory machines and fast CPUs, the approach has become tractable, and today much modern commercial CFD software is built around the concept of fully coupled solvers.

An alternative is to treat each of the governing equations in isolation, assuming all other variables are fixed, and invert the subsystem matrix on this basis. This procedure is often called the *inner iteration*. The other equations are then all solved in turn, repeating the cycle, or *outer iteration,* until all the equations are satisfied simultaneously.

The solution of the fully coupled system of equations, and the inner loop of the non-coupled system, requires the solution of a set of linear, simultaneous equations, in other words, the inversion of a matrix. Except for small problems, for which inversion by Gaussian elimination can be attempted, the solution algorithm is usually iterative. In fact, the success of finite-volume discretisation schemes in CFD is largely since the algorithms produce diagonally dominant system matrices. Such matrices can be readily inverted using iterative methods.

A multitude of such methods have been derived, ranging from the classical Jacobi, GaussSeidel, successive-over-relaxation (SOR) and alternative direction implicit (ADI) algorithms, through the more modern Krylov family of algorithms (e.g. conjugate-gradient, GMRES) up to the more up-to-date multigrid and algebraic multigrid methods. All such methods involve pivoting on the diagonal entry for each row of the matrix, and the success and speed of convergence of the iteration process is essentially governed by how much this term dominates over the sum of the others in the row (supported by under-relaxation if necessary) and the accuracy of the initial guess.

When using iterative solvers, it is important to know when to stop and examine the solution (steady state problems) or move on to the next time step (transient solutions). The difference between two successive iterates, measured by an appropriate norm, being less than a pre-selected value is not sufficient evidence for solution convergence, but the information may be used to provide a proper estimate of the convergence error as follows. The largest eigenvalue (or spectral radius), λ_m, of the iteration matrix, may be estimated from the (*rms* or L_2) norms at successive iteration steps according to:

$\lambda_m=|r^n|/|r^{n-1}|$, where $r^n = \Phi^{n+1}-\Phi^n$, Φ is a dependent variable, and n the iteration number. A good estimate of the convergence error ε^n is then

$$\varepsilon_m \approx \left\| r^n \right\| / (\lambda_m - 1)$$

Though the analysis is based on linear systems, all systems are essentially linear near convergence, and, since this is the occasion when error estimates are needed, the method can be applied to non-linear systems as well. Further details are given in Ref. [2].

It should be emphasised that with commercial CFD software incorporating sequential (i.e. partially coupled) solvers, it may not be possible to have sufficient user access to control the convergence error in the way described above. For example, many solvers based on pressure/-velocity coupling algorithms rely on minimising the mass residual in the continuity equation. It is recommended that the residuals for each of the momentum equations, as well as for the energy equation for problems involving heat transfer, be controlled as well, just as they would be for fully coupled solvers. There is another issue as well: some "juggling" between the convergence criteria for the inner and outer iterations may be necessary to avoid wasting machine time. Obviously, it is not worth insisting on high accuracy for the inner iteration when the outer iteration is still far from convergence. The reader is referred to the code documentation on how best to optimise tolerances for

maximum CPU efficiency. However, as the solution approaches convergence in the outer iteration, minimisation of all the residuals should be enforced.

Regardless of the underlying iteration scheme, CFD users should perform some simple numerical studies to understand the effect of convergence criteria on solution accuracy. After a base run, a second run should be performed with all iterative convergence criteria halved. After plotting results for key variables, the user can make a practical decision on significance of the discrepancies. To make a conservative judgement of impact, all differences in results should be doubled.

References

1. Richtmyer, R.D. and K.W. Morton (1967), *Difference Methods for Initial-Value Problems*, Wiley, New York.
2. Ferziger, J.H. and M. Perić (1999), *Computational Methods for Fluid Dynamics*, Springer Verlag, Berlin/Heidelberg.

6.5. Free surface consideration

As discussed in Section 5.4, the presence of free surfaces introduces difficulties in the CFD analysis, whichever tracking algorithm is used. This is essentially since the location and movement of the free surface must be computed simultaneously with the flow field.

- The simplest solution is not to explicitly track the interface at all. This can be accomplished within a two-phase two-fluid code by using the void fraction (gas volume fraction) variable to describe where each phase is located. This approach is only acceptable if the free surface location is only required approximately since volume fraction information is only known cell-wise and will become diffuse because of the numerical diffusion associated with the solution scheme. Though "surface-sharpening" algorithms may be introduced to offset the interface diffusion, these tend to be ad hoc schemes, and do not guarantee mass and momentum conservation. From the standpoint of BPGs:
- It will not be possible to obtain completely grid-independent results but repeat runs with different meshes should be performed to give an indication of the degree of precision of the results.
- Numerical diffusion should be minimised by employing high-order space and time differencing algorithms.
  - Mass conservation must be checked if surface-sharpening algorithms are employed.

The most popular surface tracking methods are the front-capturing, Eulerian volume of fluid (VOF) [1], and level sets (LS) [2]. In principle, for incompressible fluids, the VOF methods preserve mass exactly since the volume fraction F is a conservation property. In practice, however, a surface reconstruction algorithm must be employed to define the actual interface location from the volume fraction information in each cell and their neighbours. In the most popular of these algorithms (PLIC-VOF) the interface is piecewise linear, with discontinuities at mesh boundaries. This can sometimes lead to small, isolated parcels of one fluid becoming trapped in the other fluid domain. Cleaning up can lead to mass-loss errors.

In the LS method, the Level Set Function Φ is not a conservation quantity and is often challenged on the issue of poor mass conservation. However, some successes have been

reported, so that from a BPGs viewpoint it is possible to nominate this property as one of the target variables.

Thus, for both VOF and LS approaches:

- Mass conservation check is the ultimate test of a good solution.
- The solution of the advection equation for F or Φ should be at least the same order as for the rest of the flow solution, otherwise it is impossible to judge the overall accuracy of the solution. Schemes should be at least second order to limit numerical diffusion.
- Grid independence checks should be made, as usual. The exercise has somewhat more importance in free surface flows because of the "numerical blending width" – usually a few mesh cells – over which the discontinuous change in physical variables across the interface is handled.
- The advection of the interface is often explicit: that is, the position of the interface is treated as "frozen" over the time step, even if the basic flow solver is implicit. This means that there will be a CFL time-step limitation controlled by the interface motion through the mesh.
- The surface tension force is usually incorporated as a body force spread over several computational cells in a band adjacent to the interface [3]. Sensitivity of results to the width of the band should be investigated.

References

1. Hirt, C.W. and B.D. Nichols (1981), "Volume of fluid (VOF) method for the dynamics of free boundaries", *J. Comp. Phys.,* Vol. 39, pp. 201-225.
2. Osher, S. and R.P. Fedkiw (2001), "Level set methods: an overview and some recent results", *J. Comp. Phys.,* Vol. 169, pp. 463-502.
3. Brackbill, J.U., D.B. Kothe and C. Zemach (1992), "A continuum method for modelling surface tension", *J. Comput. Phys.,* Vol. 100, pp. 335-354.

7. Assessment strategy

Here, assessment is understood as the expression of belief (based on validation calculations) that a given computer code is able (when properly used) to simulate with acceptable fidelity a given set of situations (at least parts of a nuclear reactor transient). Assessment therefore requires validations of a verified computer code on suitable experiments.

The overall situation is schematically shown in Figure 7.1. The complete process can be separated into the following eight activities, see Oberkampf [1]:

1. Identification and specification of the intended application.
2. Planning of verification and validation activities, especially use of the PIRT (see Section 2).
3. Development, implementation and documentation of verification activities.
4. Design and execution of validation experiments based upon the PIRT results.
5. Development and definition of useful metrics.
6. Assessment of the results of the validation metrics.
7. Assessment of the predictive accuracy of the code.
8. Accurate and complete documentation of the validation planning, results and consequences, concluding with a clear statement on predictive confidence for the intended application of the code.

Verification as used here is in fact an experiment-independent activity since in a strict sense of this term only analytical solutions (including manufactured solutions, see Roache [2] and Section 8.7.2 of this report) are used in verifying that the numerical properties of a given computer code correspond to those stated in the code documentation ("solving the equations right"). Nevertheless, results of calculations performed by means of a high-precision code (e.g. DNS) or selected separate-effect and well-designed experiments in simple geometries can contribute to the verification process. A poor match of calculation to a separate effect experiment originally used to formulate a particular model indicates the potential for a coding error. A good match is an indication of correct coding. The strength of these indications depends on how strongly the experiment isolates the effects of the model in question.

Validation ("solving the right equations") should be based on well-designed separate-effects or integral experiments with instrumentation enabling elimination of user effects (e.g. mistakes in modelling of initial and boundary conditions) and determination of sources of possible differences of experimental and analytical results. In any case it must be proved that all suitable tools of the code have been utilised and user errors have been eliminated. It is a good practice to plan the validation experiments as needed during the validation process rather than just once before all needs are understood. After validation computations are finished and the results evaluated, it is possible to review the existing validations and to produce a new, updated statement on the state of assessment of the code for given range of problems. Therefore, assessment should be understood as an ongoing, iterative process.

The assessment process is not cheap and easy, especially experiments and validation calculations when done at the highest level of precision and complexity. On the other hand, safety of nuclear power plants belongs to a class of problems, where the ability to do full-scale testing is very limited, in some cases even impossible, so that computational

simulations are the only possible tool. Erroneous results of computational analyses could therefore have dangerous consequences. It is desirable to improve confidence and understanding in these simulations.

Figure 7.1. Basic components of an assessment process

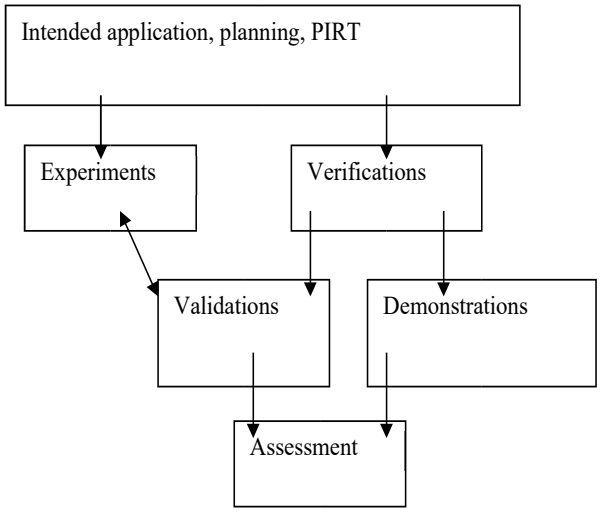

7.1. Demonstration of capabilities

Within safety analyses of nuclear power plants, there are situations where no validation calculations of the situation with the given computer code have been done so far, and even experimental data are sparse or non-existent. Under these conditions, computational simulations can be termed "demonstration calculations". These demonstration calculations, where no or limited and almost non-conclusive comparisons with experiments have been done, are frequently found in the literature. They demonstrate a certain capability of a code to perform such calculations and illustrate the required computational time and memory. These parameters could add some ground on decisions as regards to assessment of the code, but in no case can they replace verification and validation. A specific group of such "demonstration" calculations consists of simulations of experiments on mock-ups of parts of nuclear power plants. These test facilities are in some cases quite large so that only coarse computational grids are possible given the capacity of present (or available) computers. The assessment matrix should contain such experiments and simulations, but validation calculations aimed at individual physical phenomena involved in the experiment should also be made based on more detailed experiments on simpler models.

7.2. Interpretation of results

In analyses of computational results, several levels of comparisons can be observed (see Oberkampf et al [1]). At the lowest level, statements can be issued whether important physical phenomena observed in real world are seen in the analysed computation. This is a purely qualitative evaluation of results ("viewgraph norms" in the cited reference), most frequently represented by comparison of colour pictures of measured or observed situation with computed physical quantity at selected locations. Existence of maxima and minima of important state variables and their locations, existence of regions with recirculation flows or other distinguished flow regions found in real world should be the first criteria for success or failure of this qualitative analysis.

The next level of analysis of results is the quantitative comparison of target variables (see Section 9.6). These variables strongly depend on the intended application of the code and could therefore range from integral quantities like averaged values of velocity or temperature at selected planes or volumes to local quantities. Here, selection of suitable metrics is important, but simple graphical comparison of measured and computed values is the most frequent case. It is very important that both experimental uncertainty and numerical error are estimated and shown.

The highest level of comparison of results requires ensembles of experiments and computations to be performed so that experimental uncertainty and simulation results- are represented as estimated probability distributions. Then, a graph showing differences of the mean, or expected values of computational and experimental distributions with contours of one and two standard deviations can be produced.

References

1. Oberkampf, W.L., T.G. Trucano and C. Hirsch (2004), "Verification, validation and predictive capability in computational engineering and physics", *Applied Mechanics Reviews,* Vol. 57, pp. 345-384.
2. Roache, P.J. (1998), *Verification and Validation in Computational Science and Engineering*, Hermosa Publishers.

8. Verification of the calculation and numerical model

8.1. Introduction

Verification is defined as the process of determining that the implementation of a physical model accurately represents the developer's conceptual description of the model, and that the implementation of the numerical solution method precisely calculates the solution to the model. However, a distinction must be made between verification of the code itself by the developer and verification of the solution resulting from the application of the code to a particular input model by the code user. A code user clearly has responsibility for verification that quantifies and limits discretisation error and for verification of the initial conditions, boundary conditions and other special options provided in the input model. However, a code user must also confirm that the code itself has been adequately verified by obtaining and reviewing verification documentation from the developers. If such documentation is unavailable or inadequate, then appropriate caveats must be provided in documentation of results and/or the user needs to perform what code verification is possible.

A complete error evaluation for the solution of a particular simulation requires user consideration of several potential error indicators:

- quality assurance of the system input model;
- iterative convergence;
- basic consistency checks, e.g. checks on global mass, momentum and energy conservation;
- spatial grid sensitivity or convergence;
- temporal convergence.

Inconsistencies in any of these checks will quickly point to implementation problems in the input model (or on occasion the software). Once the verification checks have been passed, the validation task can start. Techniques to perform the verification tasks listed above are described in the remainder of this chapter.

8.2. Code verification

To the extent possible, code verification examines implementation of the full mathematical model through comparison to exact analytical results, manufactured solutions [1], or previously verified higher accuracy simulations. Oberkampf and Roy [2] provide a comprehensive introduction to these strategies.

Unfortunately, analytical results and manufactured solutions are only useful for verification of the portions of a code responsible for approximating partial derivatives and solving the system of PDEs associated with the flow problem. They do not help verify coding of complex algebraic expressions used for contributions such as turbulent diffusion coefficients, wall heat transfer functions, reaction rates and the equation of state. For them the first step is a good quality assurance (QA) procedure with rigorous version control and routine regression testing. End users who do not have access to the source code may consider benchmarking results of such models in independently developed codes for simplified test cases. Discrepancies strongly suggest, but do not prove, an error in the model implementation.

If the code developers' verification is inadequate, the code user needs to either independently verify the software or understand that the validation process (Chapter 9) may be effectively checking an undocumented model.

Comparison to data can also contribute to verification if there is sufficient knowledge about the expected performance of the numerical method or the physical model for a given test case. However, validation against trusted data should not be conflated with verification. They are not the same.

References

1. Roache, P.J. (2002), "Code verification by the method of manufactured solutions", *Trans. ASME, J. Fluids Engineering*, Vol. 124, pp. 4-10.
2. Oberkampf, W. and C. Roy (2010), *Verification and Validation in Scientific Computing*, Cambridge: Cambridge University Press.

8.3. Error analysis hierarchy for users

The range of errors possible in a simulation should be addressed in a logical, hierarchical sequence to obtain efficient error quantification. In the case of CFD software, this sequence starts at round-off errors and then proceeds to iteration errors, discretisation errors and, finally, model errors. Model errors are typically addressed as part of model validation rather than as part of code or solution verification.

8.3.1. Target variables

Numerical errors should be monitored for a limited number of representative target variables defined during the PIRT process as being representative of the goals of the simulation. It is usually inefficient to evaluate and check all values of all variables. These target variables can for instance be maximum or minimum dependent variable values or integral quantities like efficiencies, and heat transfer coefficients. In optimal conditions these variables are computed during run-time and for steady state solutions displayed as part of the convergence history. They should be readily available to existing post-processing tools.

8.4. Round-off errors

Round-off errors are caused by insufficient machine accuracy and are rarely considered significant with contemporary computing resources. In some cases, it may be possible to test round-off error contributions by simply running the code at higher precision.

Round-off errors can be significant for high Reynolds number flows where the boundary layer resolution can lead to very small cells near the wall if single precision memory allocation is used. Similar situations can occur in two-dimensional axisymmetric simulations where the volume of the first cell near the axis can become very small in comparison to the neighbouring cell rings if the radial cell dimension is chosen small. Local convergence might not be reached in such cases at the axis, which is visible in discrepancies in the solution variable fields. Round-off errors can also occur in multispecies or multiphase simulation if single precision memory allocation is used. Typically, one species concentration or the volume fraction of one phase steps to zero at low concentrations in such cases. In case of observed erratic behaviour of the CFD method in simulations of such high Reynolds number flows, the use of a higher precision version may improve performance.

8.5. Iteration errors

Most CFD codes use iterative schemes for matrix solution, and for dealing with the coupling and nonlinearities of the underlying equation system. In both cases, insufficient convergence can cause unacceptable errors in results. Only once these iteration errors have become sufficiently small, should discretisation errors be investigated.

In most cases, the differential equations are implemented in residual form, and a first indication of the convergence to the solution is the reduction of the residuals (or residual norms). However, different types of flows require different levels of residual reduction. For example, swirling flows can often exhibit significant solution changes, even when the equation residuals have been reduced by more than five to six orders of magnitude. Other flows can be well converged with a reduction of only three to four orders of magnitude. As a result, it is also necessary to monitor the solution during convergence and evaluate the progression of the predefined target quantities of the simulation against predetermined asymptotic convergence conditions. Common commercially distributed codes provide features to support monitoring of both residual convergence and asymptotic convergence of monitored quantities. The monitoring of the global balances of conserved variables, like mass, momentum and energy during the iterative process is often a useful first step towards diagnosis and correction of undesirable convergence behaviours.

These steps are generally easy to follow for a steady state calculation. For a transient requiring iterative equation solution at each time step, it is generally preferred that progression to the next time step be triggered by satisfaction of a predetermined convergence monitoring criteria based on residual data, global balances, asymptotic convergence of target quantities or some combination of these.

8.6. Spatial discretisation errors

Spatial discretisation errors result from the use of finite-width grids and from the approximation of the differential terms in the model equations by difference operators. Discretisation errors are the difference between the solution of the discrete approximation to the PDEs in the mathematical model and the actual PDE solution. To obtain mathematically sound solution error estimates, systematic grid width and time step reduction is necessary. Experience shows that only space discretisation methods with at least second order truncation error can produce high-quality solutions on practical grids. It is worth noting that for some grids only first order methods will produce converged steady state solutions. However, in such cases solutions need to be regarded with caution. The convergence is a result of a numerical viscosity larger than the actual turbulent viscosity. In some instances, the first order solution can be successfully used as an initial guess at the steady state for a higher order analysis. In others, the numerical viscosity may be simply masking fundamentally transient behaviour in the flow (see Section 6.1).

As the truncation error order of a given discretisation scheme usually cannot be changed by an end user, spatial discretisation errors can only be influenced by the provision of optimal grids. It is important for the quality of a solution, that the grid points are concentrated in regions of large truncation errors, which are often the regions of large solution variation. It is also important for the reduction of spatial discretisation errors, to provide high-quality numerical grids based on guidance provided in preceding sections.

For mathematically sound grid convergence tests, simulations should be carried out on at least three successively refined grids, and the target quantities should be given as a function of the grid width. Using Richardson extrapolation [1] an estimate can be made of error in the target variable due to discretisation in space as follows:

$$\varepsilon_1 = \frac{\Theta_1 - \Theta_2}{r^p - 1} \tag{8.1}$$

In this equation, Θ is the target variable (lift, drag, heat transfer coefficient, maximum temperature, mass flow rate, etc.), *r* is the grid refinement ratio (always greater than 1), and p is the truncation error order of the discretisation scheme. A subscript of one indicates results from the finest grid.

If the successive refinements of the mesh are uniform (i.e. the edge of each element is divided by two to form the refined mesh) an independent estimate of the order of accuracy for the discrete approximation can be obtained from results on three successive grids.

$$p = \frac{ln\left(\frac{\Theta_3 - \Theta_2}{\Theta_2 - \Theta_1}\right)}{ln(r)} \tag{8.2}$$

This value of p can only be expected to approach the theoretical accuracy of the numerical method when mesh size is small enough.

For practical three-dimensional simulations, limited computational resources often make it extremely difficult to obtain all three mesh solutions in the asymptotic region. In this situation useful information on mesh errors can still be obtained by driving sub-regions of the mesh with appropriate boundary conditions. A code user should also realise that practical implementations of numerical methods (particularly when flux limiters or highly distorted grids are involved) do not always perform at their advertised order of accuracy even in the asymptotic region.

It is often not possible to obtain results for three meshes within the asymptotic range. However, there is still hope for useful results from a Richardson analysis. Remember that the asymptotic range comes from consideration of terms in a classic Taylor series-based truncation error analysis of the discrete approximations to the PDEs. Richardson analysis is simply an extrapolation using a curve fit to results from a sequence of mesh refinements in the form:

$$\Theta(h) = \Theta_{exact} + ah^p \tag{8.3}$$

where h is the relevant mesh (or time step) size. If results for a target variable at the same spatial location for three grids (Θ_1, Θ_2, and Θ_3) lie on a smooth, monotonic curve, then use of Eqn (8.1) with Eqn (8.2) can be expected to give a sensible estimate of the error associated with the finest grid. Although the rigour of the results in the asymptotic range is missing, results in this case can still have value in determining regions where a mesh is inadequate.

Roache [2] deals with quality of error estimates using a grid convergence index (GCI) to measure error, and a factor of safety (F_s) to cover degradation of the error estimate due to results from a grid outside the asymptotic range. From the GCI, the error associated with the prediction of the target parameter at a specific location in the computational mesh can be calculated.

For unstructured meshes, the above considerations are only valid in case of a global refinement of the mesh. Otherwise, the solution error will not be reduced continuously across the domain. The GCI approach of Roache can be applied through the definition of grid refinement ratios to account for the non-uniform refinement of the mesh. This is the preferred strategy defined in the ASME Standard for verification and validation in computational fluid dynamics and heat transfer [3]. However, when using contemporary automated meshing strategies, satisfactory convergence characteristics can often only be obtained in regions of the unstructured mesh exhibiting fortuitous alignments of subsequent mesh refinements.

Eça and Hoekstra [4] have proposed an alternative procedure for evaluation of spatial discretisation errors using a least squares method based on solutions using meshes with

four different resolutions. This approach is more tolerant of oscillatory convergence with spatial refinement and has the advantage of always providing a meaningful error estimate associated with the predicted quantity of interest regardless of the convergence characteristics.

Characterisation of errors in predicted quantities associated with spatial discretisation using meshing strategies with ever increasing complexity remain a field of active research.

References

1. Richardson, L.F. (1910), "The approximate arithmetical solution by finite differences of physical problems involving differential equations, with an application to the stresses in a masonry dam", *Transactions of the Royal Society of London, Series A,* Vol. 210, pp. 307-357.
2. Roache, P.J. (1998), *Verification and Validation in Computational Science and Engineering*, Hermosa Publishers.
3. ASME Standard (2016), *Standard for Verification and Validation in Computational Fluid Dynamics and Heat Transfer*, ASME-V&V-20-2009(R).
4. Eça, L. and M Hoekstra (2014), "A procedure for the estimation of the numerical uncertainty of CFD calculations based on grid refinement studies", *Journal of Computational Physics,* Vol. 262, pp. 104-130.

8.7. Time discretisation errors

To reduce time integration errors for unsteady-state simulations, it is recommended to use at least a second order accurate time discretisation scheme (see discussion in Section 6.3). For oscillating flows the relevant frequencies usually can be estimated beforehand and the time step can be adjusted to provide at least ten to 20 steps for each period of the highest relevant frequency. In case of unsteadiness due to a moving front, the time step should be chosen as a fraction of:

$$\Delta t \approx \frac{\Delta x}{U}$$

In this equation, Δx is the grid spacing and U the front speed.

Sometimes, under strong grid and time step refinement, flow features can be resolved which are not relevant for the simulation. An example is the (undesirable) resolution of the vortex shedding at the trailing edge of an air foil or a turbine blade in a simulation with very fine grids and time steps. Another example is the gradual transition of a free surface flow simulation with a statistical volume of fluid method to a direct numerical (multiphase flow) simulation (DNS), with droplet formation, and wave excitation. This is a difficult situation, as it usually means that no grid and time step-converged solution exists above the DNS range, which can usually not be achieved.

In principle, the time dependency of the solution can be treated as another dimension of the solution error estimation. However, a four-dimensional grid study would be very demanding. It is therefore more practical to carry out the error estimation in the time domain separately from the space discretisation. Starting with a sufficiently fine space discretisation, the error estimation in the time domain can be performed as a one-dimensional study.

Studies should be carried out with at least two and if possible three different time steps for one given spatial resolution. The error estimators given in Section 8.5 can be used if the spatial grid width is replaced by the time step.

8.8. Software and user errors

Software errors are defined as an inconsistency in the software package. This includes the code, its version, its documentation, and the technical service support. Software errors occur when the information provided to the user on the model equations is different from the actual equations solved by the code. This difference can be a result of coding errors (bugs), deficiencies in the numerical algorithms, errors in the graphical user interface, documentation errors, and incorrect support information.

Many software errors can be detected by the verification tests described above. However, it is the task of software vendors to ensure the functionality of the software through a systematic programme of quality control, including extensive testing and non-regression between versions. If more than one software package meets a user's modelling needs, it is worth reviewing the quality control procedures for each candidate before making a final selection.

User errors result from the inadequate use of the resources available for a CFD simulation. The resources are for instance the problem description, computing power, CFD software, physical models in the software, and the project time frame. User errors can be caused by lack of experience, lack of attention to detail, and simple mistakes. Typical user errors are oversimplification of a given problem (geometry, equation system, etc.), poor geometry and grid generation, use of incorrect boundary conditions, selection of non-optimal physical models, incorrect or inadequate solver parameters (time step, etc.), acceptance of non-converged solutions, and post-processing errors.

8.8.1. Quality assurance

The most important step in error control is to understand that errors will occur regardless of the method used to generate source code or input models. Procedures must be in place to eliminate (or at least minimise) programming or user input errors. Quality Assurance (QA) procedures are a proven way to control the introduction of bugs and formalise test procedures. These procedures work well for both code development and application input model development. However, it is important to realise that rigorous adherence to international standards for a QA programme carries a heavy price in two respects. Inclusion of formal QA adds at least 30% to the cost of a project. In addition, the system can become rigid enough that the best CFD practitioners will leave to find a better work environment. However, even if a formal QA programme is not in place, it is important to understand and apply the underlying principles.

In addition to discussion of QA principles directly applicable the creation and maintenance of code input models, this section contains a significant amount of information on software QA. This has been provided to aid in judging the adequacy of software verification documentation obtained from code developers.

Four key components of QA are documentation, development procedures, testing and review. Written standards for these components should be established at the beginning of a project and accepted by all involved. Documentation of a new code or new simulation usually begins with a simple statement of requirements for what must be modelled, what approximations are and are not acceptable, and the form of implementation. A complete written description of the underlying mathematical model provides a basis for verification activities. A clear description should be provided of relevant experiments for use in

validation activities. Any uncertainties in the input model and in code models should also be described for later studies of sensitivity of results to model uncertainties. A test plan describes calculations based on the validation experiments, and any necessary verification tests including discretisation error studies described in previous sections.

For more mature codes intended for nuclear safety applications, the ASME nuclear quality assurance standard [1] defines requirements and guidelines for quality assurance programmes.

References

1. ASME Standard (2019), *Quality Assurance Requirements for Nuclear Facility Applications*, American Society of Mechanical Engineers, NQA-1.

9. Validation of results

Once the verification process has limited discretisation and iteration convergence errors to acceptable levels, validation of physical models can proceed. Ideally, validation is performed by comparing a simulation result with experimental data. This chapter discusses basic considerations for validation, as well as the associated uncertainty analysis needed to build final validation metrics, and to confirm completeness of the validation. Validation process in the frame of safety studies is also mentioned.

In the field of CFD, the real world is modelled first by a conceptual model (governing equations), and then by a computational model (computer code). Application of the computer code or, more specifically, of one concrete computational path to a scientific or industrial problem leads to a computational solution. The computational solution should be validated.

The PIRT process aims to identify the leading physical phenomena for a given application (cf. §3.2). This is useful for both experimental design and validation of the relevant model implementation in the code. Indeed, as described below, steps following PIRT must ensure that every phenomenon is well reproduced, taken separately but also combined. Applicability of the physical models describing leading phenomena to the targeted application is the object of the final step of the validation process.

As defined in Section 2.3 of this report, **validation** is a process of determining the degree to which a model is an accurate representation of the real world from the perspective of the intended uses of the model (AIAA Guide [1]). Here, real world is a system (engineering hardware), for which a reliable engineering simulation tool is needed. Such a system is typically very complex with many coupled physical phenomena, taking place in complicated geometry. Therefore, a **tiered approach** is recommended for validation of models of such systems. In Oberkampf and Trucano [2] and Oberkampf et al. [3], the following four progressively simpler tiers are defined:

- Unit Problems.
  - Benchmark Cases.
  - Subsystem Cases.
- Complete System.

The French Nuclear Safety Authority (ASN) has also elaborated a guide [4], to provide guidelines regarding qualification of codes used in nuclear safety studies, including CFD, which also enforces a tiered approach regarding validation.

Careful attention to the tiered approach minimises one of the most insidious problems in code validation, cancellation of errors. Confidence is built in relevant models contributing to the CFD simulation by first testing isolated physical processes and simple geometries, and then moving up through testing with higher levels of complexity in process interaction [7]. Relevance and sufficiency of the validation tests for the intended application must be analysed.

9.1. Separate effect tests (SET)

Validation of a CFD code should then start from the unit problems (also called “separate effects validation” in [4] and “separate effect tests” in [6]), where only one element of complex phenomenon is allowed to occur in each problem, so that dominant phenomena of complex physics are isolated as tractable items. Unit problems are characterised by very simple geometries, very often two-dimensional, or three-dimensional with important geometric symmetry features. Analytical solution of the problem can be used if available.

Experiments should be on highly instrumented test facilities producing highly accurate data supported by extensive uncertainty analysis of the data for validation calculations at this level. If possible, repeated runs should be performed, preferably at different days, even at separate facilities, to aid identification of random and systematic (bias) errors in the experimental data. All the important code input data, initial conditions and boundary conditions should be accurately measured and documented. If some significant parameters that are needed for the CFD simulation were not measured, reasonable or plausible values for the missing data should be assumed. In this case, an estimation of possible effect of missing information on computed results should be performed. A rigorous (and seldom feasible in the CFD field) approach in this case requires multiple computations and a statistical uncertainty analysis to estimate sensitivity of target variables to the possible range of unknown (or uncertain) system parameters.

Benchmark cases typically involve only two or three types of coupled flow physics in more complex geometry than in the unit problems, retaining the features, critical to these types of physics. Most of the required modelling data, initial conditions and boundary conditions are measured, but some of the less important experimental data are not measured in some cases. As in the case of unit problems, whenever missing input data are replaced by assumed values, uncertainty analysis should be performed.

9.2. Integral effect tests (IET)

For subsystems and complete systems (also called “integral validation” in [4] and “integral effect tests” in [6]), it is difficult, and sometimes impossible to quantify most of the test conditions required for thorough validation of the computational model. Three or more types of physics are coupled (some coupling reduction is typical for subsystem cases). Some of the necessary or the most important modelling data, initial conditions and boundary conditions are measured. There is typically less experimental data and less measurement precision provided at this level than in the case of unit problems and benchmark cases. Taken as stand-alone validation, these factors reduce reliability of detailed conclusions on suitability of the computational model to the intended application. However, taken in conjunction with unit and benchmark tests, subsystem and complete system tests provide necessary validation of interactions between individual process models.

Attention must be paid on the coherence between separate effects tests and integral validation, concerning physical and numerical models used. The validation areas of the models must be respected in all steps of the validation process. Potential adjustments in one step must be reported in the following ones.

9.3. CFD-grade experiments

Traditional experiments are intended to improve understanding of the physical world, whereas validation experiments have the primary goal of quantifying differences between a portion of the physical world and the equivalent portion of a virtual world. As a result, design of a validation experiment requires both skilled experimentalists, and individuals with detailed knowledge of the contents and behaviour of the simulation tool (both developers and code users). The experiment should be designed to answer questions about a specific application, and the design should be guided by the PIRT process (see Section 3.2) to capture the essential physics of interest, and to measure state variables most sensitive to the relevant model implementations in the code [6]. Special care should be taken with the experiment to obtain initial and boundary conditions for use in the simulation. This includes precision measurements of hardware geometry and instrument location rather than

use of dimensions from design drawings. This data as well as data from instrumentation during the experiment should be accompanied by reliable estimates of random (precision) and bias (systematic) errors. In the case of initial and boundary conditions, these errors form the basis of uncertainty analysis for key computed results. For physical state data these errors should be included in consideration of validation metrics.

Scoping studies with the simulation code may provide guidance to the design process. However, once the experimental facility is built and provides reliable results, experiment and simulation should be performed independently and results should only be compared after each activity is complete. The idea is to avoid recalibration of the calculation regarding experimental results. It is common to perform a second post-test round of simulation, but care should be taken that changes to the input model only reflect differences in initial and boundary conditions between design and actual execution of the experiment.

9.4. Acceptance criterion

The last step in the validation process is formulation of conclusions. Validation cannot be understood as a binary ("yes" or "no") problem. From an engineering viewpoint, validation is an estimation problem: What is the measure of agreement between the computational result and the experimental result, and how much is the measure affected by numerical error in the computational solution and by the experimental uncertainty? The answers are clearly application dependent and user dependent. Acceptance criterion is in most cases determined very vaguely, and there is also a risk of faulty conclusions. There is a "model builder's risk", that is risk of rejection of a model when the model is valid, based on errors on both computational side and the experimental side, and there is also a "model user's risk" in accepting the validity of a model when the model is invalid and the original favourable agreement has compensating, or cancelling errors in the comparisons. Oberkampf and Trucano believe that compensating error in complex simulations is a common phenomenon. It is also well known that model user's risk is potentially the more disastrous since it produces a false sense of security. It is also more likely to occur in practice since there is a tendency to find agreement of results and not to spend more time and resources pursuing possible problems in either the computations or the experiments.

9.5. Lack of experimental data

In case of lack of experimental data regarding specific phenomena or integral results, numerical studies can provide reliable data to help the validation. Such numerical studies must be performed with an already qualified tool. This tool can be another CFD code, but also more macro-scaled codes (like system codes), or local-scale codes (like DNS approach [8]), depending on the application case. Interpretation of the results must be taken carefully if the physicals models to validate are similar between the codes.

9.6. Target variables and metrics

Target variables for validation should be selected during the PIRT process (Section 3.2) by the panel of experts. Because PIRT is recognised to be an iterative process, it should be realised that the list of target variables may change as experience is gained with the experiment or with computational scoping studies. Note that target variables may be fundamental quantities such as velocity, temperature, and pressure, or derived quantities such as flow rates, heat transfer coefficients or a maximum, minimum, or average over more fundamental data.

Selection of suitable validation metrics is a very important part of the validation process. Oberkampf and Barone [9] provide a detailed discussion of considerations for selection of metrics. Two key considerations are that the metric include a comparison to a reliable measure of experimental uncertainty, and that presentation of metric values do not include qualitative judgements such as "very good agreement". It is not the analyst's job to make such judgements. To obtain reliable values for experimental uncertainty, results should be available from redundant validation experiments. With the data from multiple runs of the same experiment, a basic metric would be the difference between a computed value and the mean of the experimental values at the same location, presented with a confidence interval for true experimental data. In this case the metric involves statement of three numbers: the estimated error between results of the simulation and the true experimental value, an estimated range within which the true value of this error lies, and the confidence level that the error lies within the quoted range (usually chosen as 90% or 95% for the statistical analysis). Useful global metrics can be constructed by integrating the local error estimates or corresponding fractional errors over time or space as appropriate. However, the corresponding integration of confidence intervals (or intervals ratioed to the mean experimental value) simply become confidence indicators, due to loss of rigour in the interpretation of the resulting interval. Care must also be taken in using such global metrics because regions with relatively large error may be masked by the averaging process.

To place the metric in the proper perspective, information on experimental error should also be provided that, to the extent possible, clearly distinguishes between truly random error and systematic (bias) error. Consider the hypothetical comparison in Figure 9.1 of calculated and measured mass flow rate at a specific location. The error bars could be the result of phenomena that vary randomly with time during any run of the experiment. Another possibility is that they reflect calibration error resulting in a fixed offset (bias) of data in any given experiment. This offset might vary randomly from experiment to experiment because of the calibration process. In later evaluation of validation metrics, the nature of the experimental error in Figure 9.1 can make a significant difference in conclusions about the quality of one or more models used in the numerical simulation. If the error is truly random within each experiment, one might conclude that the simulation adequately captures the physical phenomena. However, if the error is a bias, the simulation misses a key trend in the data, and depending on needs for the final application, one or more relevant models could be judged to be inadequate.

Figure 9.1. Comparison of a calculation to data references

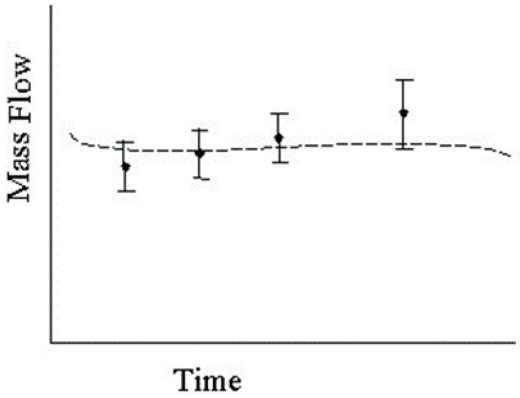

9.7. Transposition

Once the validation of physical models has been carried out, the next step is the transposition. It is rare that experiments cover the entire range of identified parameters, mainly dimensionless numbers, of the application case, mainly reactor case. Transposition aims to justify that validated models (at a specific scale and under specific conditions) can predict phenomena at another scale and other running conditions. Transposition leans on dimensionless numbers of studies and similarities. It can valorise other elements, for example new experimental data, sensitivity studies and expert judgements. Coherence of modelling between validation and applications cases must be verified. Additionally, coherence in meshing (type, characteristics like the use of inflation layers at walls, and refinement level of the mesh) and temporal resolution (time step size for unsteady simulations) between validation and application cases should be considered.

9.8. CFD for safety applications

Another possibility is to carry out sensitivity studies to demonstrate that key parameters of the safety study are not impacted using different physical models or modelling choices. Thus, it can provide confidence in the ability of the simulation tool to predict the global physical phenomena correctly, or at least in a conservative way.

Using CFD in the frame of safety applications, validation is a crucial step during the studies. In case of lacks in the process (lack of experimental data or gaps between computed and reference data), it is possible to penalise the figure of merit by conservative choices. Sufficiency of these conservatisms must be justified to validate the CFD-based methodology. Insufficiencies in the validation process should conduct such CFD studies to be rejected by safety authorities, as illustrated in this article [5].

References

1. AIAA (1998), *AIAA Guide for the Verification and Validation of Computational Fluid Dynamics Simulations*, American Institute of Aeronautics and Astronatics, peport G-077-1988.
2. Oberkampf, W.L. and T.G. Trucano (2002), "Verification and validation in computational fluid dynamics", *Progress in Aerospace Sciences,* Vol. 38, pp. 209-272.
3. Oberkampf, W.L., T.G. Trucano and C. Hirsch (2004), "Verification, validation and predictive capability in computational engineering and physics", *Applied Mechanics Reviews,* Vol. 57, pp. 345-384.
4. ASN (2017), "Qualification of scientific computing tools used in the nuclear safety case – 1st barrier", ASN Guide No. 28, www.french-nuclear-safety.fr/regulation/asnr-guides/asn-guide-no.-28.
5. Ruyer, P. et al. (2020), "Using CFD in the frame of safety studies – Some IRSN experiences", in *Proceedings of CFD4NRS-8 Workshop,* Saclay, France.
6. Bestion, D. et al. (2018), "Requirements for CFD-grade experiments for nuclear reactor thermalhydraulics", in *Proceedings of CFD4NRS-7 Workshop,* Shanghai, China, September 2018.
7. Bieder, U. and E. Graffard (2008), "Qualification of the CFD code TRIO_U for full scale nuclear reactor applications", *Nuclear Engineering and Design*, Vol. 238 (3), pp.671-679, https://doi.org/10.1016/j.nucengdes.2007.02.040.

8. Rosa, D., A. Shams and E.M.J. Komen (2016), "Towards the benchmarking direct numerical simulations of a single phase pressurised thermal shock", in *Proceedings of CFD4NRS-6 Workshop*, Cambridge, United States.

9. Oberkampf, W.L. and M.F. Barone (2006), "Measures of agreement between computation and experiment: Validation Metrics", *J. Comp. Phys.,* Vol. 217, pp. 5-36.

10. Uncertainty quantification

Uncertainty quantification (UQ) of simulations is an increasingly common component of validation and can be an important enabler for industrial application, especially in the nuclear community. In France, for example, the safety authority ASN clearly expressed in their Guide No. 28 [1] the requirement of a UQ process for CFD simulations. This short guide gives a brief overview on the idea of UQ as seen by the regulator. Evaluated uncertainties from performed validations play a central role in the evaluation of the UQ for the plant application and shall be used whenever possible. If it is not possible to validate simulation results against experimental data or to compare them to results from previously qualified codes, the guide [1] advises to evaluate the uncertainties based on comparisons to results of other simulation codes, on expert assessments and on sensitivity studies. Also, an alternative "conservative" approach may be used according to [1] in cases where determining the various uncertainties is particularly complex: It has to be shown that conservative hypotheses on the initial or boundary conditions or on the physical models lead to conservative values for the variables of interest in the validation cases.

Specific methods for UQ like deterministic sampling and polynomial chaos expansion are collected for example in the special guide issued by the NEA [2] in a first version in 2016. Thus, the UQ process in detail is not given in this BPG. A dedicated chapter of the guide [2] deals with the methodology of the ASME V&V 20 standard [3] for the steady state CFD applications. This standard constitutes a solid basis shared by academic and industrial CFD communities. Especially the similar treatment of uncertainties in experiment and simulation in this standard as a symmetric concept reflects the modern view on simulations as virtual experiments. Three main uncertainties are worked out: numerical, input and the a priori unknown model uncertainty. The last one can finally be evaluated in the validation process when all other uncertainties are known. In case the model uncertainty is dominating the others, model constants like those for the turbulence model can also be evaluated by declaring them as uncertain input variables[9] as described in the paper [4] from NRG, dealing with the GEMIX mixing experiment. This GEMIX experiment was especially dedicated to UQ, see the final report [5]. As a further example, EDF used for GEMIX the WAVE method, described in [2] and additionally in [6] for the use at PTS.

References

1. ASN (2017), "Qualification of scientific computing tools used in the nuclear safety case – 1st barrier", ASN Guide No. 28, Version of 25/07/2017.
2. NEA (2016), "Review of Uncertainty Methods for Computational Fluid Dynamics Application to Nuclear Reactor Thermal Hydraulics", OECD Publishing, Paris, www.oecd-nea.org/jcms/pl_19700.
3. ASME (2009), *Standard for Verification and Validation in Computational Fluid Dynamics and Heat Transfer*, American Society of Mechanical engineers, ASME V&V 20-2009.
4. Cutrono A. et al. (2020), "Uncertainty quantification method for CFD validated for turbulent mixing experiments from GEMIX", *Nuclear Engineering and Design, Volume.*, Vol. 358, 2020.

9. However, modifying turbulence models' constants should be performed with caution and respect some physical criteria.

5. NEA (2019), "NEA Benchmark Exercise: Computational Fluid Dynamic Prediction and Uncertainty Quantification of a GEMIX Mixing Layer Test", OECD Publishing, Paris, www.oecd-nea.org/jcms/pl_19838.
6. Barthet, O., H. Brero, Cordier and R. Camy, "Uncertainty quantification for a pressurised thermal shock experiment using the wave method", presented at the 5th workshop on Computational Fluid Dynamics for Nuclear Reactor Safety, 9-11 September 2014, Zurich, Switzerland.

11. Documentation

It is necessary to document the content and results of any thermal-hydraulic computation, especially of verification or validation of a code/computation. Relevant information must be recorded, archived and disseminated. The documentation must be complete, consistent and readable.

In any organisation doing thermal-hydraulic computational analyses, a record management system must be established and documented. This represents a long-term activity. A good record of the simulation should be kept with clear documentation of assumptions, approximation, simplifications, geometry and data sources. The documentation of the calculations should be organised so that another CFD expert can follow what has been done. The level of documentation required can depend strongly on the customer requirements as specified in the problem definition.

The ECORA project Best Practice Guidelines [1] contain proposals for the structure of three types of documents (Test Case Selection Report, Existing CFD Results Evaluation Report, and Validation Report) to be used within the project. General guidance on the content and form of appropriate documentation based on a long-term experience can be found in Trucano et al. [2]. According to this source, the following information should be included in any report on a thermal-hydraulic analysis (abridged):

1. Information about the code application, the origin of this application, the modelling requirements that this application creates, and characterisation of uncertainties that are associated with the application.
2. Detailed discussion of the physical phenomena in the PIRT that are being validated by the computation.
3. A comprehensive discussion of verification activities, both code and calculation, centred on the intended application.
4. Documentation of how the code was used in the definition, design and analysis of each validation experiment. Enough information should be included to allow the reproduction of the described calculations by others. Such information includes mesh construction information, calculation geometry, computational initial and boundary conditions, computational model inputs such as material-model input specifications, and selection of computational algorithm parameters such as iterative tolerances and numerical smoothing parameters.
5. A complete description of each experiment, sufficient to allow experimental replication in the future.
6. A description of the analysis of experimental data. It is important to document information about the uncertainty in the acquired experimental data, including estimation of both random and bias errors with information on the methods of these estimations.
7. The methods and results of the validation metrics (a synonym for “measure”) applied in the validation experiment activity including definition of success and failure criteria for these metrics.
8. A characterisation of the credibility of the code for the specified application, based on the results from the application of the defined validation metrics and the assessment.
9. Information about the contribution of the validation activity to the BE+U (“best-estimate + uncertainty”) paradigm for predictive code application. A discussion

should be given for the sources of uncertainty that were considered, as well as those sources that were neglected. Assumptions should be discussed concerning any probabilistic analyses.

Given the scope of this information, it should be evident that one or more documents will sometimes be required to archive all the proposed content. Especially in the case of code validation, detailed description of experiment(s) is needed including evaluation of measurement uncertainties. When a demonstration simulation of a real industrial problem is attempted, preparation of a PIRT before the start of simulation is essential together with corresponding scaling considerations.

References

1. Menter, F. (2002), *CFD Best Practice Guidelines for CFD Code Validation for Reactor-Safety Applications*, European Commission, 5th EURATOM Framework Programme, report EVOLECORA-D1.
2. Trucano, T.G., M. Pilch and W.L. Oberkampf (2002), "General concepts for experimental validation of ASCI code applications", Sandia National Laboratories, SAND2002-0341.

12. Special consideration of specific NRS cases

The present section focuses on specific studies that illustrate different aspects of NRS applications. It was not planned to select studies that perfectly enforce all the aspects of the present guidelines but rather to present real-life examples that provide a practical orientation to the report. Because these are simply intended as examples, no independent assessment has been performed on results presented in this section.

Several validation and verification databases relevant to NRS are also available such as:

- ERCOFTAC QNET-CFD: http://qnet-ercoftac.cfms.org.uk, with a section dedicated to NRS applications; and
- NUREG: www.nrc.gov/reading-rm/doc-collections/nuregs.

12.1. Boron dilution

Boron dilution has been and still is a topic of interest for the international community (OECD: NUREG/CP-0158, ISP43, European initiatives: CA EUBORA, ECORA, FLOMIX, etc.). For an illustration of the use of CFD for this type of study, the reader may refer to Ref. [1])

The present section provides a useful example of a study carried out by Prasser et al. at the Forschungszentrum Dresden-Rossendorf [2].

The choices and conclusions reflect the opinion of the authors and must be considered as purely illustrative and not as guidance for Boron dilution studies. Other strategies may be selected for representing the geometry (core inlet plate description, core model, upper plenum, and outlet nozzle), other choices may be adopted for grid refinement and turbulence models.

References

1. Hemström, B. et al. (2005), "Validation of CFD codes based on mixing experiments (Final report on WP4)", EU/FP5 FLOMIX-R Report, FLOMIX-R-D11, Vattenfall Utveckling, Sweden.
2. Prasser, H.-M. et al. (2003), "Coolant mixing in a pressurized water reactor: deboration transients, steam-line breaks, and emergency core cooling injection", *Nuclear Technology*, Vol. 143 (1), p. 37.

12.1.1. Key phenomena

During so-called boron dilution transients at pressurised water reactors, slugs of weakly borated water might be formed in one of the primary systems loops due to different external or internal mechanisms (failure of the water make-up system, steam generator tube break, reflux-condenser mode during small break LOCA). By starting the coolant circulation in the corresponding loop (inadvertent pump start-up, restart of natural circulation) the under-borated slug might enter the reactor core. This results in the insertion of positive reactivity and possibly leads to a power excursion. In this case the amount of reactivity insertion depends on spreading of the cold leg flow at the core barrel and subsequent turbulent mixing in the downcomer and lower plenum of the reactor pressure vessel (RPV). In the case of start-up of the main coolant pump, the mixing is momentum controlled. In the case of low flow rates and higher density differences between the slug and the ambient water, the mixing forced by buoyancy forces. The specific case of slug mixing during pump start-up will be described below. Key phenomena include: the transition from resting fluid via

laminar flow to turbulent flow; the jet impingement at the core barrel; the splitting of the flow into two main jets to the left and to the right of the core barrel; secondary flows in various parts of the downcomer; and a recirculation area below the injection nozzle.

12.1.2. Solution strategy

The solution strategy is based on the validation of the CFD models against experiments at test facilities before simulating the real plant transients. An experimental data base on turbulent mixing has been created within the EC research project FLOMIX-R [1]. The objective of the project was to obtain complementary and confirmatory data on slug mixing using improved measurement techniques with enhanced resolution in space and time. Results have contributed to the validation of CFD codes for the analysis of turbulent mixing problems. A few benchmark problems based on selected experiments have been used to study the effect of different turbulent mixing models under various flow conditions, to investigate the influence of the geometry, the boundary conditions, the grid, and the time step in the CFD analyses according to the ECORA Best Practice Guidelines [2].

The CFD analysis described here is for a slug mixing test performed at Rossendorf's ROCOM mixing test facility. This is a 1:5 scaled model of a German Konvoi type reactor, including four loops with fully controllable main coolant pumps. The RPV model is manufactured from transparent acryl. Mixing is determined from electrical conductivity measurements of the distribution of a salt tracer solution [3]. Higher measured salinity corresponds to higher boron dilution, or lower boron concentration.

References

1. Rohde, U. et al. (2005), "Fluid mixing and flow distribution in the reactor circuit – Part 1: Measurement data base", *Nuclear Engineering and Design*, Vol. 235, pp. 421-443.
2. Menter, F. (2002), "CFD best practice guidelines for CFD code validation for reactor-safety applications", European Commission, 5th EURATOM Framework Programme, report, EVOLECORA-D1.
3. Prasser, H.-M. et al. (2003), "Coolant mixing in a pressurised water reactor: deboration transients, steam-line breaks, and emergency core cooling injection", *Nuclear Technology*, Vol. 143 (1), p. 37.

12.1.3. Geometry, grid, numerical schemes, and model features

The geometric details of the vessel internals have a strong influence on the flow field and hence on the mixing. Therefore, an exact representation of the inlet region, extension of the downcomer below the inlet region and the obstruction of the flow by the outlet nozzles cut through the downcomer is necessary.

In the CAD-File all geometrical details are modelled accurately, such as: inlet nozzles including the diffuser; orifices of the outlet nozzles; the downcomer extension; the lower plenum; the core support plate; the perforated drum; the core simulator; the upper plenum; and the outlet nozzles. No additional physical models (Porous media, Body Forces) are necessary. The following internals were modelled in detail:

- The core plate contains 193 orifices with a diameter of d=20 mm each.
- The core contains 193 fuel element dummies. The fluid flows through the hydraulic core simulator inside the tubes. Although it was found by Hemström et al [1] that

the influence of the core structure on the flow and mixing pattern at the core inlet is rather small, this region was also modelled in detail.

- The perforated drum contains 410 orifices of 15 mm diameter. The advantage of modelling the drum with the original geometry is a detailed study of the flow phenomena in the lower plenum, the disadvantage is the high numerical effort. Sensitivity tests on the influence of different ways of modelling the perforated drum (e.g. porous media, resistant coefficients, reduced number of holes) are presented in [1].

Figure 12.1. Hybrid mesh based on tetrahedral and hexahedral elements

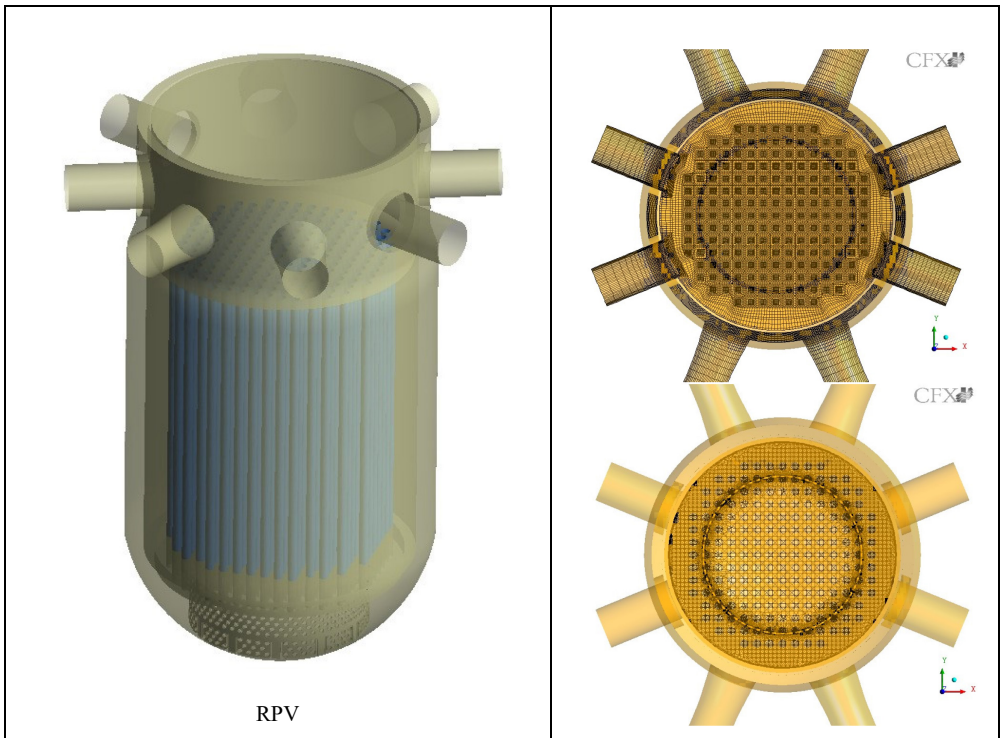

Note: Grid features. Horizontal cut: Inlet nozzle plane (Hexa), Lower Plenum (Tetra).

The CFD code used for this analysis was ANSYS CFX-10. A hybrid mesh was used to model the RPV. The upper part was modelled with 1.2 million hexahedral cells, and the lower plenum including the perforated drum with 2.3 million tetrahedral elements. In addition, 470 000 wedges and 26 000 pyramids were needed to optimise the grid (Figure 12.1). Mesh refinement was used in the perforated drum and in the lower core support plate, and the Laplace grid-smoothing algorithm has been utilised.

Discretisation schemes

The calculations were done with the CFX "High resolution" option for spatial discretisation, which adjusts local discretisation to provide something close to second order spatial accuracy. The CFX "Fully implicit second order backward Euler" option was chosen for integration in time. For both discretisation schemes the target variable does not change significantly for iteration convergence criteria below 10^{-4}. The round-off error was

studied by comparing the results obtained with single and double precision. No significant difference was observed in results between single and double precision calculations.

Time step

Calculations have been performed with three different time steps: 0.05 s; 0.1 s and 0.5 s. An optimum with respect to computation time and convergence of the solution was achieved for a time step size of 0.1 s. The differences in the solutions between 0.05 s and 0.1 s time step sizes were small.

Boundary conditions and model selection

The inlet boundary conditions (velocity, mixing scalar etc.) were set at the inlet nozzles. No specific velocity profile is given. As an initial guess the CFX defaults for the turbulent kinetic energy and the dissipation rate were used. The outlet boundary conditions were pressure controlled and set at the outlet nozzles. Passive scalar fields were used to simulate transport of water salinity, used in the experiment to describe the boron dilution processes. In loop 1 the pump starts linearly from 0 to 185 m^3/h in 14 s, after 14 s the mass flow rate is constant at 185 m^3/h, counter flows are developing at the other three loops. The initial space averaged value of the mixing scalar at the inlet nozzle of Loop 1 was used as the inlet boundary condition.

Calculations have been performed with the following turbulence models and wall boundary conditions:

- k-ε-standard turbulence model, wall treatment adiabatic with scalable logarithmic wall functions
- Shear stress transport turbulence model, wall treatment adiabatic with automatic Menter modified wall functions
- Reynolds stress turbulence model, wall treatment adiabatic with scalable logarithmic wall functions

In the case of a highly turbulent flow, these three selections for turbulence modelling gave almost the same results for the velocity and mixing scalar profile in the downcomer. However, the SST model was preferred as it is more accurate than the k-ε model near the wall.

References

1. Hemström, B. et al. (2005), "Validation of CFD codes based on mixing experiments (Final report on WP4)", EU/FP5 FLOMIX-R report, FLOMIX-R-D11, Vattenfall Utveckling, Sweden.

12.1.4. Results of the boron dilution transient

Due to a strong impulse driven flow at the inlet nozzle, the horizontal part of the flow dominates in the downcomer (Figure 12.2). The injection is distributed into two main jets by impact on the core barrel, the so-called butterfly distribution. In addition, several secondary flows are seen in various parts of the downcomer. Especially strong vortices occur in the areas below the non-operating loop nozzles and below the injection loop. Here a recirculation area develops, which controls the size of other small swirls. The maximum value of the passive scalar field at the core inlet (representing the minimum boron concentration) is an indicator for possible reactivity insertion during a transient (Figure 12.3a). In the experiment as well as in the calculation the maximum value at the core inlet is determined at each time step over all fuel element positions, therefore the position can

vary. The calculated maximum mixing scalar at the core inlet is very close to the experimental value. The local time-dependent mixing scalar at the fuel element position in the centre of the core inlet is shown in Figure 12.3b.

Figure 12.2. Time-dependent mixing scalar distribution in the downcomer, CFX-5

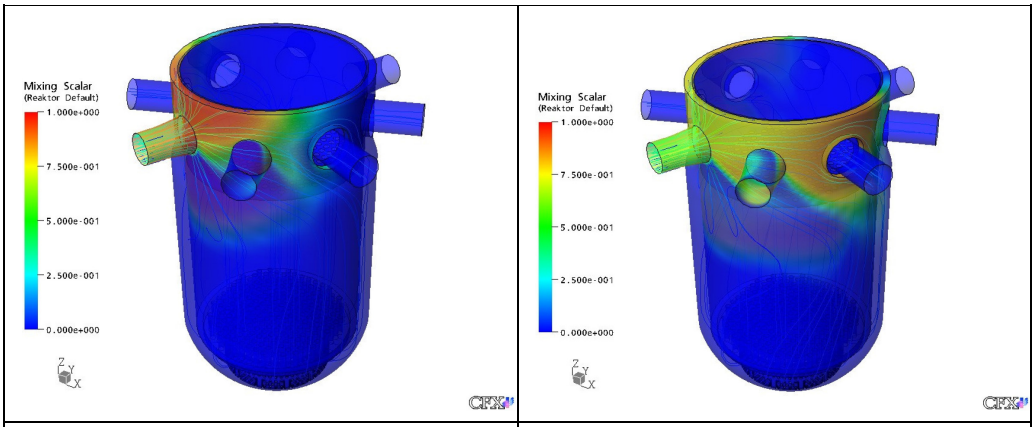

9 s after start-up	10 s after start-up

Figure 12.3a and 12.3b. Comparison of the time-dependent mixing scalar at the core inlet sensor position (experiment, CFX-5 calculation)

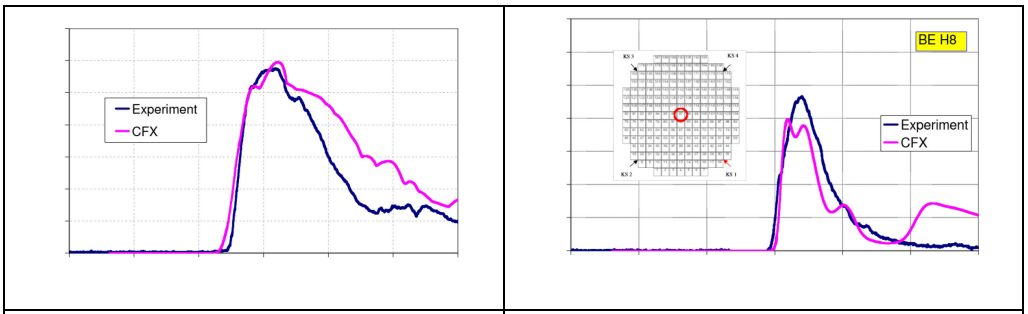

a) Time dependent global maximum of the mixing scalar on the core inlet plane	b) Time dependent local mixing scalar at the core inlet, center position

12.1.5. Conclusions

The CFD calculations were carried out with ANSYS CFX-10. All internals of the RPV of ROCOM were modelled in detail. A production mesh with seven million elements was generated. Detailed and extensive grid studies were made. With the refinements considered in this study, it was observed that a detailed model of the perforated drum made it possible to obtain a better agreement with the available experimental data. However, no full grid independence of the CFD solutions was achieved and further analysis would be required before drawing final conclusions.

Sensitivity studies have shown that the SST turbulence model and the automatic wall functions together with higher order discretisation schemes can be used.

12.2. Pressurised thermal shock: UPTF Test 1

The upper plenum test facility (UPTF) was a full-scale representation of the primary system of the four-loop 1 300 MWe Siemens/KWU pressurised water reactor (PWR) at Grafenrheinfeld in Germany. The test vessel upper plenum internals, the downcomer, and the primary coolant piping were replicas of the reference plant. However, other important components of the PWR such as the core, the coolant pumps, the steam generator, and the containment were replaced by simulators which simulated the thermal-hydraulic behaviour in these components during end-of-blow down, refill, and reflood phases of a large break loss-of-coolant accident (LOCA). Both hot leg and cold leg breaks of various sizes have been simulated in the UPTF. The emergency core Cooling (ECC) injection systems of the UPTF were designed to simulate the various ECC systems of PWRs in Germany, Japan and the United States.

The present section provides a useful example of study carried out by the Nuclear Research and Consultancy Group (NRG) [1].

Temperature measurements have been performed at various locations in the UPTF geometry. The results of CFD simulations have been compared at those positions most relevant for pressurised thermal shock (PTS). The temperature measurements in the intact cold leg, where the ECC injections occur, and the measurements in the downcomer directly under this cold leg were selected. These measurement positions are indicated in Figure 12.4.

Figure 12.4. Location of the key temperature measurement positions, and probe numbering

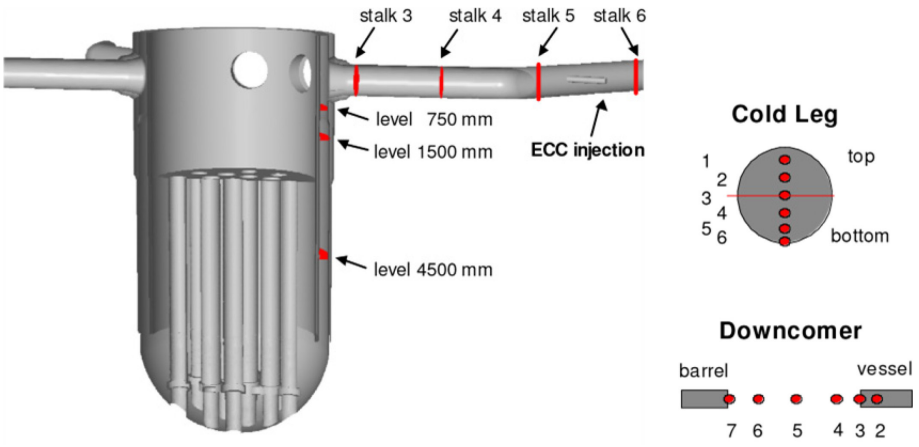

12.2.1. UPTF test 1 conditions

UPTF test 1 was performed to investigate fluid-fluid mixing in the cold leg and downcomer during a small break LOCA. This fluid-fluid mixing results from the high-pressure injection of the cold ECC water into the cold leg at a time when the reactor coolant system is at an elevated temperature. The level of mixing controls the fluid temperatures in contact with pipe and vessel walls and hence the potential for a PTS safety issue. In general, if the mixing is good, a slow cool down occurs which provides sufficient time to prevent the development of significant temperature gradients in the wall of the reactor pressure vessel (RPV). Good mixing takes place when there is flow in the loops, even when the flow only results from natural circulation. However, in certain SBLOCA scenarios, it is possible that

stagnant flow conditions occur in one or more loops. For this situation, the flow in the cold leg is thermally stratified. Namely, the ECC injection results in a cold stream, which flows along the bottom of the cold leg from the injection nozzle to the downcomer, whereas a hot stream flows along the top of the cold leg counter current to the cold stream. This situation was investigated in UPTF Test 1.

For UPTF Test 1, the primary system was initially filled with stagnant hot water at 463 K (190°C). The cold ECC water was injected into a single cold leg. The ECC water injection mass flow rate was equal to 40 kg/s and the temperature of this ECC water was 300 K (27°C).

12.2.2. Summary of results calculated using CFX-5

Calculations summarised here were performed by the Nuclear Research and Consultancy Group (NRG). The different turbulence models and meshes used in these computations are summarised in Table 12.1. Cases A and B have been executed to determine whether detailed modelling of the UPTF internals is required. Simulations showed spurious circumferential flow oscillations in the downcomer for an empty lower plenum in combination with the commonly applied porous medium approach for representation of the UPTF core. Furthermore, it has been shown that the pump volume must be taken into account, since a large amount of the ECC water flows towards the pump and accumulates there. In a real accident scenario, it is therefore important to correctly predict the amount of ECC water flowing towards the pump, since this water will never reach the core.

Table 12.1 Overview of the performed CFX-5 computations for UPTF Test 1

Case	Turbulence model	Turbulence modification	Core model	Pump volume	Time step	Discretisation space , time	Mesh size
A	SST-k-ω	none	porous	no	0.5 s	1^{st}, 1^{st}	1.155.153
B	SST-k-ω	buoyancy	internals	yes	0.5 s	1^{st}, 1^{st}	2.052.315
C	k-ε	buoyancy	internals	yes	0.5 s	1^{st}, 1^{st}	2.052.315
D	SST-k-ω	buoyancy	internals	yes	0.5 s	2^{nd}, 1^{st}	2.052.315
E	SST-k-ω	buoyancy	internals	yes	0.05 s	2^{nd},2^{nd}	2.052.315
F	SST-k-ω	buoyancy	internals	yes	0.05 s	2^{nd},2^{nd}	2.871.450
G	RSM	buoyancy	internals	yes	0.05 s	2^{nd},2^{nd}	2.871.450

Turbulence modelling has been investigated by comparing results of a simulation using the SST k-ω turbulence model without (case A) and with (case B) inclusion of the turbulence production/destruction term due to buoyancy. From a comparison of these two cases, it has been concluded that this modification to the standard turbulence model is required to achieve a good representation of the stratification occurring in the cold leg. Once this term is included, the results of the SST k-ω (case B) and standard k-ε turbulence model (case C) are practically identical. Finally, an k-ω-based Reynolds stress turbulence model has been used (case G). The results from this calculation show a better agreement with experimental observations for the amplitude of the oscillations in the downcomer. These oscillations are overpredicted by the two-equation turbulence model (case F). It is important to notice that correct prediction of these oscillations is required to analyse phenomena like PTS and thermal fatigue. Since these oscillations have a significant effect on the wall temperature, and thus on the correct prediction of the severity of the PTS, an attempt was made to quantify the oscillations in the experiments. However, the Fast Fourier Transformation of the experimentally observed oscillations did not show any dominant frequencies present in

the signals. Besides determining the effect of the geometrical assumptions and turbulence modelling, as described before, the other calculations in Table 12.1 are related to the ECORA best practice guidelines. Since modelling the UPTF geometry is computationally very demanding, it is impossible to strictly follow the BPG, which, e.g. Tate that a 2×2×2 refinement should be performed. Instead, a first order solution (case B) has been compared with a 2nd order solution (case D). This comparison demonstrated that it is plausible to assume that the mesh in the cold leg is sufficiently fine; but that the results in the downcomer are still mesh dependent. Therefore, a mesh which is locally refined in the downcomer was generated. In this new mesh, care was taken to ensure correct y+ values (case F). The temporal discretisation has been checked by performing a simulation with a reduced time step size and second order temporal discretisation (case E). This reduced time step size is needed to reliably capture the oscillations in the downcomer which determine the vessel wall temperature.

Case F in Table 12.1 is the reference case, since here the best mesh and time step size was used. In Figure 12.5 the temperature distribution on the vessel cold leg walls can be seen. Strong mixing of the cold ECC water with the hot liquid, initially present in the system, is observed in the region of the upward directed ECC injection tube. Further downstream, strong stratification is observed in the cold leg. The cold-water flows towards the reactor vessel and in the direction of the pump simulator, where the cold water accumulates until it has reached the level of the top of the cold leg (after about 160 s). The stratification in the part of the cold leg leading to the reactor vessel remains at a constant level throughout the transient. The cold-water plume flows downwards past the vessel wall. Some slow oscillations can be observed in the circumferential direction. In the same figure, a detailed view of the flow in the downcomer is presented. At the connection of the reactor vessel with the cold leg, the flow remains attached to the vessel wall but starts to detach and re-attach at a lower level in the downcomer. These oscillations, which are much faster than the circumferential oscillations, cause hot and cold regions to emerge. In the bottom of the reactor vessel, the hot and cold regions are fully mixed by the turbulent flow between the lower plenum internals.

Figure 12.5. Vessel and fluid temperatures on the vessel and cold leg walls (left) and a cross-section through the middle of the cold leg with ECC injection (right)

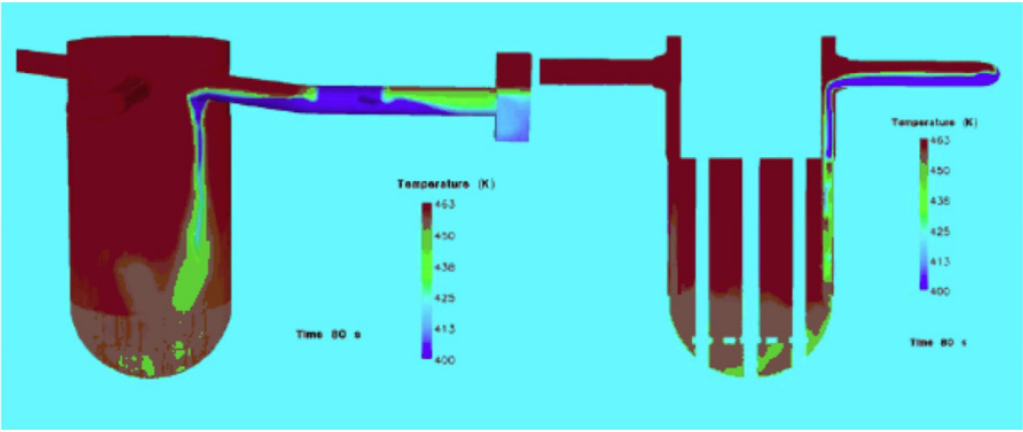

The computed temperature profiles in the cold leg are compared with the experimental results from the UPTF test 1 in Figure 12.6. From this comparison, it is concluded that the stratification in the cold leg is accurately predicted by the CFD code. The calculated lowest temperature in the cold leg, which is the most important factor for determining the severity of the thermal shock, is within 3% of the experimental value. A second comparison is made

for the results in the downcomer in Figure 12.7 and Figure 12.8. In the experimental results, large oscillations are observed at every height in the downcomer. In the CFD results, these oscillations are not found at the highest measurement positions. This is caused by the previously mentioned attachment of the cold plume to the vessel wall, which results in an overestimation of the cooling of the vessel wall. The predicted temperature drop $\Delta T=T-T_{initial}$ is typically overestimated by 50 to 100%. At the lower level (see Figure 12.8) oscillations are observed, but the temperature drop remains overestimated by 60 to 90 %.

Figure 12.6. Stalk 3 results of the CFX-5 reference calculation (left) and UPTF experiment (right). For location see Figure 12.4.

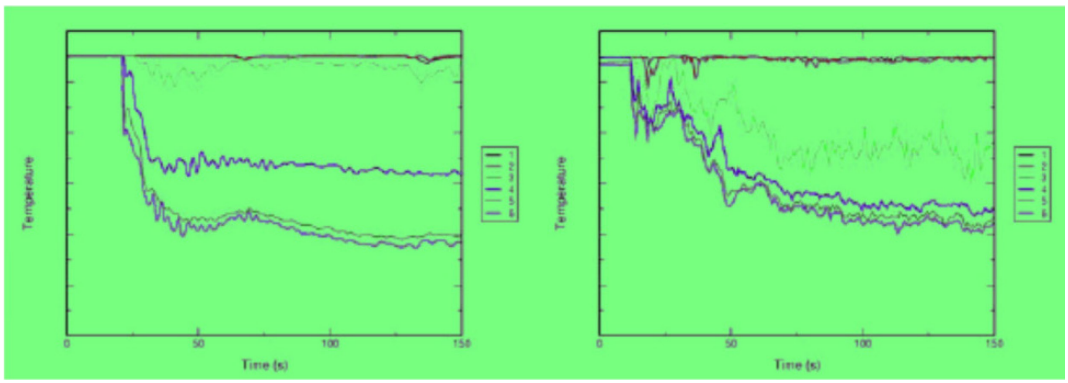

Figure 12.7. Level 750 mm results of the CFX-5 reference calculation (left) and UPTF experiment (right). For legend see Figure 12.4.

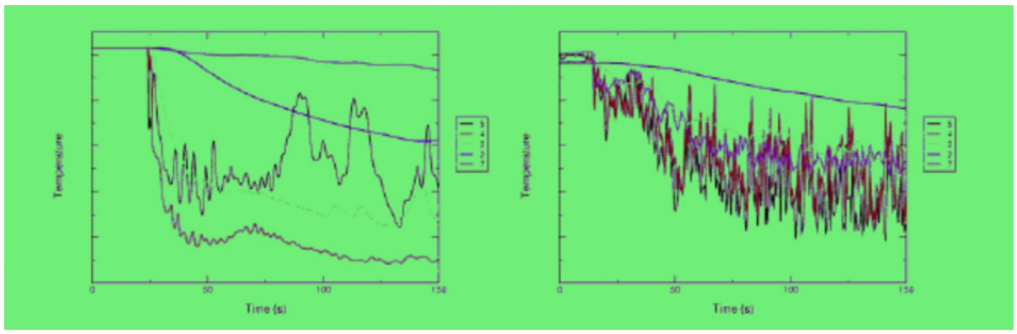

Figure 12.8 Level 4500 mm results of the CFX-5 reference calculation (left) and UPTF experiment (right). For legend see Figure 11.4.

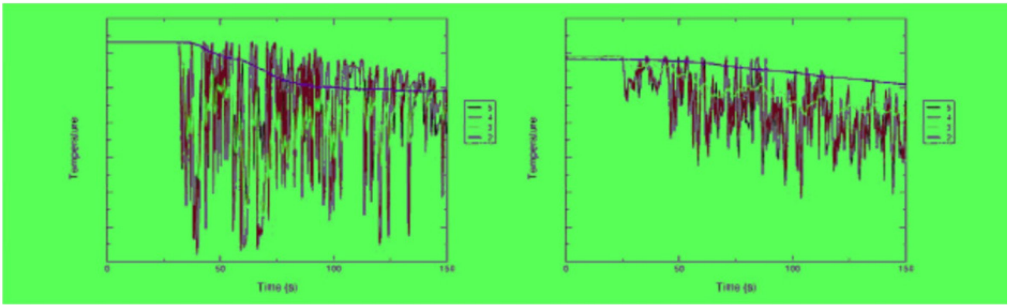

12.2.3. Conclusions

This study clearly indicated a need for buoyancy modifications to turbulence source/sink terms. Further work is needed in nodalisation and model studies to resolve serious discrepancies in results within the downcomer.

12.3. Spent fuel dry storage cask

The present section provides a useful example of study carried out by the US Nuclear Regulatory Commission.

The objective of this task was to validate a general purpose computational fluid dynamics (CFD) method to perform thermal evaluations of a ventilated concrete storage cask VSC 17 system. In addition, the effectiveness and validity of an effective thermal conductivity model k_{eff} was quantified and validated. The (k_{eff}) model is used to represent the combination of radiation and conduction heat transfer by an equivalent thermal conductivity in the region that houses the spent fuel. The (k_{eff}) method has long history of use with finite element analysis (FEA) codes and has been proven to favourably predict a dry cask's thermal response. In the presented analysis, FLUENT [1], a commercially available CFD software package was used. FLUENT is finite control volume based, more suited than FEA codes like ANSYS to model convection in open flow regions of the storage system. As such, there is a need to investigate the applicability of a k_{eff} model in the context of FLUENT.

Two types of flows exist in spent fuel dry storage casks such as the VSC-17. Inside the sealed canister, compressed helium flows through the fuel rod assemblies due to buoyancy forces, while air flows outside the canister in an open system manner also because of buoyancy (density difference). The standard k-ε model with standard wall function is often used to bridge the viscous layer near the wall to the fully turbulent core region in the middle of the channel. As such, the second objective of this validation is to compare the performance of different turbulence models as well as the laminar flow option.

Run #1 among the runs shown in Table 12.2 of the VSC-17 experiments performed in 1990 at Idaho National Laboratory [2] was selected for detailed modelling with the FLUENT code. The VSC-17 is a multi-assembly storage cask comprised of a ventilated concrete storage module. Detailed temperature data was taken during testing and is available for multiple locations and axial levels throughout this cask.

References

1. Fluent Inc. (2004), *FLUENT User Guide*, Version 6, New Hampshire.
2. McKinnon M.A. et al. (1992), "Performance testing and analyses of the VSC-17 ventilated concrete cask", TR-100305, Electric Power Research Institute, Palo Alto, California.

12.3.1. Description of the VSC-17 spent fuel storage cask experiments:

The VSC-17 spent fuel storage system is a passive heat dissipation system for storing 17 assemblies/canisters of consolidated spent nuclear fuel. The VSC-17 system consists of a ventilated concrete cask (VCC) enclosing a multi-assembly sealed basket (MSB) containing spent nuclear fuel as shown in Figure 12.9 and Figure 12.10. Decay heat generated by the spent fuel is transmitted through the containment wall of the MSB to a cooling air flow. Natural circulation drives the cooling air flow through an annular path between the MSB wall and the VCC liner wall and carries the heat to the environment without undue heating of the concrete cask. The annular air flow cools the outside of the MSB and the inside of the VCC.

The cask weighs approximately 80 tonnes empty, and 110 tonnes loaded with 17 canisters of consolidated fuel. The VCC has a reinforced concrete body with an inner steel liner and a weather cover (lid). The MSB contains a guide sleeve assembly for fuel support and a composite shield lid that seals the stored fuel inside the MSB. The cavity atmosphere is helium at slightly sub-atmospheric pressure. The helium atmosphere inside the MSB enhances the overall heat transfer capability and prevents oxidation of the fuel and corrosion of the basket components. This is evident when reviewing the comparison for different gases and near vacuum conditions for the measured temperatures inside the MSB (see Figure 4.10 of Reference 1). Even though the higher density of nitrogen would shift the temperature peak location towards the top of the canister, a helium environment would still result in lower temperatures as compared to a nitrogen and a vacuum environment.

The performance testing consisted of loading the MSB with 17 fuel cans containing consolidated pressurised water reactor (PWR) spent fuel from Virginia Power's Surry reactors and Florida Power & Light's Turkey Point reactors. At the time of the cask tests, this fuel was generating about 14.9 kW of total decay heat. Temperatures of the cask surface, concrete, air channel surfaces, and the fuel compartments (containing the fuel cans) were measured, as were cask surface gamma and neutron dose rates. Testing was performed with vacuum, nitrogen, and helium backfill environments in a vertical cask orientation, with air circulation vents open, partially blocked, and completely blocked. Of these tests, run#1 is the nominal case (no blocked vents) with helium gas in the MSB.

Detailed descriptions of the VSC-17 experiments, including system geometry, instrumentation locations, specifics of fuel loading, and estimates of the heat generation rates in the spent fuel assemblies are included in the original documentation of the testing [1]. The availability of as-built information and an extensive amount of data make this an excellent choice for evaluation of the accuracy and completeness of computer models for spent fuel storage systems.

Figure 12.9. Photo of the concrete shell and sealed canister

Figure 12.10 Schematic of the ventilated concrete cask system

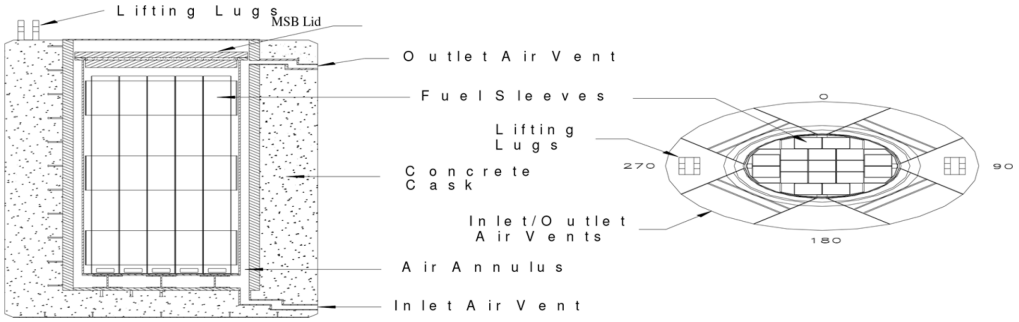

References

1. McKinnon M.A. et al. (1992), "Performance testing and analyses of the VSC-17 ventilated concrete cask", TR-100305, Electric Power Research Institute, Palo Alto, California.

12.3.2. Effective thermal conductivity model for consolidated fuel canister:

The tightly packed fuel rods within the stainless-steel fuel canisters are modelled as a homogeneous solid material region with a specified uniform heat generation rate and an effective thermal conductivity. The option in FLUENT for anisotropic thermal conductivity was used to represent the different effective conductivities of the fuel region in the axial and radial directions. For axial heat transfer, the conductivity of the fuel (UO_2) material and the fill gas was ignored, and it was assumed that significant axial conduction occurs only in the zircaloy cladding of the fuel rods. The effective conductivity in the axial direction was represented as an area-weighted fraction of the conductivity of zircaloy-4, using an area-weighted ratio of the cladding to the total cross-section of the homogeneous

region. This relationship was implemented in FLUENT based on the temperature-dependent thermal conductivity of Zircaloy 4.

For heat transfer in the radial direction through the fuel region, the FLUENT model makes use of the effective thermal conductivity values for consolidated 17x17 fuel. The k-effective values for the consolidated fuel cans in the VSC-17 are based on a calculational "database" generated by a separate 2-D FLUENT analysis for consolidated WE 17x17 fuel using a detailed two-dimensional model of a single fuel can. The 2-D heat transfer model includes both conduction and radiation based on the discrete ordinate's method. The model explicitly represents the fuel pins (including the fuel pellet, gas gap, and cladding) and the backfill gas bounded by the can walls. Calculations were performed with FLUENT for a single consolidated fuel can of WE17x17 fuel rods for fuel can wall temperatures ranging from 93°C to 400°C. A "database" was created for fuel can total decay heat rates of 0.5 kW, 0.75 kW, 1.0 kW and 1.2 kW, somewhat exceeding the range of decay heat values of the fuel cans loaded into the VSC-17 cask. However, there were only very small differences (less than 3%) in the effective thermal conductivity values as a function of wall temperature obtained with the standard methodology for the full range of heat rates evaluated. The calculated effective conductivity values were tabulated as a function of wall temperature are shown in Tables 12.4 and 12.5. Therefore, the effective thermal conductivity obtained for a heat load of 1.0 kW was used for all fuel cans in the CFD calculations, regardless of actual fuel can heat load, which varied from about 0.744 kW to 1.048 kW in the quadrant represented in the FLUENT model.

The effective thermal conductivity values in the radial direction of the fuel region were obtained as a function of temperature using the standard k-effective methodology [1]. This is the approach generally employed in vendor's Safety Analysis Report (SAR) analyses to determine peak fuel temperatures in spent fuel casks when the fuel assemblies are modelled as a homogeneous material. Following the documented form of the basic k-effective model, this approach yielded an effective thermal conductivity for the homogeneous fuel "block" as a function of local computational cell temperature. The model is implemented in FLUENT as temperature-dependent k-effective values.

References

1. US DOE (1996), *Spent Nuclear Fuel Effective Thermal Conductivity Report*, prepared by TRW Environmental Safety Systems, Inc. for US DOE, 11 July 1996.

12.3.3. Decay heat generation (thermal source term) for consolidated fuel cans

Individual consolidated fuel cans in the VSC-17 had heat generation rates ranging from 0.707 kW to 1.05 kW. The fuel cans were loaded in the basket to give as close to a symmetrical heat load as possible, with fuel cans near 1.0 kW in the central 3x3 grid, and fuel cans with heat loads near 0.7 kW on the periphery of the basket (refer to Figure 3.13 of McKinnon [1]). Most of the temperature measurements obtained within the fuel cans and the basket are from thermocouples located in one quadrant of the basket. In this quadrant, the peripheral fuel cans all have decay heat values of approximately 0.744 kW, and the inner fuel cans have decay heat values ranging from 0.962 kW to 1.048 kW. The specific heat generation rates for these fuel cans were applied to the homogeneous regions modelling the corresponding fuel cans in the 1/4 section of symmetry representation of the MSB in the FLUENT model.

The decay heat for a given fuel can was applied as a uniform volumetric heat generation rate throughout the homogeneous region, modified only to include an axial power profile based on the measured axial power distribution in the fuel cans (refer to Figure 3.14 of

McKinnon [1]). The heat generation is applied over 388 cm (153 inches). The actual heated length for this fuel is estimated at 145.5 inches (i.e. an original length of 144 inches, plus 1.5 inches of growth due to burn-up.). This approximation will result in slightly lower peak fuel temperature predictions than would be obtained if the shorter (actual) heated length were to be used.

References

1. McKinnon M.A. et al. (1992), "Performance testing and analyses of the VSC-17 ventilated concrete cask", TR-100305, Electric Power Research Institute, Palo Alto, California.

12.3.4. Mesh considerations and turbulence modelling in the air annulus region

Figure 12.11 shows the VSC-17 computational domain and the mesh used for the different cask components, including the MSB and the VCC. The mesh spacing between the VCC liner and MSB outer shell wall is an important consideration in selecting turbulence model for airflow through this annular gap. The near-wall modelling significantly impacts the fidelity of numerical solutions, since walls are the main source of mean vorticity and turbulence. After all, it is in the near-wall region that the solution variables have large gradients, and the momentum and other scalar transports occur most vigorously. Therefore, accurate representation of the flow in the near-wall region determines successful predictions of wall-bounded turbulent flows. In this study, two types of mesh distribution were used in the annular region. The first mesh was chosen to use semi-empirical formulas called "standard wall functions" to bridge the viscosity-affected region between the walls and the fully turbulent core region. The use of wall functions obviates the need to modify the turbulence models to account for the presence of the wall. This type of modelling is usually used for high Reynolds number flows. In the second mesh, the viscosity-affected region is resolved with a mesh all the way to the wall, including the viscous sublayer. This type of approach is referred to by "near wall modelling" approach. The dimensionless distance between the wall and the cell centre near the wall (y+) for the second mesh is around 1, while the first mesh used y+ of around 20.

Reynolds number estimates were made using velocities from initial runs for the cooling air in the annulus and helium fill inside the MSB. Cooling air in the annulus between the MSB and VCC had an average velocity of 1 m/s, corresponding to a Reynolds number above 3 000 based on the channel hydraulic diameter. This is just above the critical Reynolds number of 2 300 for internal flows, putting the flow in the transitional range between the laminar and turbulent zone. As we are dealing with buoyancy driven flows, both the Rayleigh (Ra) number based on the hydraulic diameter of the channel and the modified Rayleigh number defined as ($Ra_{modified}$ = Ra* W/H) where W and H are the width and height of the air channel) were also calculated. Based on both, Rayleigh and the modified Rayleigh number, laminar flow was obtained. On the other hand, buoyancy driven helium flow cooling the inside of the canister was calculated as laminar based on both the Rayleigh and the Reynolds numbers due to the higher kinematic viscosity, and the low achieved velocities of the helium gas within the MSB resulting in a Reynolds number of around 200. This is clearly in the laminar flow regime. The MSB internals were represented explicitly, except for the consolidated fuel cans that were modelled as non-porous solid using the effective thermal conductivities obtained from the 2-D FLUENT thermal model of a single assembly. Since the fuel is consolidated, there is limited space for helium to go through the fuel rods. However, there are other regions between the consolidated cans and the MSB inside wall where convection occurs and these spaces are explicitly represented in the MSB model as shown in Figure 12.12.

These preliminary calculations showed that a turbulence model was not needed for the buoyancy driven recirculation of the helium gas within the basket, and laminar flow conditions were assumed in this region of the model. The airflow in the inlet and outlet vents and annular gap between the MSB and the concrete outer shell, however, is expected to be in the transitional regime. It was therefore necessary to specify an appropriate turbulence model for the airflow to obtain accurate predictions of local velocities and temperatures in the air stream, and local wall temperatures on the surfaces of the annulus and inlet/outlet vent structures.

As noted above, two types of meshes were used in the air annular region and in the inlet/outlet regions to define conditions that would be more consistent with both types of turbulence modelling. Additionally, as the calculated Reynolds number was close to the critical Reynolds number of 2 300, a laminar model with finer mesh was also tested.

Figure 12.11. Control volumes of VSC-17 showing canister and overpack models

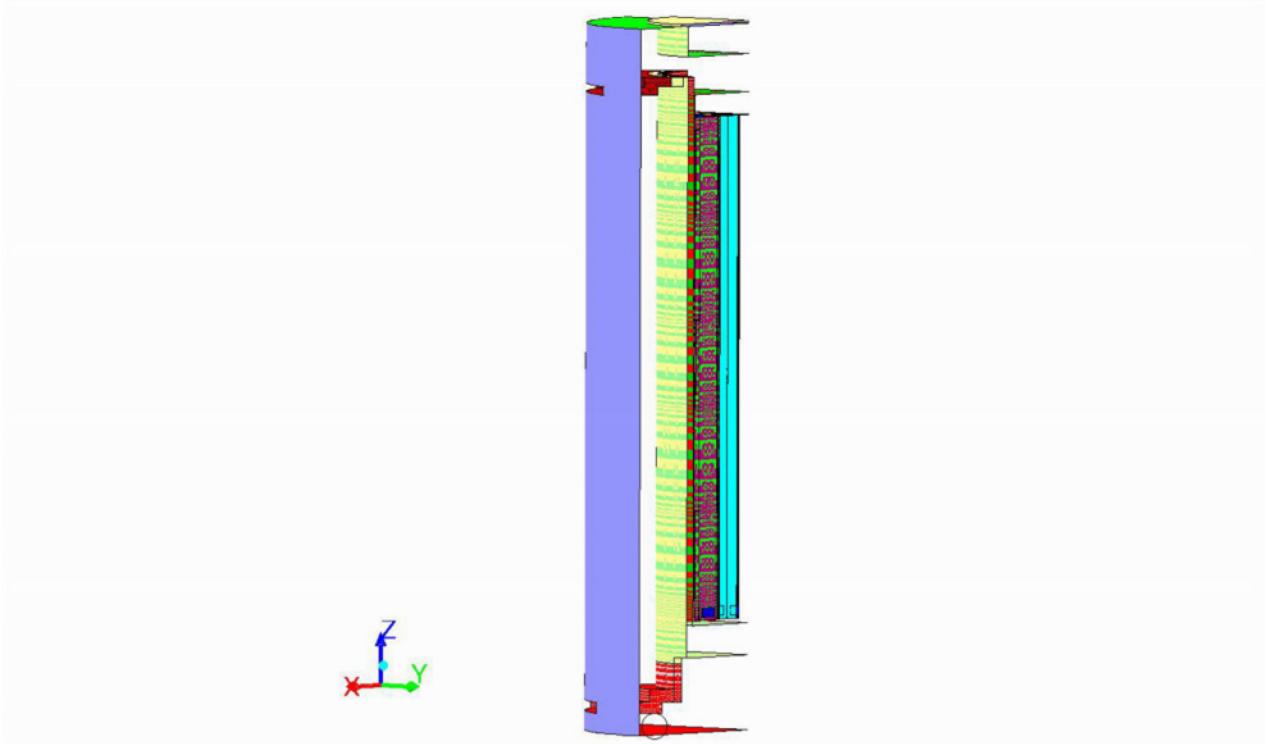

Figure 12.12. Geometry of VSC-17 dry cask

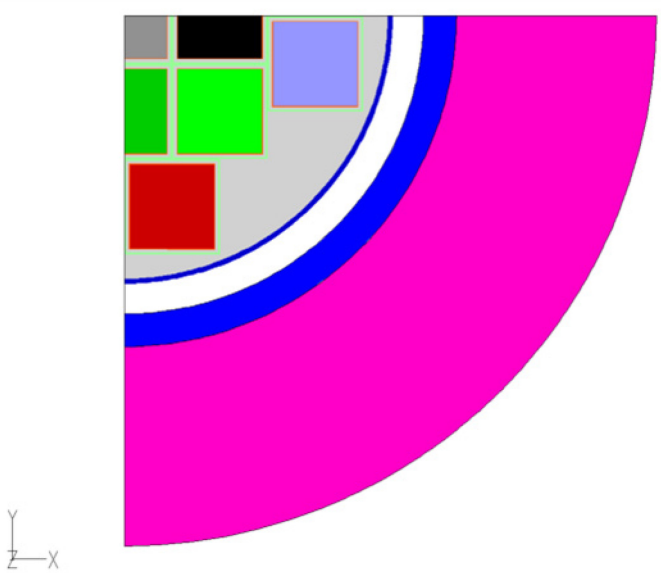

12.3.5. Thermal radiation modelling within the VSC-17 system

There are quite a few radiation models that are implemented in FLUENT. Each model has its advantages and limitations. In previous applications, both the discrete transfer radiation (DTRM) and discrete ordinate (DO) models were used and gave comparable results. As a result, the DO model was chosen. In this approach the radiative transfer equation (RTE) for an absorbing, emitting and scattering medium is solved for a finite number of discrete solid angles. The fineness of the angular discretisation is controlled by the user. Unlike the DTRM, the DO model does not perform ray tracing. Instead, the DO model transforms the RTE equation into a transport equation for the radiation intensity in the spatial coordinates (x, y, z). The DO model solves for as many transport equations as there are directions defined by the angular discretisation. The helium was treated as a transparent medium that neither absorbs nor scatters. The solution method is identical to that used for the fluid flow and energy conservation equations. In the solution of the VSC-17 problem, four angular discretisations were used in each direction of the spherical coordinates system (theta (θ) and phi (ϕ)). A sensitivity study was performed based on two, four, and six angular divisions and it was found that the results did not change much between four and six divisions.

12.3.6. Boundary conditions

The external boundary conditions on the VSC-17 consisted of free convection to ambient air on the top and side surfaces, radiation to the ambient, and conduction through the base to a concrete pad and its underlying soil. Since the experiment was conducted inside a building, solar insolation was not considered. These boundary conditions were represented in the FLUENT model of the VSC-17 by specifying appropriate convective heat transfer coefficients on the cells representing the outer surface at the top and sides of the VCC, and an appropriate thermal resistance on the cells representing the base of the system. Thermal radiation properties and resolution control for the view factor calculations were set via internal boundary conditions on solid cells adjacent to fluid (gas) cells. The specified values for these boundary conditions are summarised below:

- Ambient temperature of 21°C (based on test report).
- Solar heat loading not accounted for.

- Ambient pressure boundaries at the inlet and outlet vents.
- Heat transfer coefficient of 5 W/m^2-K on the top and sides of the VCC.
- Heat transfer coefficient of 10 W/m^2-K on the top of the VCC weather cover.
- Conduction resistance 5.87 m^2-K/W on the base of the VCC, to a 15°C fixed soil temperature (equivalent to conduction through 3 m of soil).
- Surface emissivities set to:
  - 0.4 for fuel cans,
  - 0.6 for basket, supports and MSB body, and
  - 0.7 for A36 steel used for VCC annulus and inlet/outlet liners.

The values of heat transfer coefficients were determined using standard correlations for convective heat transfer and were adapted to include additional losses through thermal radiation determined via simple hand calculations. The heat transfer coefficient on the weather cover is higher than that of the surrounding concrete to account for its higher temperature and consequently higher heat transfer rate due to thermal radiation.

The values of surface emissivities were selected based on "typical" values for the corresponding materials, since measured values for the components of the VSC-17 were not obtained in the testing. The most complete set of data is Hottel's measured values as listed in McAdams [1]. Most other textbooks reference this data. For the 304 stainless steels used in the consolidated fuel can walls, McAdams lists an emissivity range of 0.44-0.36 for temperatures ranging from 420 to 914°F for a sample described as "light silvery, rough, brown, after heating". Since the measured temperatures for the VSC-17 fall in the middle of this range, a value of 0.4 is selected as the baseline. Values for non-stainless steels span a large range. McAdams [1] shows emissivity for mild steel with a very thin oxide layer can range from 0.1 to 0.3, whereas oxidised steel surfaces are shown as 0.66 for rolled sheet, 0.79 for steel oxidised at 1 100°F, and 0.8 for sheet steel with a strong, rough oxide layer. A value of 0.7 for the A-36 steel of VCC liner was assumed. A-516 pressure vessel steel is the primary material for the MSB. The internal components will operate at elevated temperatures but will not see an oxidising environment. The outside shell of the MSB is subject to rust and oxidation, however it would be expected to be less likely to oxidise than the A-36 steel used in the liner and MSB lid. The assumed emissivity for all the A-516 components is 0.6.

References

1. McAdams, W.H. (1954), *Heat Transmission*. McGraw-Hill Book Company, Inc., New York.

12.3.7. Material properties

Thermal properties for the solid materials in the VSC-17 were obtained from the test documentation (specifically, from Table 5.2 available in [1]). Gas properties for air and helium were determined using the functions provided in the FLUENT material set. Temperature-dependent thermophysical properties were used for cooling air and helium.

References

1. McKinnon, M.A. et al. (1992), "Performance testing and analyses of the VSC-17 ventilated concrete cask", TR-100305, Electric Power Research Institute, Palo Alto, California.

12.3.8. Spatial differencing and solution method

The steady state solution for the VSC-17 model in FLUENT was performed with the SIMPLE algorithm using a conjugate-gradient solver. Second order Upwind spatial differencing was used for all variables except the pressure equation (continuity equation), where a body force weighting method was used.

These simulations were run from a zero-flow initial condition using a pressure boundary at the airflow inlet. The criterion for solution convergence is typically when the total heat flux is within 20 W, corresponding to an energy error of approximately 0.5%.

12.3.9. Thermal performance data

The VSC-17 tests provided a large amount of thermocouple data of recorded temperatures inside the fuel cans, within the basket structure, and on the inner and outer surfaces of the VCC structure. The measured data and the locations of the instrumentation are given in the background references for the experiment (specifically, in Table C.1 of McKinnon 1992 [0]). From this information it is noted that the peak measured temperature was consistently recorded at thermocouple location L6-3. This thermocouple location was at the 3 050 mm elevation of the thermocouple lance in the central fuel can. Therefore, location L6-3 was used as the Peak Clad Temperature (PCT) for evaluating the FLUENT model results, although additional comparisons were also made with temperatures measured in the basket, on the MSB shell surfaces, and on various surfaces of the VCC.

A total of 98 thermocouples (TCs) were used to measure the thermal performance of the cask. The inside of the MSB was instrumented using seven TC lances, as shown in Figure 12.13. Each TC lance contained six calibrated Type J (Iron-Constantan) insulated junction TCs, which provided a total of 42 internal lance TCs. A total of 53 Type J TCs were used to determine the temperature of the MSB, cask lid and concrete. Ten TCs were attached to the outer surface of the cask; five were attached to the MSB lid; two were attached to the weather cover; ten were imbedded in the concrete; nine were attached to the outside barrel of the MSB; nine were attached to the inner liner of the VCC; and one TC was installed in the centre of each air inlet and outlet vent. An additional three TCs were used to monitor the ambient temperature in the Hot Shop. The location of the TC lances and the elevations of the TCs are shown in Figure 12.14. Each TC lance had six TCs installed in an 8-mm-diameter (0.315-inch) tube as shown in Figure 12.13. Lances were inserted through instrumentation penetrations in the test lid and into selected guide tubes placed in six fuel canisters and into one simulated guide tube attached to the basket. The selected axial and cross-sectional locations of the TC lance thermocouples made it possible to evaluate temperature symmetry and to determine axial and radial temperature profiles for the cask.

Figure 12.13. Thermocouple lance

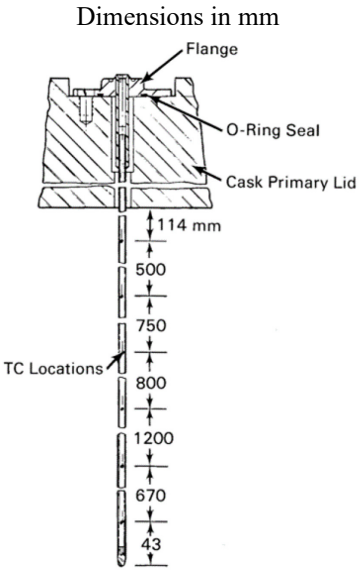

Figure 12.14 Temperature measurement locations used during the VSC-17 performance test

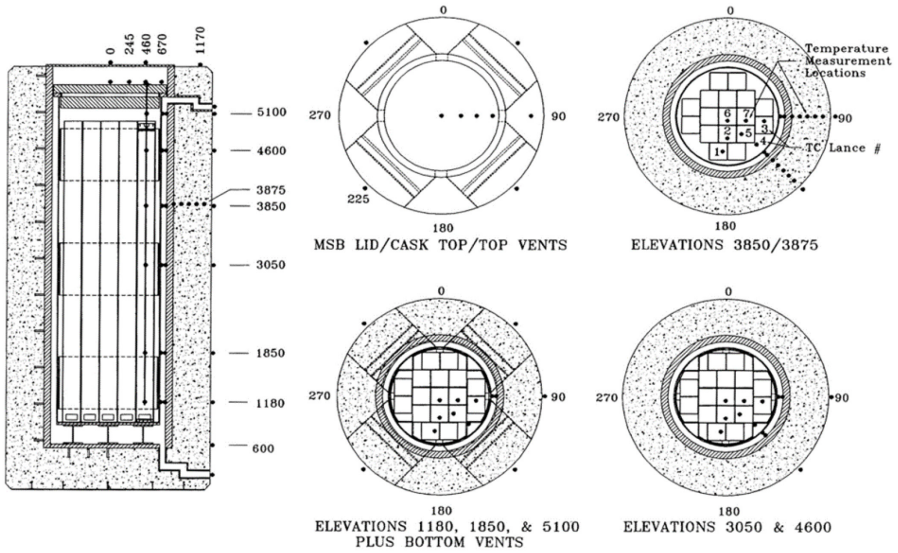

Note: Dimensions in mm.

Table 12.2 Performance test run designation

Test #	1	2	3	4	5	6
Backfill gas	Helium	Helium	Helium	Helium	Nitrogen	Nitrogen/vacuum
Pressure, mbar absolute	817.5	1 074.1	935.3	975.2	843.6	8.6

References

1. McKinnon, M.A. et al. (1992), "Performance testing and analyses of the VSC-17 ventilated concrete cask", TR-100305, Electric Power Research Institute, Palo Alto, California.

12.3.10. Summary of results

Three turbulence models as well as a laminar regime were used to model the air flow passage between the MPC and the concrete liner. The first two models among the three chosen turbulence models were the transitional SST k-ω model, and the low-Reynolds k-ε model. Both models use damping functions that consider the effect of the cell Reynolds number on the calculation of the time and length scale of turbulence. Both models are used with the fine grid near the wall (y+ ~1) to enable integration through the viscosity-affected near-wall region. The third chosen turbulence model was the standard k-ε in conjunction with standard wall function to bridge the fully turbulent core region to the viscosity-dominated region near the wall. This model does not use finer mesh near the wall. In the present application a y+ close to 20 was used.

Temperature profiles from the four CFD approaches described above are compared to the experimental data and shown in Figure 12.15 through Figure 12.27. The axial temperature profile experimental data for Lances three, five, six and seven inside the fuel region, liner wall and MPC wall were chosen to compare to calculated CFD results. Additionally, radial profiles from the centre of the fuel region to the periphery of the overpack concrete shield at elevation of 3.0 m and 3.85 m were used to compare the experimental data to the CFD results.

As a first observation, all the four options used to model the turbulence in the air-cooling channel were successful in predicting the location of the peak cladding temperature. The peak cladding temperature value is of great importance in dry cask applications. For long-term normal storage conditions, dry cask peak cladding temperature is limited to 400 C to avoid spent fuel rod failure due to thermal loads. CFD results obtained for the laminar option are shown in Figure 12.25 through Figure 12.27. Modelling air flow using the laminar option overpredicted the peak cladding temperature as well the axial temperature distribution in the entire fuel region as shown in Figure 12.25. Additionally, the liner wall axial temperature distribution as well as the MPC wall axial temperature distribution was overpredicted using the laminar regime option to model the air-cooling channel. The over-prediction of the temperature distribution inside the cask and the air channel led to the over-prediction of the radial temperature profile in the overpack region. The standard k-ε model was a better choice than the laminar option, but due to the lack of grids near the MPC wall and the liner wall, this model was unable to capture the exact temperature distribution at the liner wall. This model overpredicted the heat exchange between the two walls. Usually, a standard k-ε model combined with standard wall function is used when high Reynolds number flow exists. In case of transitional Reynolds numbers, as in this example, some type of damping function to enable computation across the laminar viscous sublayer is required in conjunction with fine mesh near the wall, as was done with the first two turbulence models chosen in this analysis. The standard k-ε predicted the peak cladding temperature as shown in Figure 12.22 but under-predicted the liner wall axial temperature distribution as shown in Figure 12.24, for the reasons enumerated above. In the review and confirmation of CFD calculations of other dry cask designs, the standard k-ε model proved to be non-conservative and under-predicted the peak cladding temperature when compared to transitional k- ω turbulence and low Reynolds k-ε model.

Both, the transitional SST k-ω and the low Reynolds k-ε turbulence models predicted the temperature distribution well in the fuel region inside the canister as well as the passage of cooling air. Considering that the reported experimental measurements are within +- 6 degrees and possible discrepancy in the material properties, the predicted results are acceptable. Both Figure 12.15, and Figure 12.19 show that these two models predicted the location and the value of the peak cladding temperature. Additionally, the axial temperature profile of the liner wall and MPC wall were well predicted given the complex nature of this buoyancy driven flow as shown in Figure 12.18 and Figure 12.21. The improvement in the prediction of the liner wall distribution was the result of the fine mesh used near the walls and the capability of these two models to handle low Reynolds turbulent flow. Additionally, the radial temperature distribution at 3.05 m and 3.85 m compares favourably using these two models as shown in Figure 12.16 and Figure 12.20.

Higher values for the emissivity were considered for surfaces outside the MPC due to surface oxidation. However, surfaces inside the MPC were not considered oxidised.

Figure 12.15 Fuel region axial temperature, using SST k-ω turbulence model

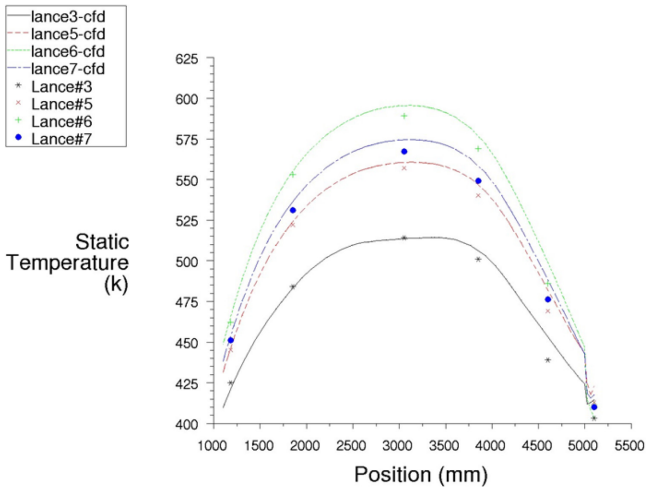

Figure 12.16 Radial temperature plot at 3.05 and 3.85 m elevation using SST k-ω turbulence model

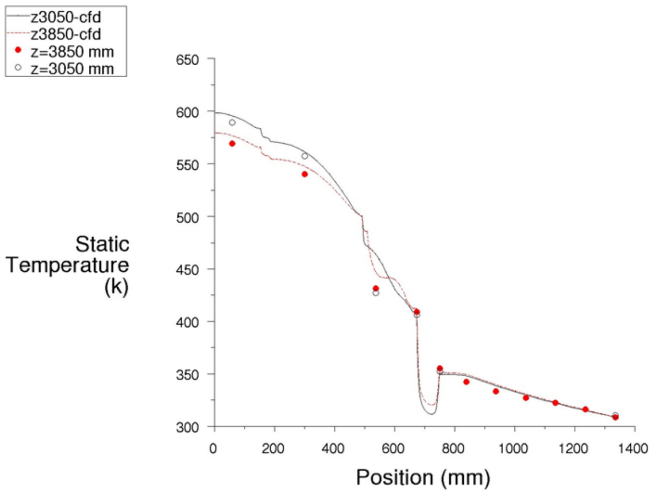

Figure 12.17 Z-velocity (direction along the cask) contours (showing the flow direction of helium inside the MPC and flow of air outside the MPC)

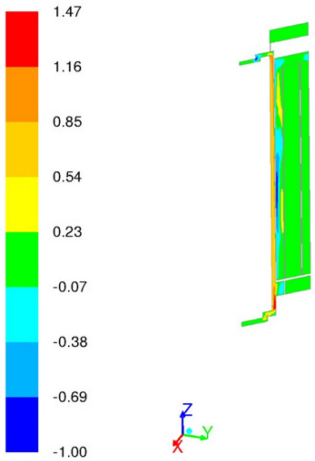

Figure 12.18. MPC and liner walls axial temperature, using SST k-ω turbulence model

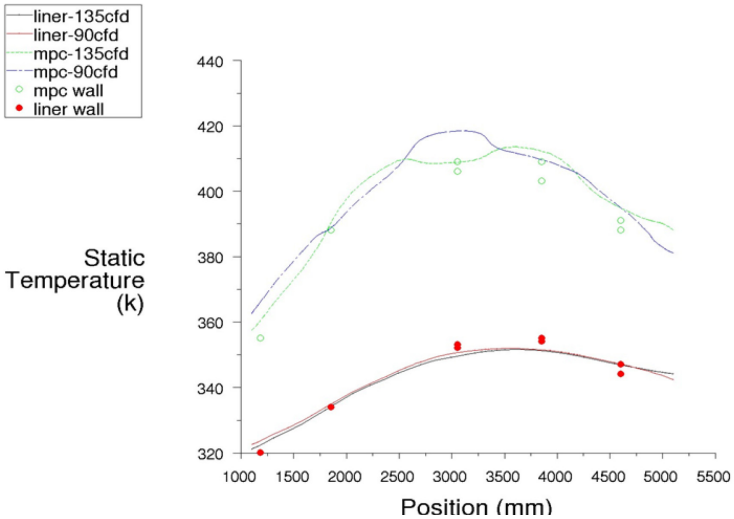

Figure 12.19. Fuel region axial temperature, using low Reynolds k-ε turbulence model

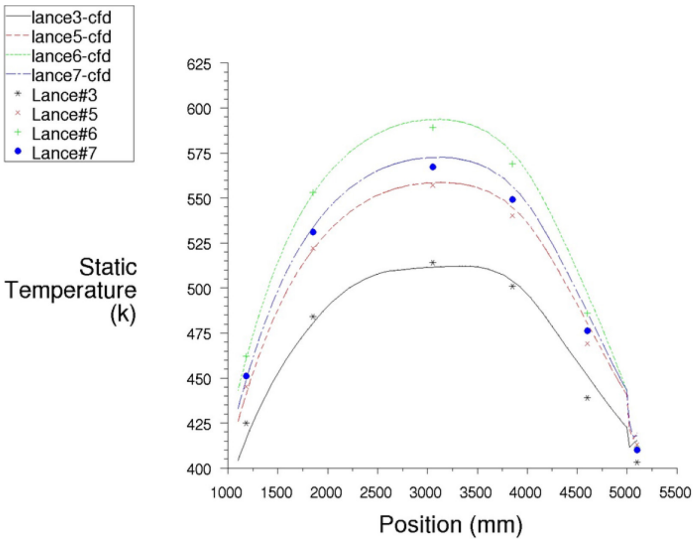

Figure 12.20. MPC and liner walls axial temperature, using low Reynolds k-ε turbulence model

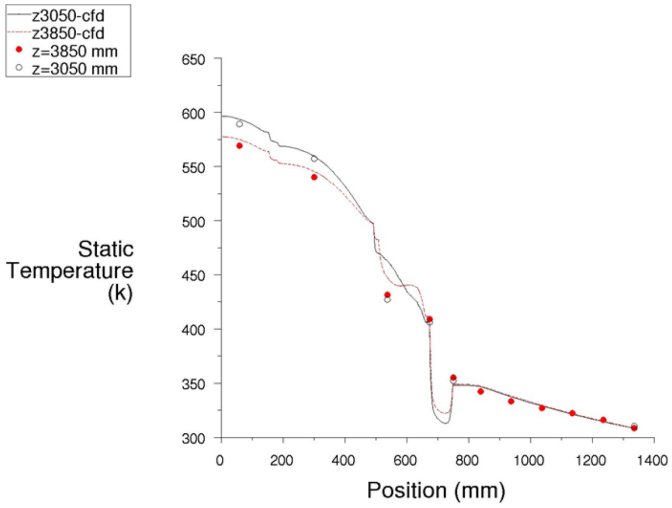

Figure 12.21. MPC and liner walls axial temperature, using low Reynolds k-ε turbulence model

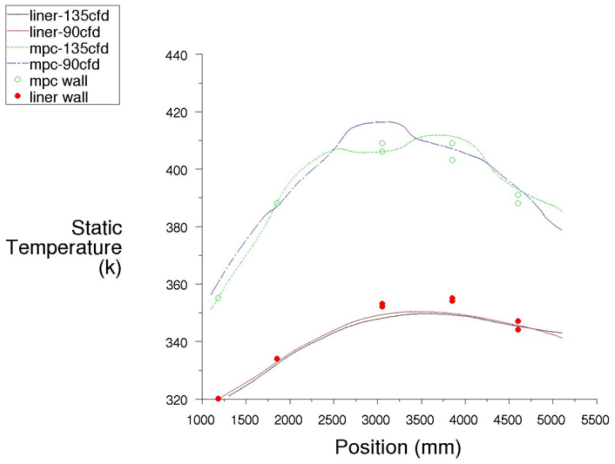

Figure 12.22. Fuel region axial temperature, using standard k-ε turbulence model

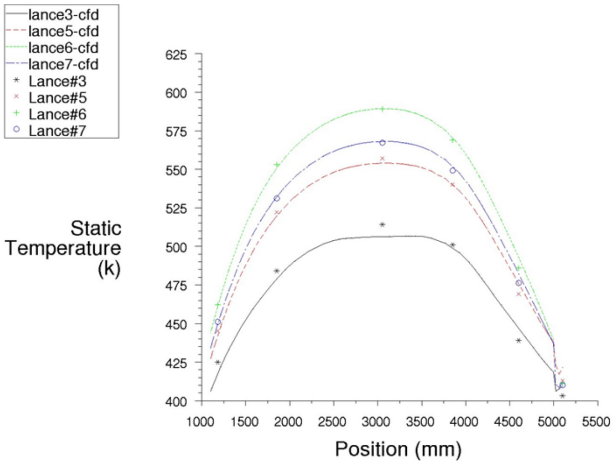

Figure 12.23. Radial temperature at 3.05 and 3.85 m, using standard k-ε turbulence model

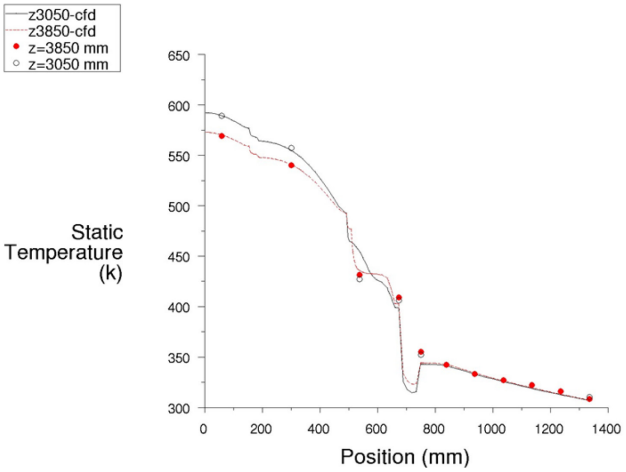

Figure 12.24. MPC and liner walls axial temperature, using standard k-ε turbulence model

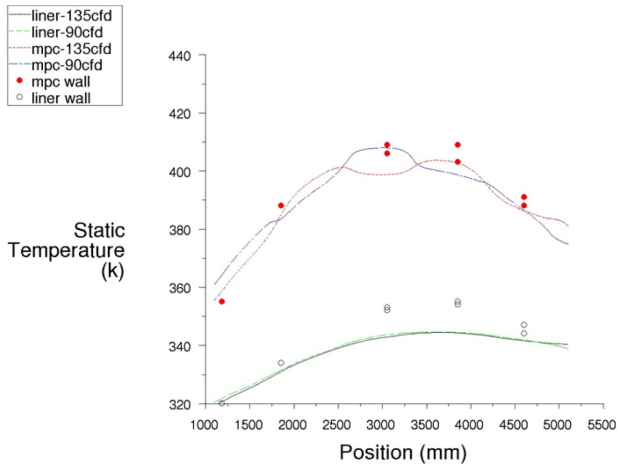

Figure 12.25. Fuel region axial temperature, using laminar option

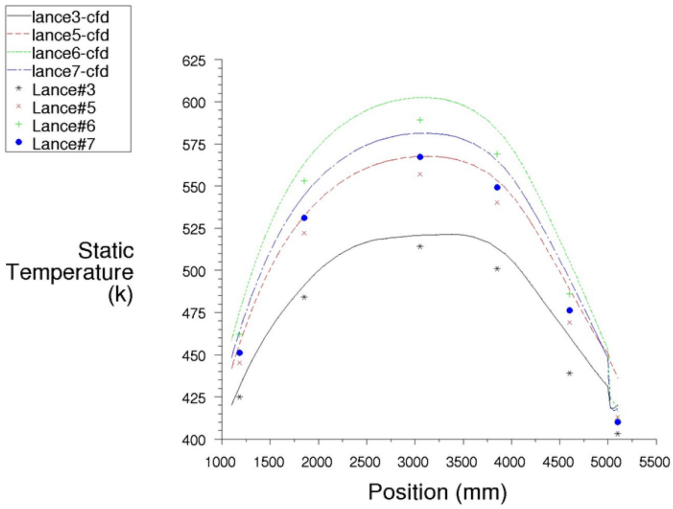

Figure 12.26. Radial temperature at 3.05 and 3.85 m, using laminar option

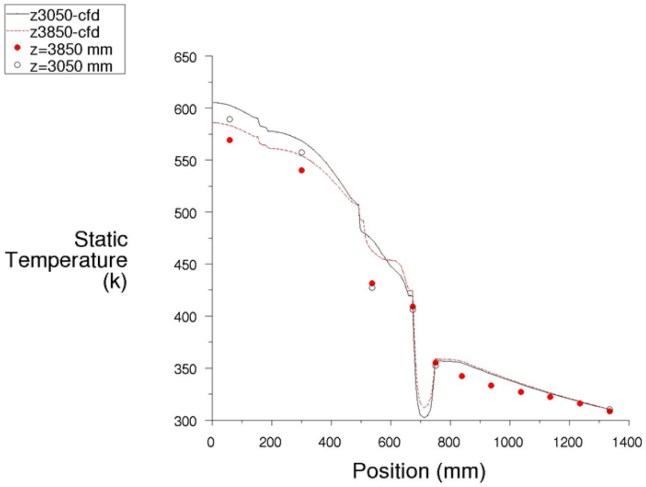

Figure 12.27. MPC and liner walls axial temperature using laminar option

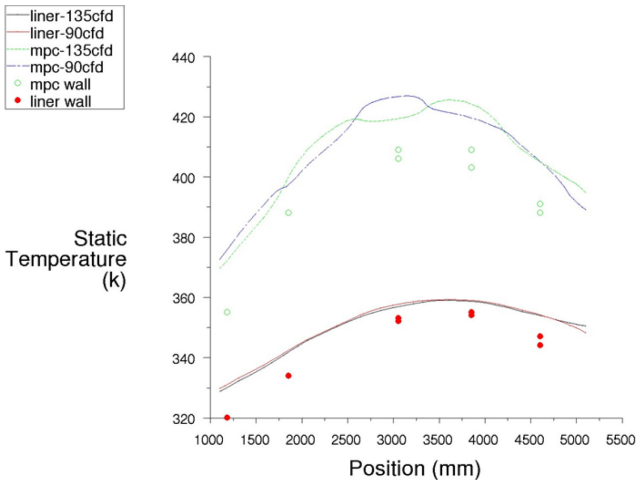

Table 12.3. Fuel radial k_{eff} for VSC-17 with helium

Temperature (Kelvin)	Keff (W/(m-k))
370	1.383
509	1.770
647	2.01
676	1.99
703	1.85

Table 12.4. Fuel axial k_{eff} for VSC-17 with helium

Temperature (Kelvin)	Fuel with helium (W/(m-k))
366	5.75
505	5.84
644	4.99
673	4.75
720	4.36

12.4. Hydrogen mitigation in the containment of the PAKS Nuclear Power Plant

Within the PHARE project “Hydrogen management for the VVER-440/213 containment” [1] of the EC, the project partners were requested to provide simulations for the hydrogen behaviour in the containment during a severe accident. The problem was selected from existing probabilistic safety assessments (PSA), and flow boundary conditions for steam and hydrogen into the containment were provided by a MAAP calculation [2] of the reactor system response to the severe accident. A comparison was made of the consequences for two variations on the accident scenario. The first case had no countermeasures against

hydrogen accumulation and the second case included catalytic recombiners to remove as much hydrogen as possible from the containment atmosphere. Ignition of the atmospheric gas mixtures was not considered but could be included as an extension of the project scope. The main result of the project was information on the effectiveness of different arrangements of catalytic recombiners in removal of atmospheric hydrogen and therefore reduction of the risk of damage by ignition.

The problem was complex in geometry (full containment with numerous internals and additional engineered systems) and spanned a long time (25 000 s of transient). Additionally, none of the available commercial CFD codes were equipped with all the models needed. Special models had to be implemented before running the simulations:

- bulk condensation of steam;
- wall condensation of steam as a single-phase implementation.

The following engineered systems were modelled:

- condensation of water vapour in pressure suppression pools of the bubble condenser system (found in VVER-440 containments);
- catalytic recombiners for hydrogen removal.

For the given type of problem CFD codes were selected for application because hydrogen mixing is a typical 3-D problem which requires a high spatial resolution of the given geometry to detect potential agglomeration of hydrogen. The use of full Navier-Stokes solvers was necessary to capture the momentum of the flow from the reactor pipe break as well as through various flow paths within the containment.

Experimental data for validation of CFD codes are not available for the interplay between all phenomena expected in the containment. However, combined-effect tests addressing mixing like the HYJET [3] experiments at Battelle model-containment and SETH tests at the PANDA facility [4] were used before this project started to validate CFX and FLUENT and to improve skills of the analysts. Recombiners in a multi-room arrangement (Battelle model-containment) were investigated in the HYMI [5] project of the EC and analysed with CFX. ISP 47 [6] simulations were used to extract information about the validity of the condensation models in CFX.

Best practice guidelines were applied in the sense that the experience collected from previous validation steps was applied. For example, the numerical investigation of jets through openings (important for flame acceleration) led to a minimum resolution of 3x3 to 5x5 cells. Another aspect is to enable the possibility of counter-current flows through openings, which also require at least three or four or more cells over the height of the opening [4].

Computational times were high, requiring about 50 days for one of the two cases on six to eight processors in a PC-cluster. This prevented the direct investigation of mesh influence and turbulence models on the results. Instead, to ensure a higher reliability of results the project partners used different meshes and different codes for the same problem. For all user models implemented in the codes prior to the containment simulations, special verification tests were carried out and differences carefully analysed.

References

1. Huhtanen, R. (Editor) (2005), “Hydrogen management for the VVER-440/213 containment”, *Phare project service contract No HU2002/000-632-04-01, Final Report*, Dec. 2005.

2. Téchy, Z. (2001), "Assessment of the Paks nuclear power plant safety for large radioactive release, E1: Containment event trees and severe accident analyses", *VEIKI Report 20.22-017*, October 2001.

3. Heitsch, M., H. Wilkening and D. Baraldi (2005), "CFD modelling of gas-transport and mixing phenomena in the battelle experimental facility for nuclear safety applications", 7th World Congress of Chemical Engineering, Glasgow.

4. Andreani, M. and al. (2006), "A benchmark exercise on the use of CFD codes for containment issues using best practice guidelines: A computational challenge", *Nuclear Engineering and Design*, Vol. 238, Issue 3, 2008, pp. 502-513, ISSN 0029-5493, https://doi.org/10.1016/j.nucengdes.2007.01.021.

5. Carcassi, M. and al. (1999), "Improved modelling of turbulent hydrogen combustion and catalytical recombination for hydrogen mitigation (HYMI)", *4th Framework Programme of the EC, Final Summary Report*, Pisa.

6. Fischer, K. (2004), "International standard problem ISP-47 on containment thermal- hydraulics, step 2: ThAI. Volume 1: Specification Report", Becker Technologies GmbH, Eschborn, Internal report Nr. BF-R 70031-1, Revision 4, December.

12.4.1. Calculations performed

The codes involved in the simulations were FLUENT (VTT Finland), CFX (SERCO UK, GRS Germany) and GASFLOW (VEIKI Hungary). GASFLOW as a nuclear in-house code uses a completely different approach for mesh generation than CFX and FLUENT. VTT and GRS created two independent meshes of the PAKS containment. SERCO used the VTT grid in CFX. VTT implemented all necessary user models in FLUENT, while SERCO and GRS shared the same modelling work for CFX.

The following table gives some details of the simulations performed.

Table 12.5. Details of the simulations performed

	FLUENT (VTT)	CFX (SERCO)	GASFLOW (VEIKI)	CFX (GRS)
Grid	Hexahedral (body-fitted)	Hexahedral (body-fitted)	Rectangular	Hybrid (Hexas, Tetras, Pyramids) (body-fitted)
Number of Cells	167 170	167 170	23 030	237 400
Wall Condensation Model	User Model	User Model	Built-in	User Model
Bulk Condensation	User Model	User Model	Built-in	User Model
Recombiner Model	User Model	User Model	Built-in	User Model
Bubble Condenser System	User Model	User Model	User Model	User Model
Mitigation Option (# of Recombiners)	30	20	30	20

Results reported from the calculations include pressures and temperatures as well as distributions of hydrogen, steam and oxygen within all compartments of the containment. Additionally, sometime dependent quantities useful for describing the ignition potential of the actual gas mixture in the containment were calculated. These are the lower and upper ignition limits (lower: >4 % hydrogen, >5 % oxygen and <55 % steam; upper: >8 % hydrogen, >5 % oxygen and <55 % steam), the size of ignitable clouds and the AICC (adiabatic isochoric complete combustion) pressure for selected regions in the containment. This pressure is easily calculated and can serve as an upper limit for most combustion situations if these really occur.

12.4.2. GRS simulations

Results from GRS for the two scenarios with and without hydrogen mitigation are summarised in this section. More details of these calculations can be obtained from references [1] and [2].

The final grid for the simulation without recombiners is shown in Figure 12.28. In this picture the main equipment of the primary circuit can be seen. In the upper part of the picture, two channels establish the connection to the pressure suppression system of this reactor system. This pressure suppression system (bubble condenser) consists of a tower to guide the hydrogen-steam-air mixture to 12 large water pools, where the steam condenses. The non-condensable gas components leave the water pools and flow to four large air spaces (air traps), from which they cannot return to the reactor system.

The mesh in the bubble condenser (only the lower section is visible in Figure 12.28) is considerably coarser than in the main part of the containment. In the bubble condenser detailed flow fields are not of interest; only gas composition and pressure need to be known to establish the link to the main part of the containment.

The SST (shear stress transport) turbulence model available in CFX (version 5.7.1) was chosen for this work in conjunction with a combined linear and logarithmic wall function. This selection was made based on comparisons between simulations of several SETH tests [3] using SST and k-ε turbulence model options.

Figure 12.28. View of main components and the surface mesh of the modelled containment

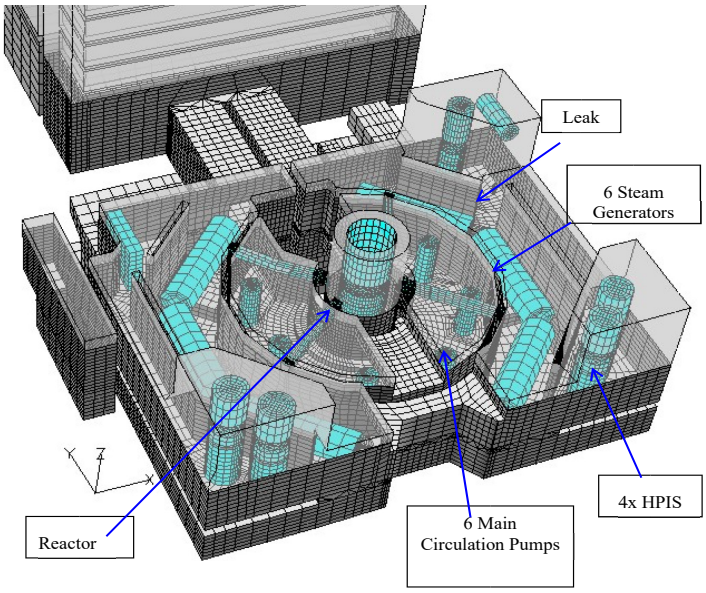

The non-dimensional wall distance (see Section 6.2.3) was detected to stay well within an upper boundary of about 300.

All main components were built from hexahedral cells. Cylindrical bodies were handled by an internal "H-type" grid to avoid strongly distorted cells. To restrict the propagation of internal mesh structures too far from the location where they are needed, layers of tetrahedral cells were introduced. One example of this method can be seen in the upper end of the connecting channels before they merge into the tower of the bubble condenser.

The CFX grid for the simulation case including recombiners was modified from the grid in Figure 12.28 by splitting appropriate blocks down to the size of the recombiner boxes which is about 1.5 m by 1.4 m by 0.3 m (WxHxD).

Figure 12.29. Distribution of hydrogen in the containment in the unmitigated case

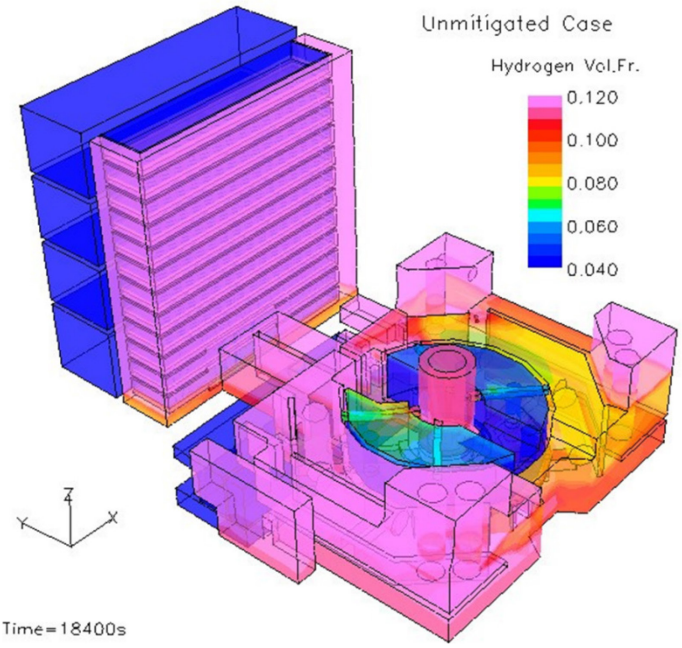

Figure 12.29 and Figure 12.30 provide the hydrogen volume fraction in the containment for the unmitigated and mitigated cases. The time selected is after the first hydrogen release peak. In the unmitigated case there are many locations with hydrogen fractions higher than 12%. However, high steam and low oxygen volume fractions in many locations at the same time (not shown) avoid ignitability even in this case. This illustrates the danger in looking only at hydrogen concentrations to reach a conclusion on combustion consequences. The integrated size of ignitable clouds (all cells with ignition limit fulfilled) in the containment is shown in Figure 12.31. This figure illustrates how drastically recombiners reduce the chance of ignition.

Figure 12.30 in comparison to Figure 12.29 proves the strong removal effect of catalytic recombiners in a more illustrative manner. The coloured surface contours in Figure 12.30 show that there are no more locations exceeding 8% of hydrogen. In combination with oxygen and steam molar fractions the history of burnable cloud sizes (Figure 12.31) can be deduced.

Figure 12.30. Distribution of hydrogen in the containment with 20 recombiners installed

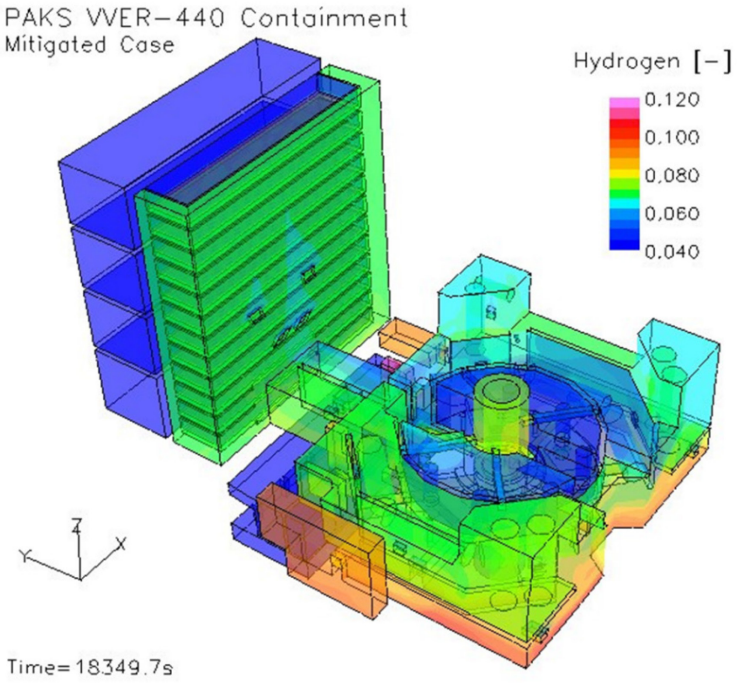

SG-Tube Rupture Accident in PAKS Containment - Size of Ignitable Cloud -

Figure 12.31. Size of ignitable clouds for unmitigated and mitigated cases

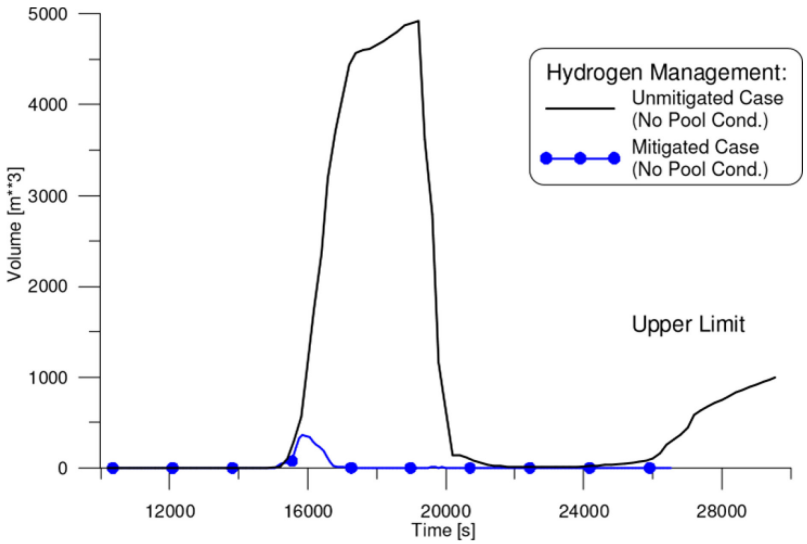

References

1. Heitsch, M. and B. Schramm (2005), *Simulation of the Unmitigated SG-Tube Rupture Accident at PAKS with CFX, Hydrogen Management for the VVER-440/213 Containment*, HU2002/000-632-04-01, GRS Cologne.
2. Heitsch, M. and B. Schramm (2005), *Simulation of the Unmitigated SG-Tube Rupture Accident at PAKS with CFX, Hydrogen Management for the VVER-440/213 Containment*, HU2002/000-632-04-01, GRS Cologne.
3. Andreani, M. et al. (2008), "A benchmark exercise on the use of CFD codes for containment issues using best practice guidelines: A computational challenge", *Nuclear Engineering and Design*, Vol. 238, Issue 3, pp. 502-513, ISSN 0029-5493, https://doi.org/10.1016/j.nucengdes.2007.01.021.

12.4.3. Conclusions

Some results of the work carried out in the project "Hydrogen management for the VVER-440/213 containment" were presented to demonstrate the increasing capabilities of CFD in evaluating containment problems. The application of Best Practice Guidelines is currently restricted due to the prohibitive numerical effort to carry out mesh sensitivity studies and comprehensive investigations on different turbulence models. In the given context code benchmarks were defined to test the proper implementation of user models.

There is a continuous need to get more detailed information on hydrogen behaviour associated with severe accidents to design mitigation measures as reliably as possible. The work summarised gives new insights for this type of problems. There is also a generic significance of the simulations described because it is relatively easy to apply the same strategy to the containment of other and more recent reactor systems like the EPR. It might even be easier to perform simulations as the complex bubble condenser system will not be available and containments consist of more open space.

13. Summary

As reflected in the content of this report, computer simulation is much more than generating input and observing results. In an NRS project producing trusted results, these activities do not even occupy most of the staff time expended. A project must begin with a clear written statement of the problem, including identification of the specific system and scenario to be analysed. This statement is then reviewed by a panel of experts in a PIRT process to identify parameters of interest and to rank the physical phenomena (and, by inference, regions of the system) that most strongly influence these parameters. This identification of important phenomena guides the analyst in the selection of an appropriate CFD code and in selecting optional physical models within that code. With knowledge of the system and significant physical phenomena, the panel is also responsible for identification of existing information that can be used to validate models over the range of conditions in the specified scenario.

The panel's identification of significant physical phenomena, and associated validation, is also an initial guide for spatial (and if appropriate temporal) discretisation. If a specific validation problem has already been performed with the selected code, it should be reviewed for appropriate nodalisation. If new validation calculations are required, a verification process is necessary to estimate errors associated with discretisation before any comparison with data. This may result in an iterative adjustment of discretisation until a quantitative assurance is available that error associated with the selection of the spatial mesh (and where appropriate time step) does not contaminate the conclusions of the validation exercise.

If validation does not include simulations of the full system considered by the project, verification of the final discretisation will also be needed before accepting the results. Frequently, the available time and computer resources restrict the rigour in estimation of discretisation error. However, analysts must not use these restrictions as an excuse to abandon verification. Useful information can be obtained from comparisons with results from a mesh that is coarser than the one used for results, and verification tests with subsections of the mesh can also be productive.

This report suffers from two major shortcomings. The first is that a snapshot of guidelines is produced at a relatively early phase in the use of CFD for nuclear reactor safety applications. In addition, general claims of maturity for single-phase CFD technology ignore the fact that most applications still must strike a balance between detail of modelling and reasonable execution time for the simulation. As computer speed and memory continue to grow, opinions on the optimal discretisation and model selection will shift. As practical capabilities and associated experiences expand, extensions and revisions to all Best Practice Guidelines are expected. The second limitation is in the necessary decision to cover a wide range of CFD safety applications. As more experience is gained through NEA-sponsored benchmarks and other activities, it is recommended that this report be used as a template for the application of specific best practice guidelines. For example, experience with ISP 47 could be used to generate detailed guidelines for modelling hydrogen mixing and combustion in a containment building.

Examples have been provided for two safety issues with a relatively long history of CFD analysis: boron dilution and pressurised thermal shock. In addition, CFD analyses are described for the more recent issues of dry cask fuel storage and hydrogen mixing in containment. None of these are intended as sample implementations of the guidelines provided in this report. They do, however, demonstrate important considerations in model selection, and provide references to validation data for four specific problems in nuclear reactor safety.

Annex I: Checklist for a calculation

Initial preparation

Produce a clearly written problem description, specifying the system and scenario requiring analysis, and clearly listing study objectives (Section 3.2).

Assemble a panel of experts and go through the PIRT process based upon the problem description (Section 3.2).

Do special phenomena such as containment wall condensation require addition of models to a standard CFD code or use of a special purpose CFD package? (Section 3.3)

With knowledge of the problem and physical processes select an appropriate CFD code and if necessary, develop enhancements. (Section 4.3)

Does the problem require full CFD or are classic thermal-hydraulic (TH) codes adequate? (Chapter 4)

Is coupling required between a CFD and a TH code to supply boundary conditions to the CFD? (Section 4.4)

Geometry generation

Is the coordinate system correct?

Are the units correct?

Have any substantial modifications been made to the geometry?

Is the geometry complete?

Are there oversimplifications due to symmetry assumptions, etc.?

Are inlet, outlet, symmetry, and cyclic boundary condition regions located correctly?

Selection of physical models

Develop a basic understanding of the prevalent physical phenomena and flow fields (part of the PIRT process)

Select the appropriate level of turbulence representation (see Section 5.1.4)

For RANS or T-RANS select an appropriate statistical model for turbulence (Section 5.1.4).

Either resolve the wall boundary layer or choose a wall function model (Sections 5.1.4 and 6.2.3).

Establish boundary conditions consistent with your choice of turbulence model. (Section 5.1.4)

Grid generation (Section 6.2.3)

Are the grid angles larger than 20° and less than 160°?

Are the ratios of adjacent volumes less than 2?

Are the aspect ratios below the values given in the solver manual (typically, 10 … 50)?

Is the grid scalable?

Are grid nodes concentrated in areas of foreseeable physical significance?

Does the grid contain non-matching grid interfaces in critical regions?

Is the grid compatible with the physical models (turbulence model, wall treatments, etc.)?

Numerical methods

Generally, avoid use of first order upwind spatial discretisation, and first order implicit time integration schemes.

If first order methods are used, compare the numerical diffusion coefficient to an estimate of the turbulent diffusion coefficient at several locations in your mesh (Section 6.3).

When using LES, select a higher-order central-difference method, preferably fourth order.

Verification

Check for round-off errors (Sections 8.2 and 8.3).

Check for errors associated with selection of iteration convergence criteria (Sections 8.2 and 8.4).

Check for errors associated with discretisation of space and time (Sections 8.2, 8.5 and 8.6)

Follow procedures to limit and locate user errors (Section 8.7) including: − selection of a high-quality user interface to the CFD code; and − use of quality assurance practices.

Validation

Follow a tiered approach comparing first to separate effects experiments (unit problems) and working up through complete system experiments (Section 9.1)

Where possible use repeat experiments to help quantify experimental error

Using guidance from the PIRT process, select target variables and metrics for agreement between calculation and experiment (Section 9.2).

Characterise experimental uncertainty for all target variables, distinguishing between random and systematic (bias) contributions to the uncertainty (Section 9.3.1).

If sufficient computer resources are available, perform uncertainty analysis on the simulation, to place bounds on results, and to cross-check the initial PIRT assumptions about relative importance of physical phenomena (Section 9.3.2).

Annex II: Major modifications of the BPG

Modifications in NEA/CSNI/R(2014)11 with respect to NEA/CSNI/R(2007)5.

Modifications were introduced in Chapters 2, 3, 4, 5 and 11. Major modifications were introduced in the following sections of Chapter 3, Chapter 5, and Chapter 11, as listed below:

Chapter 3: Problem definition

Section 3.3.1 - Complements to the containment wall condensation (two-phase approach) were added.

Section 3.3.2 - Clarifications in pipe wall affected by flow-accelerated corrosion were provided.

Section 3.3.3 - The thermal cycling section was also modified.

Section 3.3.4 - Complements in hydrogen explosion were provided.

Section 3.3.8 – Regarding natural convection, clarifications related to turbulent heat flux treatment were introduced.

Chapter 5: Selection of physical models

In general, turbulence modelling was clarified, and complements were provided as follows:

-research and validation are still in progress on hybrid methods, SAS, or RANS/LES coupling;

-merge buoyancy with heat transfer section;

-introduce clarifications and complements in thermal cycling;

-clarifications in thermal cycling.

Chapter 11: Special considerations of specific NRS cases in which clarifications and complements were provided for boron dilution and spent fuel dry storage cask.

Major modifications in the present version with respect to NEA/CSNI/R(2014)11.

A quick guide introduction was added to better drive the reader through the report.

Modifications/updates were introduced in several chapters:

3.2: PIRT, including an example

3.3.1 Containment wall condensation

3.3.7 Liquid Metal Systems

3.3.8 Molten Salt Systems

4.4 The 1D-3D multiscale coupling

5.1 Guidelines for turbulence modelling in NRS applications.

5.2 Heat Transfer

5.4 Fluid-Structure Interaction

8. Verification of the calculation and numerical model

9. Validation of results

10. Uncertainty quantification